DETECTION, IDENTIFICATION AND LOCATION OF FAULTS IN DISTRIBUTION SYSTEM

Ph. D. THESIS

by

PRATUL ARVIND

DEPARTMENT OF ELECTRICAL ENGINEERING
INDIAN INSTITUTE OF TECHNOLOGY ROORKEE
ROORKEE – 247 667 (INDIA)
FEBRUARY, 2016

DETECTION, IDENTIFICATION AND LOCATION OF FAULTS IN DISTRIBUTION SYSTEM

A THESIS

Submitted in partial fulfilment of the requirements for the award of the degree of

DOCTOR OF PHILOSOPHY
in
ELECTRICAL ENGINEERING

by

PRATUL ARVIND

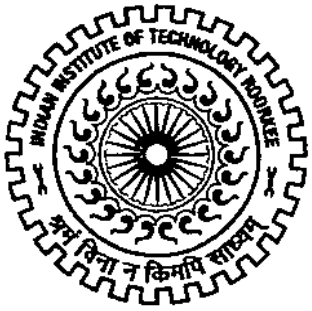

DEPARTMENT OF ELECTRICAL ENGINEERING
INDIAN INSTITUTE OF TECHNOLOGY ROORKEE
ROORKEE – 247 667 (INDIA)
FEBRUARY, 2016

Dedicated in the Lotus Feet of

Jai Mahakaleshwar, Ujjain

Jai Maa Maha Kali, Jahangira

Late Shri Maheshwar Prasad – Great Grandfather

Late. Dr. Chittranjan Prasad & Late. Smt. Shiela Prasad – Grand Parents

Dr. Arvind Kumar Sinha & Mrs. Neelam Sinha – Parents

Er. Piyush Prashar & Mrs. Shilpi Prashar – Bhaiya & Bhabhi

Kshitij Prashar – Nephew

Dedication would be incomplete without the following names:

Dr. Anil balaji Gonde – Guardian at IIT Roorkee

Dr. Subrahmanyam Murala – Friend, Brother at IIT Roorkee

Er. Ashish & Ar. Neetu – Brother & Bhabhi at IIT Roorkee

Akshaj & Atharva (Betti) – Stress Reliever

INDIAN INSTITUTE OF TECHNOLOGY ROORKEE
ROORKEE

CANDIDATE'S DECLARATION

I hereby certify that the work which is being presented in the thesis entitled **"DETECTION, IDENTIFICATION AND LOCATION OF FAULTS IN DISTRIBUTION SYSTEM"** in partial fulfilment of the requirements for the award of the degree of Doctor of Philosophy and submitted in the Department of Electrical Engineering of Indian Institute of Technology Roorkee is an authentic record of my own work carried out during a period from January 2009 to October 2014 under the supervision of Prof. R. P. Maheshwari**.**

The matter presented in the thesis has not been submitted by me for the award of any other degree of this or any other Institute.

(PRATUL ARVIND)

This is to certify that the above statement made by the candidate is correct to the best of my knowledge.

Date: 12th February 2016 **(R. P. MAHESHWARI)**

The Ph. D. Viva-Voce Examination of **Mr. Pratul Arvind**, Research Scholar, has been held on **12th February 2016.**

Chairman, SRC **Signature of External Examiner**

This is to certify that the student has made all the corrections in the thesis.

(R. P. MAHESHWARI) **Head of the Department**
Dated: 12th February 2016.

ABSTRACT

Electrical power distribution network is an integral part of electrical power systems since it is the last stage in the delivery of electricity to customers. Analogous to humans' circulatory system, if transmission system can be termed as the arteries of a human body, then the distribution system are the capillaries. The distribution network is responsible for distributing power to consumers at desired voltage levels with higher reliability. Alternating Current (AC) three-phase four-wire structure is the standard distribution system that exists throughout the world.

With the growth in urban population and development of industries, distribution grids now consider a considerable amount of power. The large number of lines in a distribution system experience regular faults which lead to high values of line currents. A fault which occurs on a distribution network is defined as an irregular condition of circuit that results in energy being dissipated in a manner other than the serving of the intended load.

As compared to transmission system lesser research works has been carried out for detection, identification, classification and location of faults in distribution system. The algorithms which have been developed for transmission system cannot be directly applied to distribution system because of certain constraints. Several techniques have been developed in order to get an errorless fault detection, identification and location. Traditionally, impedance based methods were developed but it suffered from the problem of multiple estimation. With the evolution of time, travelling based approaches also found its existences, but the measuring device required high sampling devices. With the introduction of artificial intelligence, there is a need for development of hybrid algorithm which not only detects, identify faults but also locate them accurately.

Feature extraction is the basic need for development of protection algorithms using digital signal processing tools. It transforms data of high dimension to a lower dimension. But at the same time, the embedded information content is kept intact. Also the dimensionality of data is reduced. Further, the complexity for the purpose classification or regression is decreased. This chapter presents a brief concept of the tools used for feature extraction. It covers a brief overview of the different signal processing tools involved in the development of algorithm. Wavelet Transform, Wavelet Packet Transform, Gabor Transform, M – Band Wavelet Transform and Complex Dual

Tree Wavelet transform have been dealt. Also, it presents a brief overview of Artificial Neural Network meant for the classification and regression.

The thesis gives an introduction of distribution system and the need for identification, classification and location of fault. Further, an extensive literature reviewed throughout this research work. During this the focus was on fault detection, identification and its location. Further, the detailed literature of signal processing tools used for feature extraction such as Wavelet Transform, Wavelet Packet Transform, Gabor Transform, M Band Wavelet Transform, Complex Dual Tree Wavelet Transform and the neural network employed for carrying out classification and location can be seen in next chapter.

In the next work wavelet transform and wavelet packet transform has been used in order to collect the features. It has been extensively used by power system engineers for fault detection and location. However, it should be kept in mind that only approximations of the signal are decomposed to next level. It fails to accurately capture high frequency information in signals. Hence, in order to capture more information content in a signal, Wavelet Packet Transform is used which is an expansion of classical wavelet decomposition. It represents high frequency information in a better manner as compared to wavelet transform. A comparative result of wavelet and wavelet packet transform over different "daubechies" family*"db1, db2, db4* and *db8*" has been presented. The result justifies the use of Wavelet Packet Transform which gives more accurate result than Wavelet Transform.
Further, another technique based on the use of Gabor Transform for collecting features is presented in the next chapter. In Gabor Transform, one obtains the coefficients through high pass filter only. It gives detail information which is required to trap the sudden changes in the fault signal. In the present work, a level decomposition is used for fault classification and four levels decomposition have been used for fault location. A comparison is presented between Gabor Transform and Wavelet Packet Transform. Results obtained are very promising for Gabor Transform.

In the subsequent work, M- Band Wavelet Transform has been used to extract the feature. M-band decomposition gives both logarithmic and linear frequency resolution. Further, its decomposition yields large number of sub bands which further helps more information about the signal. In M-Band transform for one level decomposition one obtains the one low pass filter decomposition and two high pass filter decomposition. A comparison is presented between Gabor Transform and M-

Band Wavelet Transform. Results obtained are very promising for both the databases in case of M-Band Wavelet Transform.

Another technique based on extraction of features of Dual Tree Complex Wavelet Transform is presented. The Dual-tree complex wavelet transform is used to overcome the two fundamental problems of wavelet transform as already discussed, while retaining the properties of nearly shift invariance and directionally selectivity. A comparison is presented between M- Band Wavelet Transform Dual Tree Complex Wavelet Transform. Results obtained for both the databases are very good that it proves that it is the best transform which give almost errorless result.
At, the end an alternative solution to the problems associated with interruptions by means of a statistical modeling of current sample database applied to determine the fault location in power distribution systems in order to reduce the system restoration time. The current samples collected from the sample distribution systems are subjected to FCM to obtain clusters and fed to expectation maximization algorithm

Eventually, the summary of work in the thesis is presented and also focuses on the scope for future work. An attempt has been made in the thesis to give an almost errorless fault location with the use of various digital signal processing tools and statistical based methods. It gives an edge over the conventional impedance based methods and also the problem of multi estimation has been successfully deal

ACKNOWLEDGEMENT

I express my deep gratitude to Dr. R. P. Maheshwari, Professor, Department of Electrical Engineering for his valuable guidance through my research work. His minute technical discussion, everlasting moral support, and faith on me has led to the completion of my thesis work. Apart from the above qualities, his immense concern during bad or good times of my Ph. D span is indeed memorable and appreciable.

I would like to extend my sincere thanks to Head of the department, Prof. S. P. Srivastava for providing me the facilities to carry out my research work. I am also thankful to previous Head of Departments, Prof. Vinod Kumar and Prof. Pramod Agarwal for constantly encouraging and supporting my research work. I extend my thank to the members of student research committee Prof. R. C. Mittal, and Prof. B. Das for their valuable suggestions and assistance during my tenure at I.I.T. Roorkee. I wish to thank Dr. R. Balasubramaniam, Dr. Ashish Pandey, Dr. Rajesh Chandra, Dr. Mahendra Singh, Dr. Barjeev Tyagi for constantly encouraging and motivating me for my research work.

I extend my thanks to office superintendent Mr. K.C. Tiwari, Mr. Mohan Singh, Mr. Mahaveer Prasad, Mr. Sushil, Mr. Amir Ahmad and other office staff who were always helpful during my work. I also wish to thank Instrumentation & Signal Processing lab supporting staff, Mr. Jogeshwar Prasad, Mr. Rajiv Gupta, Mr. Dinesh Kumar and Mr.Veer Chandji (*Veeru*) for all the necessary help provided by them. I would like to specially thank Mr. Vineet Goyal, D. O. S.W. office for supporting me and helping my stay comfortable at M. R. C. Hostel.

I extend my thanks to Prof. G. M. Dhole of S.S.G.M.C.E, Shegaon, Prof. S. B. L. Seksena, N. I.T. Jamshedpur and Prof. B. S. Sahay, B.I.T Mesra for motivating me for carry out my Ph. D program at IIT Roorke

I sincerely thank Dr. G. P. Govil, Director, Northern India Engineering College for granting me study leave at Ideal Institute of Technology, Ghaziabad and motivating and emotionally supporting me so that I can carry out my Ph. D Program as a guardian.

I owe a deep sense of respect for my Aunt Dr. Asha Sinha, and uncle Mr. A. B. Prasad and Neeraj. I extend my love to my dearest brother Arya Shamang and Hemang Pushkar and my sister Tanvi Verma for praying for my successful completion of Ph. D.

Further, I would like to thank my dearest friends Dr. Anil Balaji Gonde,, Dr. D. K. Rajoria, Dr. Subrahmanyam Murala, Dr. Jayendra Kumar, Dr. Nagshettappa Biradar, Dr. Roshan Kumar, Dr. Sachin Singh, Mr. Vandan Raj Alluri, Mrs. Rashmi Jain, Mrs. Katrina Kaif, Mr. Saurabh Srivastava, Mr. Neeraj Kumar, Mrs. Alka Sharma, and Ms. Monica Gupta "Monks" and my dearest Mr. Yusuf Ali for always standing with me by my side and supporting me during my good as well as bad period.

I owe a respect and thank specially to Ashish, Neetu, and cute kids Akshaj (Shammi), Atharva (Betti) for spending vital time with me and relieving my stress and especially to Ar. Neetu Mam for giving me food and making my stay comfortable despite her hectic schedule. I would also like to thank all the members of my family and friends whose name could not be included but motivated me and encouraged me to pursue my research work.

I sincerely thank my friend Dr. Umesh Kumar for morally supporting me and specially Supriya Vats (Watts) for correcting the typographical errors in thesis sincerely and wishing her successful life at abroad.

This acknowledgement would be incomplete if I do not thank my great grandparent Late. Shri Maheshwar Prasad who was an academically excellent member of the family, my grandparents Late. Dr. Chittranjan Prasad, Late Smt. Shiela Prasad for constantly showering blessing upon me. My parents Dr. Arvind Kumar Sinha, Mrs. Neelam Sinha, my brother Er. Piyush Prashar who bestowed their love and confidence on me and always boosted my confidence and kept a check on my day to day activity. I also like to thank sister – in -law Shilpi Prashar and my sweetest cutest nephew Kshitij Prashar (KP). I would also like to thank my dearest uncle Late. Ratan Kishore Verma who was could not be in this world to see my defense.

At the end, I bow my head in front of almighty, especially Mahakaleshwar Bhole Nath, Ujjain and Maa Maha Kali of my home town village Jahangira, Sultanganj, Bhagalpur for blessing me so that I can complete my Ph. D program.

(PRATUL ARVIND)

TABLE OF CONTENTS

LIST OF FIGURES

LIST OF TABLES

LIST OF ABBREVIATION

SD 1	Sample Distribution System 1
SD 2	Sample Distribution System 2
ANN	Artificial Neural Network
WT	Wavelet Transform
WPT	Wavelet Packet Transform
DWT	Discrete Wavelet Transform
CWT	Continuous Wavelet Transform
ANN	Artificial Neural Network
GT	Gabor Transform
MBWT	M – Band Wavelet Transform
DTCWT	Dual Tree Complex Wavelet Transform
MLP	Multi-Layer Perceptron

LIST OF SYMBOLS

TC_{err} :	Total Classification Error (%)
N_{ms} :	Number Of Misclassified Sample
N_S :	Total Number Of Samples
L_{err} :	Location Error
D_O :	Output Distance Calculated
D_A :	Actual Distance
CWT	Continuous Wavelet Transform
(c)	Scale Factor
(d)	Translation Factor
$s\ (t)$	Given Signal
$p(t)$	Mother Wavelet
q	Integer Variable
o(v)	Discrete Time Sequence
R	Length Of Discrete Time Sequence
O(ω)	Orthogonal Sub Band
T	Sampling Period
I	Total Number Of Resolution Levels
g	High Pass Discrete Filters
h.	Low Pass Discrete Filters
$u_I(q)$	Scaling Coefficients
$y_l(v)$	Wavelet Coefficients,
$y_l(q)$	Difference Level
o(q).	Discrete Wavelet Transform Representation of Faulted Signal
P(x)	Sequence Function of Wavelet Packet Transformation
j	Scale Factor of Wavelet Packet Transformation
q	Time Factor
r	Oscillating Factor
$P_0(s)$	Scaling Function

$P_1(s)$	Wavelet Function
w_q	Conjugate Mirror Filter
e_q	Conjugate Mirror Filter
p (t)	Wavelet Energy of Coefficients
s_i	Probability Distribution of the Energy Contained in the Wavelet Coefficients
$p(t)$	Window Function
$\lambda:$	Window Width
$\chi:$	Phase Constant of the Changing Oscillations
$f_0:$	Frequency of the Oscillations
$t_0:$	Window Function Centre
$\Delta(t):$	Resolution of Time
$\lvert p(t)\rvert^2:$	Distribution of Energy
$\Delta(f)$	Resolution of Frequency
$\sigma(t).$	Unit Impulse Function
$o(t)$	Unit Step Function
n	Temporal Sampling Indices
k	Frequency Sampling Indices
"N"	Shift Parameter
$p(t)$	Gaussian Window Function in Gabor Transform
a_{mr}	Basis Function in Gabor Transform
d	Positive Integer in Gabor Transform
b_{nk}	Coefficient in One Dimensional Gabor Transform
$P^2(N)$	Square Integrable Functions in M Band Transform
D	Set Of Integers in M Band Transform
$\xi_a(s):$	Wavelet Function in M Band Transform
g_0	The Scaling Filters in M Band Transform
F	Scaling Filters Of Length in M Band Transform
C	Regularity Of Scaling Function in M Band Transform
V_b	Spaces Spanned By The Scaling in M Band Transform

W_b	Spaces Spanned By Wavelet Functions in M Band Transform
$h_0(n)$	Low-Pass for the Upper Filter Bank
$h_1(n)$	High-Pass for the Upper Filter Bank
$b_0(m)$	Low-Pass for the Lower Filter Bank
$b_1(m)$	High-Pass Filter for the Lower Filter Bank
$\phi_a(t), \phi_b(t)$	Real Wavelet Transforms
P_a	Square Matrix of DTCWT
P_b	Square Matrix of DTCWT
n_a	Real Part of the DTCWT
n_b	Imaginary Part of the DTCWT
s	Real Signal
Pf	Performance Function
mse	Mean Sum of Squares of Errors.
t", "a"	Vector of the Input Model
msereg	Mean of the Sum of the Squares of the Network Weights and Biases
Υ	Performance Ratio
U_{ij}	Membership
C_i	Cluster
D	Distance Between the Cluster Center and Data Point
μ	Mean Vector
V	Covariance Matrix
p	Weight/ Coefficient Of Mixture
$\hat{\tau}_{ij}$	Posterior Probability
ϕ	Normal Multivariate Density
$f(x_j)$	Estimated Mixture of Distributions
d	Dimensions

Introduction

Chapter 1

1.1 ELECTRICAL POWER DISTRIBUTION NETWORK

Electrical power distribution network [1] is an integral part of electrical power systems since it is the last stage in the delivery of electricity to customers. Analogous to humans' circulatory system, if transmission system can be termed as the arteries of a human body, then the distribution system are the capillaries. Figure 1.1 represents an electrical distribution system.

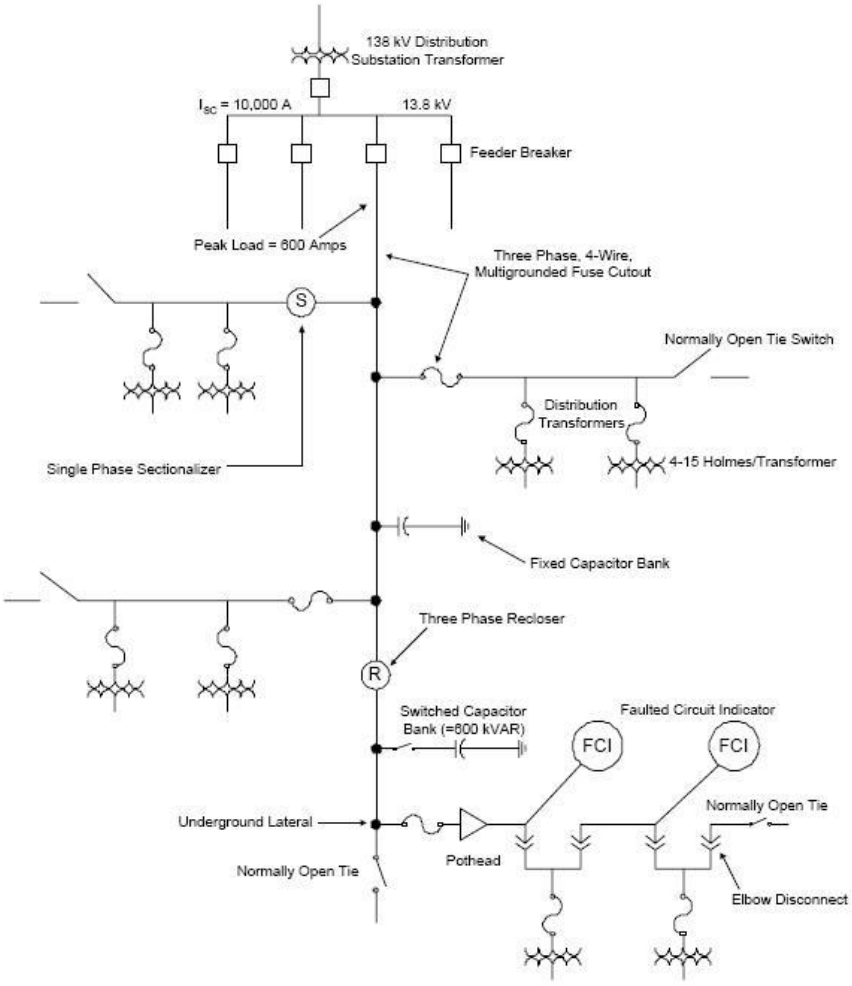

Figure 1.1: An Electrical Distribution System

Electrical power is normally generated at 11 – 25 kV in power stations. It is stepped up at sending end substations to HV/ UHV/ EHV levels for transmission over long distances. These lines run into hundreds of kilometers and deliver the power into a receiving end substation. Here, the voltage is being stepped down to values i.e. 66 kV or 33 kV or 11 kV. The secondary transmission system transfers power from these receiving end substations to secondary substation. Further, the voltage is stepped down to 11 kV/ 6.6 kV/ 3.3 kV at secondary substation. The segment of the power network that lies between a secondary substation and consumers' installation is known as the distribution system. The distribution network is responsible for distributing power to consumers at desired voltage levels with higher reliability. Alternating Current (AC) three-phase four-wire structure is the standard distribution system that exists throughout the world.

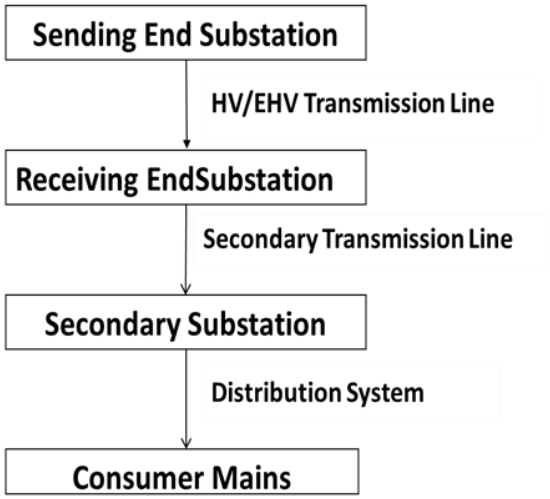

Figure 1.2: Block Diagram Representation of the Distribution System.

1.1.1 Categorization of Distribution System

Distribution System [2] has two components: (i) Feeder (ii) Distributor. A Feeder in a distribution network is a circuit carrying power from a main substation to a secondary substation such that current loading is same all along its length. The main criterion for the design of feeder is the current carrying capacity (thermal limits rather than voltage drops). A Distributor on the other hand, has variable loading along its length due to the service conditions, tapping off at intervals by individual consumers. The voltage variations at the consumer's terminals, as per electricity acts [3], must be maintained within $\pm$ 5%. Thus, the main criterion for the design of a distributor is to limit on percentage of voltage variations. The distribution system can be categorized into primary

and secondary distribution systems. The primary distribution system consists of main feeder and laterals. The main feeder acts as main source of supply to sub-feeders, laterals or direct connected distribution transformer.

Based on the topology of the feeding system, it is further categorized into radial feeder, parallel feeder, loop feeder and primary network. Figure 1.3 gives the block diagram of type of distribution system.

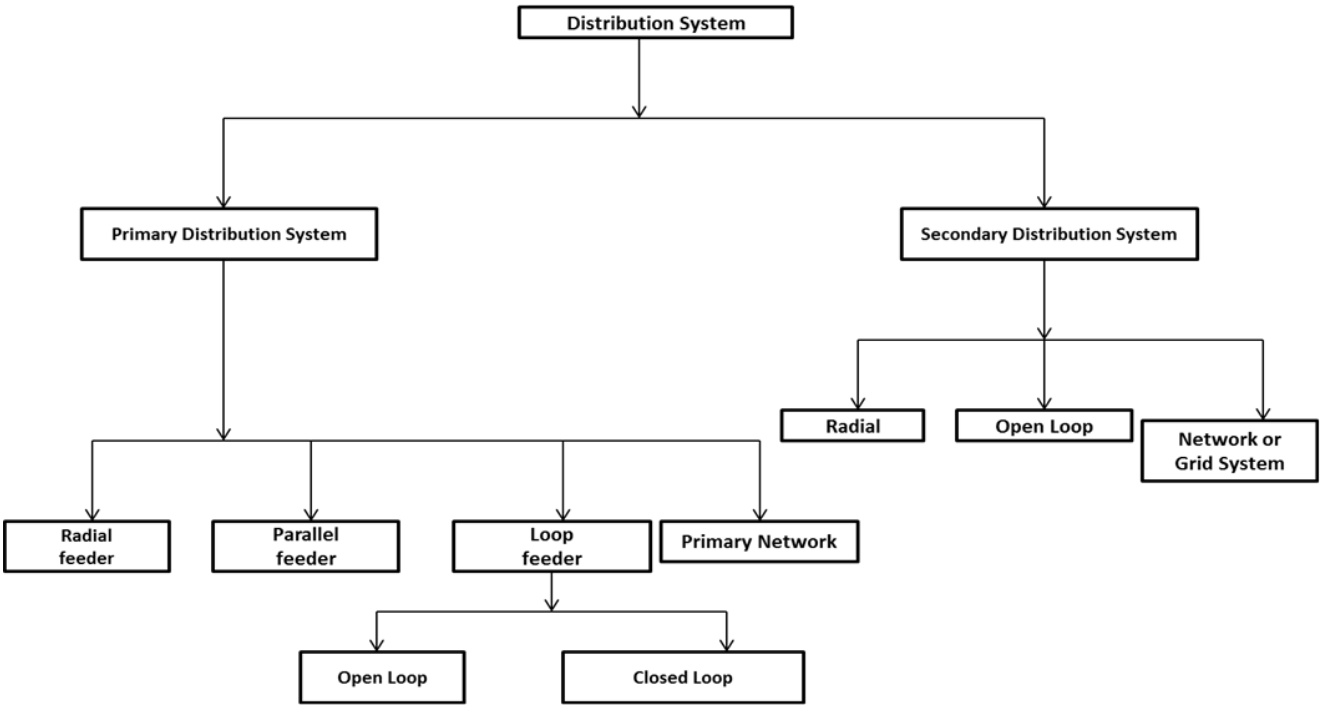

Figure 1.3: Types of Distribution System

1.1.2 Radial Feeder

A radial feeder is the simplest and the most commonly used as seen in figure 1.4. It is used extensively to supply small and medium residential, commercial, industrial loads. It is a feeder which radiates from the secondary substation. Further, it branches into sub feeders and laterals that is available for the areas where power needs to be delivered. The feeders and sub – feeders are three – phase three – wire (or four wire circuits). The laterals may be of three – phase or single phase. They are most economical, but least reliable since a fault in a feeder means disruption of supply towards the faulty section.

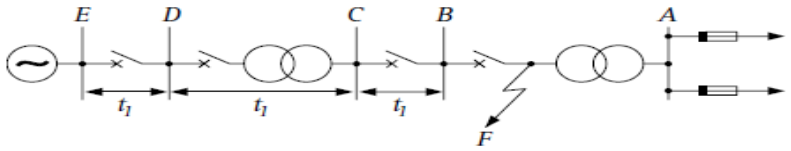

Figure 1.4: Radial Distribution System.

1.1.3 Parallel feeder

Parallel feeder consists of two radial feeders running in parallel which may originate from the same or different secondary substation as seen in figure 1.5. Each feeder supplies about half of the total load of that area but has the capability to supply the entire load in the event of an outage of other feeder. They are costlier than radial feeders, but substantially reduce the frequency and duration of outage.

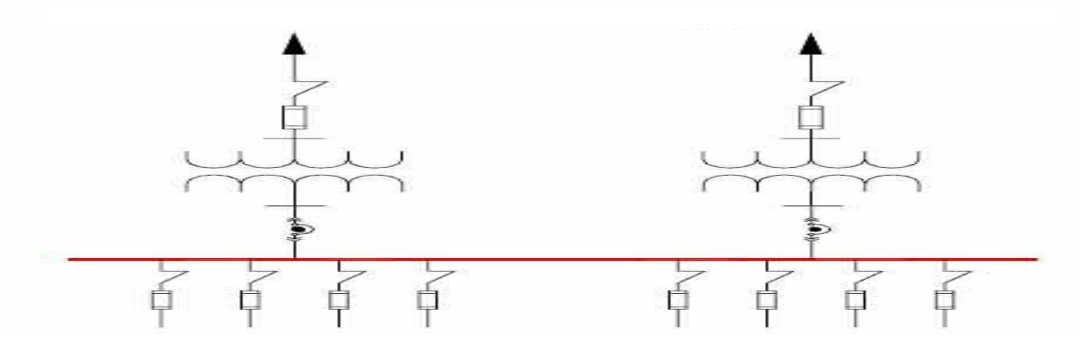

Figure 1.5: Parallel Feeder.

1.1.4 Loop Feeder

It may be defined as the system that contains two or more radial feeders which originates from the same or different secondary substations and are separately routed through the load areas. It is further classified into open loop system if the ends of the two feeders are tied together through normally open switches and ring feeder if the ends are tied together through normally closed switches.

1.1.5 Primary Distribution System

Primary Distribution System consists of number of interconnected feeders. Two or more sub transmission circuits supply two or more secondary substations from which the feeders take off. In urban areas the length of 11 kV feeders is generally up to 3 km whereas in rural areas, it extends up

to 20 -30 km. This system provides good flexibility and reliability and preferred for large distribution areas for large loads which have to be supplied with greater reliability with all other advantages of grid (interconnected) system. The system gives better voltage regulation.

1.1.6. Secondary Distribution System

Secondary Distribution System consists of 3 phase four wire 400 V distributors laid along the road side. The service connections to consumers are tapped off the distributors at convenient points in the form of single phase two wire circuits or three phase four wire circuits. It is used in the form of radial, open loop and network configuration. A radial distributor takes off from the distribution transformer and runs through the area to be served by it. An open loop system consists of two distributors taking off from the same distribution transformer and running in different directions and supplying different areas with far ends tied together by normal open switching device. If two or more distribution transformers feed the distribution network and operate continually in parallel, then this type of system is known as network or grid system. It consists of a number of interconnected distributors.

1.2 MOTIVATION

With the growth in urban population and development of industries, distribution grids now consider a considerable amount of power. The large number of lines in a distribution system experience regular faults which lead to high values of line currents. A fault [4] which occurs on a distribution network is defined as an irregular condition of circuit that results in energy being dissipated in a manner other than the serving of the intended load. Depending upon its nature, it may either be temporary or permanent. A permanent fault is a condition in which permanent damage is done to the system. It comprise of failures of insulator, broken wires etc. It usually causes continuous interruptions. In order to get rid of the fault, a fuse, re-closer or circuit breaker must operate to disrupt the circuit. In case of a temporary fault, the circuit is interrupted and then reclosed after a delay; thereby making the system operate normally. It accounts to 50 to 90% of faults on overhead distribution network. Lightning, slapping of conductors in the wind, tree branches that fall across conductors and then fall or burn off, animals that cause faults and fall off, and insulator flashovers caused by pollution are some examples of temporary fault. If the fault persists for a longer duration temporary faults can turn into permanent faults. The fault can do permanent damage to conductors, insulators, or other hardware associated with the distribution

system. In order to give uninterrupted supply to the consumer, faults occurring in the distribution system needs to be identified and located accurately. Also, for proper operation of protective relays, correct determination of fault type is a prerequisite in digital protection schemes. Fault detection, identification and location on distribution system have become a prominent issue.

As compared to transmission system lesser research works has been carried out for detection, identification, classification and location of faults in distribution system. The algorithms which have been developed for transmission system cannot be directly applied to distribution system [5] because of certain constraints. Several techniques have been developed in order to get an errorless fault detection, identification and location. Traditionally, impedance based methods were developed but they suffered from the problem of multiple estimation. With the evolution of time, travelling based approaches also found its existences, but the measuring device required high sampling devices. With the introduction of artificial intelligence, there is a need for the development of a hybrid algorithm which not only detects, identifies faults but also locates them accurately.

1.3 SAMPLE DISTRIBUTION SYSTEM

In the present work, two standard distribution systems were considered to evaluate the algorithms developed for the purpose of identification, classification and location of fault. Recent literature survey suggests that Saskan Power distribution model has been used as a standard model to evaluate the accuracy in many of the relevant recent work. Additionally, IEEE 13 – node feeder is also tested in order to establish the effectiveness of the algorithm.

1.3.1 Saskan Power Distribution Network

SaskPower Canada is a 25 kV distribution system proposed in [6] has been used in order to create the current and voltage sample database. It is considered as the sample distribution system 1 (SD 1). The single line diagram of SaskPower in Saskatchewan (Canada) is shown in fig. 1.6. The line between nodes 1 and 11 is 37 km long and consists of sections of different length that are made up of different conductors. Single or three phase loads (values shown in kVA) are tapped at all nodes except for nodes 3, 4, 5, 7, 10, 11 and 17. A detailed description of the system is presented in Appendix A.

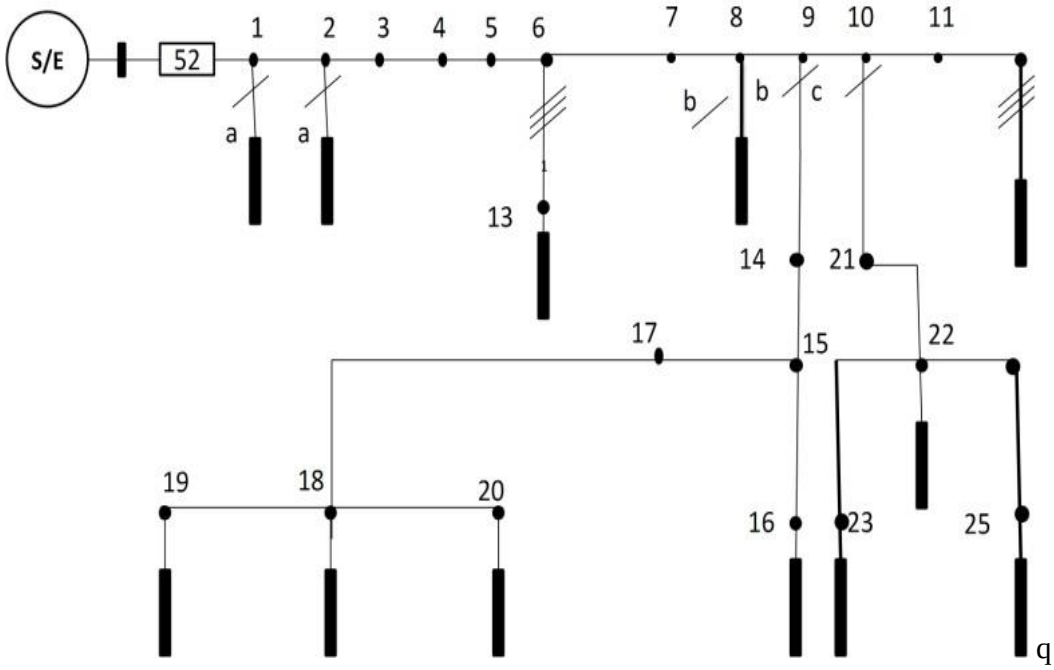

Figure.1. 6: SaskPower in Saskatchewan (Canada)

Keeping in view the multiple estimation problems, sample distribution system has been categorized into different zones as presented below in Table. 1.1.

Table 1.1: Zone-wise Categorization of Sample Distribution 1 (SD 1)

S. No	Zone	Nodes
1	Zone 1	1 - 4
2	Zone 2	5, 6 & 13
3	Zone 3	7 - 12
4	Zone 4	14, 15 & 16
5	Zone 5	17 - 20
6	Zone 6	21 - 23
7	Zone 7	24 - 25

1.3.2 IEEE 13 – Node Feeder

IEEE 13 node feeder [7] has been created as a common set of data which could be used by researchers and users to verify the accuracy of their solutions. It is considered as the sample distribution system 2 (SD 2). Fig. 1.7 gives single line diagram of IEEE 13 node system. Some of

the characteristics are as follows:

(a) It is short and relatively highly loaded for a 4.16 kV feeder

(b) It consists of one substation voltage regulator that comprises of three single-phase units having wye connection.

(c) It has overhead and underground lines with variety of phasing.

(d) It consists of shunt capacitor banks.

(e) It has In-line transformer.

(f) It also has unbalanced spot and distributed loads.

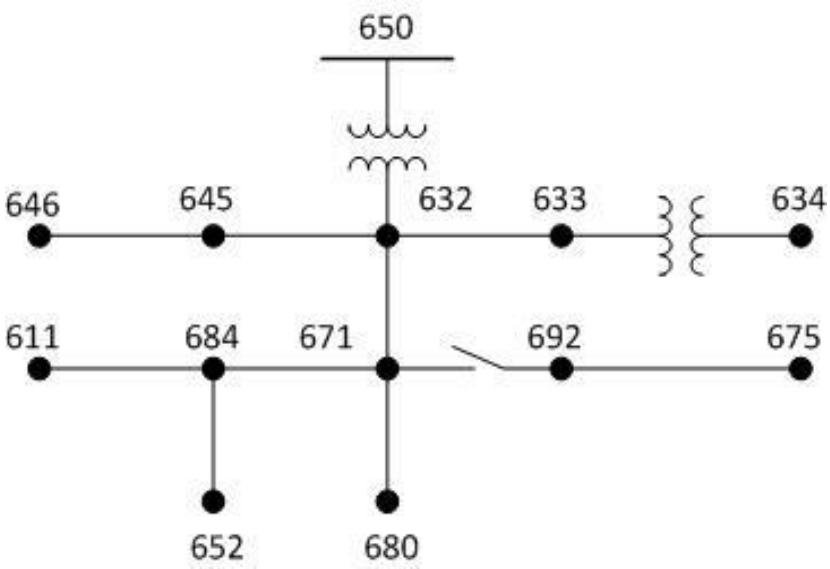

Figure1.7: IEEE 13 node feeder

A detailed description of the model is presented in Appendix B. As mentioned above, it has also been categorized into different zones as seen in Table 1.2.

Table 1.2: Zone-wise Categorization of Sample Distribution 2 (SD 2)

S. No	Zone	Nodes
1	Zone 1	632 – 633, 633 - 634
2	Zone 2	632 – 645, 645 - 646
3	Zone 3	650 – 632, 632 – 671, 671 - 680
4	Zone 4	671 – 684, 684 – 652, 684 – 611

These systems were simulated in PSCAD (Power System Computer Aided Design) [8]. Extensive simulations were carried out to collect current and voltage samples over different range of fault resistance and fault inception angle for all the ten types of faults. Ten types of faults comprises of single – line to ground fault, double – line to ground faults, phase to phase faults and triple phase to ground fault respectively.

1.4 EVALUATION MEASURES

The effectiveness of the algorithm meant for identifying, classifying and locating faults system have been evaluated by the use of following performance parameter:

1.4.1 Classification of Faults

The results of the faults classified are calculated by the following equation:

$$TC_{err}(\%) = \left| \frac{N_{ms}}{N_S} \right| \times 100 \tag{1.1}$$

TC_{err} : Total Classification Error (%)

N_{ms} : Number of misclassified sample

N_S : Total number of samples

1.4.2 Location of Faults

The result is expressed in terms of error for location. Error in percentage is expressed by the following equation:

$$L_{err}(\%) = \left| \frac{D_O - D_A}{D_A} \right| \times 100 \tag{1.2}$$

Where,

L_{err} : Location error

D_O : Output Distance Calculated

D_A : Actual Distance

1.5 OUTLINE AND CONTRIBUTIONS OF THESIS

Present chapter gives an introduction of distribution system and the need for identification, classification and location of fault. Chapter 2 presents an extensive literature reviewed throughout this research work. During this the focus was on fault detection, identification and its location. Chapter 3 gives the detailed literature of signal processing tools used for feature extraction such as Wavelet Transform, Wavelet Packet Transform, Gabor Transform, M Band Wavelet Transform, Complex Dual Tree Wavelet Transform and the neural network employed for carrying out classification and location. Chapter 4 focuses on the algorithm developed by extracting the features of Wavelet and Wavelet Packet Transform. Chapter 5 shows the intricacies to improve result by using the features of Gabor Transform. Further, the accuracy was improved using M Band Wavelet Transform is presented in chapter 6. Chapter 7 gives the use of Complex Dual Tree Wavelet Transform to increase the accuracy and the results obtained are very promising. Fuzzy C-Means (FCM) and Statistical based approach is used for locating faults in chapter 8. Finally, in chapter 9 conclusions from this research work are derived and further directions for future work are also suggested. Later, Appendix – A gives the details for designing the model of Saskan power and Appendix – B gives the detail parameters for modeling IEEE 13 node feeder.

Literature Survey

Chapter 2

During the past five decades, there has been a rapid growth in electric power systems. Due to which, there has been an increase in length of the line and its operation. Now, faults occur frequently on these lines. They may be due to the occurrence of storms, thunderstorm and lightning, snowfall, chilling rain, breakdown of insulators, and short circuit faults caused by animals, birds and other external sources. It has been observed that these faults results in mechanical damage of the system. It should be attend in priority in order to restore the service. If one detects, identifies the type of faults and its location then the restoration process can be fast. There exists a dire need for speedy identification and location of fault which helps in fast service restoration. It also reduces the outage time. This may increase the reliability of the system. This chapter makes an attempt to present the literature review of the works carried out for identification, classification and location of fault. The review extends itself from the traditional approaches to the recent developments in the field of development of algorithm for the above purpose.

2.1 IDENTIFICATION AND CLASSIFICATION OF FAULTS

Fault identification [9] based on data acquisition, data preprocessing, transient identification, participant phase identification, participant phase detection; participant phase classification is suggested in the literature reviewed. The author in [10] utilizes the concept of characteristics vector which is proposed to symbolize the different faults based on pre-fault characteristics vector data base. Classification is done by matching a fault current with one of the vectors in database. This vector is formed by taking into consideration fault current values at all relay locations. A comparative survey of fault section estimation has been made in [11]. It suggests that upon occurrence of fault, the improvement of speed and accuracy in fault identification, classification and location can be seen using hybrid based technique. The author in [12] proposed a fuzzy logic

based algorithm with three line currents at the substation. Author has claimed to identify the fault in less than one cycle period with significant variation of fault resistance. The effectiveness of the algorithm was tested on IEEE 13 and 34 node feeders. The classification is based on angular difference among the sequence components of the fundamental current and their relative magnitude. As the accuracy is dependent on threshold selection hence selection of proper threshold is a tricky affair. Fault [13] has also been identified based on analytical approach. Protection devices have been used to acquire the data from data acquisition system and the fault distance has been estimated for open and short circuit faults in a distribution network. Logistic regression and neural network as fault classifier has been used in [14]. The problem associated with the dichotomous dependent variable is analyzed using a parametric model i.e. logistic regression. It is used since artificial neural network ANN fails to determine. It is due to the lack of existence of any principle to determine the number of neurons in the hidden layer of ANN. Classifiers based on logistic regression and ANN [15] with a data collected over a span of 08 year have been tested. Although ANN performs better, but suffers due to insufficient data for various categories of faults. Knowledge based fault detection and identification for power system faults has been introduced in [16] making the use of granular computing after signal decomposition The proposed method uses the supervised clustering based neural network for fault diagnosis method. Several other techniques such as clustering algorithm for detection and classification [17], rule based approach [18] by comparing the sharp variations of detail signals in different phases are also proposed. Identifying a section affected with undetected open circuit fault using three phase voltage and by decoupling into three independent systems [19] is also used. Genetic algorithm [20] has been used to optimize the fault identification. With the introduction of wavelet transform, features have been extracted from utilizing the concept of initial travelling wave. The features of initial travelling wave from post fault signals [21] have been utilized to identify the fault. The concept of grounding system has been discussed in [22]. It also focuses on its advantages and disadvantages. An attempt to identify single phase to ground faults in a non – effectively grounded system can be observed in [23] – [28]. Attempt has been made to utilize the features extracted by the use of wavelet transform and correct determination is made. Wavelet entropy energy [29] is fed to ANN for classification is used in many cases. It should also be kept in mind that accurate fault identification and classification is the first step in for evaluating the fault location. Wavelets, Wavelet Packet Transforms are used as a tool so as to collect the features of voltage and current samples in order to develop the algorithm for the above said purpose.

2.2 LOCATION OF FAULTS

Maximum number of interruptions about (80%) is due to the occurrence of faults in distribution networks. It is indeed a tedious task to employ the algorithms developed for transmission system [30] on distribution system due to its topology and different operating principles.

2.2.1 Topology of Distribution System

The characteristics of distribution system play a pivotal role in the development of algorithm for location of faults in distribution system. These are summarized below:

(a) The feeders are heterogeneous in nature. Since, they have a variety of size. It also has different length of cables. Overhead and underground lines are also present.
(b) Unbalances occur in distribution network due to the existence of untransposed lines. Variety of loads i.e. single, double and three phase loads too makes it unbalanced.
(c) Laterals can also be found along the main feeder.
(d) Tapped loads can be found along the main feeder and laterals.

The above features are responsible for introducing errors in the estimating the fault locations in a distribution network [31]. Also, it leads to the problem of multi – estimation. This in turn creates problem for the team responsible for maintenance of the power network. It should be also kept in mind that the network is usually spread out and has a complex configuration. Due to which the location and thus restoration of the service is an uphill task. Usually, the distribution network is the lumped-parameter model [32] and thus basically algorithms based on calculation of phasors have been developed. These algorithms employ symmetrical components of the current and voltage readings. Short circuits faults usually occur in distribution system. They are basically single line-to-ground fault, line-to line fault, double line-to ground fault, three phase and three phase-to-ground faults. Basically the fault resistance involved during these faults lies between 0.05 Ω and 50 Ω.

2.3 CATEGORIZATION OF FAULT LOCATION METHODS

Some of the techniques proposed for fault location in distribution system are summarized below. Based on the analysis, these methods can further be grouped into three categories, which are as follows:

i. Calculation of Impedance and Fundamental Frequency Component
ii. Travelling Wave and High frequency components
iii. Acquiring of Knowledge

Further, Knowledge-based method may be categorized into these groups: Artificial intelligence and statistical analysis based methods, Distributed device based methods and Hybrid methods.

Traditionally, in the occurrence of outage, customers used to call for restoration of the power supply. But, the restoration was dependent on the geographic location from where the call has been made. Hence, the connectivity of area with the distribution network had to be considered in order to find out the accurate location of occurrence of fault. Sometimes the fault remains unattended due to the precise location of the network. Also, during night hours it was difficult for the engineers to restore the power. With the advancement of time, techniques have been developed for the locating faults for radial distribution system. The algorithm developed was based on an iterative approach which was evaluated by updating the fault current.

2.3.1 Calculation of Impedance and Fundamental Frequency Component

The fault distance from the primary distribution bus to the location of fault is evaluated by methods based on calculation of impedance. These methods employ the measurement of voltage and current values at one end or both ends of the line. This method [33] develops mathematical equations to estimate location of the fault. These methods are basically meant for radial distribution system. On the other hand, these methods also require information such as the circuit breaker status, waveforms of fault current, and status of fault indicators for non-radial system. During this process, first the type of the fault and faulty phases are identified. Henceforth, by the use of selected voltage and selected current, the apparent impedance is calculated. Due to non-consideration of load currents at different taps, these algorithms suffer with estimation errors.

Girgis in [34] presented equations to compute all kinds of short circuit faults that occur at the main feeder and also at single-phase lateral. Here, loads were assumed as constant impedance loads. The dynamic nature of the loads was not taken into account. The technique was not able to perform where cables were involved. Saha et al. [35], proposed a method for locating faults on radial medium voltage (MV) system. It included several intermediate load taps. Even, the non – homogeneity of the feeder was considered. A MV distribution networks was used for the testing the effectiveness of the algorithm. It should be kept in mind that the system was assumed to be balanced. The author in [36], developed equations in order to estimate fault distance for all types of faults that occurred at the main feeder and single-phase lateral. Another method proposed to be used for address the issue emerging from fault résistance. The author in [37] proposed a technique which used the fundamental frequency component of the voltages and currents that was measured at a line terminal before and during the fault. The fault location technique was meant only for single-phase-to-ground fault on a radial system. Also, the lines were considered to be fully transposed. However, the proposed algorithm gave results with reasonable accuracy but it was only meant for line-to-ground faults. Quadratic equation formed the direct circuit analysis for locating faults was developed in [38]. It was implicated that all load impedance present in the network was considered. Intelligent Electronics Devices (IEDs) with built-in oscillography function installed at the substation was employed by some methods to furnish information about fault location. The database stored information about the network topology and its electrical parameters. This method was not effective for 11kV networks, since it was difficult to establish reliable statistical estimates. Also, they were time consuming because of the iterative procedure. Prior knowledge of the fault type was must before specific equation could be developed. A fault location algorithm, using synchronized or unsynchronized pre-fault and fault voltage and current measurements from both ends of the line without taking into account the line parameters is presented in [39]. This method was applied to power line parameter estimation. It was dependent on synchronized phasor measurements. Different system operating conditions from which the parameters needs to be estimated was also required. The main lacuna of impedance-based methods is the multi-estimation. It is due to the existence of multiple fault points at the same distance. It also depends upon the power system model. Hence, it can be concluded that these methods gives an accurate fault locations but are doubtful.

2.3.2 Travelling Wave and High Frequency Components

This method uses the concept of the reflection and transmission of the fault generated travelling waves on the faulted power network. Faults can be located with a high accuracy. But the execution of this method is very complicated. On the financial aspect this method is very expensive when compared with impedance based techniques. This is due to the fact that it needs several equipments, such as the GPS system, fault transient detectors and diagnostic software. Keeping in mind the complex configurations of distribution systems, the fault transient detectors installation is also a hectic task. The cross –correlation function between the incident wave and the reflected wave was used in [40] to locate faults in distribution systems. In the development of algorithm the single-ended method and the double-ended method was used. The single-ended method failed to fetch good result. Also, the double-ended method was unable to provide a precise result. The result was obtained only if the fault occurred at the line, when the fault recorders were installed, and fault occurred at the line or at the main feeder. Another disadvantage of these methods is that it requires measuring devices with a very high sampling rate (MHz). The author could not fetch solution for multiple faults occurring in the system at the same time.

The author in [41], developed a new fault locator unit to locate faults which distinguished the reflected wave from the fault point and that from the remote bus bar. It captured high frequency voltage signals between 1 and 10 MHz. Accurate location of fault was a problem due to the presence of tapped-off loads. The proposed method was unable to give solution for locating faults due to existence of loads. The author in [42] suggested a technique where the difference between the device's terminal voltages magnitude was considered. It is required to install some equipment into the distribution feeders. It was possible by only using the terminal measurements. Another method based on the high frequency signals measured at the substation was established in [43]. The discrete wavelet transform (DWT) was used in this method. It is because it can be implemented easily due to its reduced computational time. A correlation analysis between transmitted and reflected waveform was required for the purpose. In order to implement this method, extensive simulation was to be carried out for each branches and sub – branches of distribution system. The wavelet coefficients of different fault laterals were then calculated which were able to identify the faulted lateral. It was indeed difficult for the utilities to implement this method separately for every distribution feeder. Also, separate modeling for each specific feeder was required. Borgheti et al. [30], proposed a method on the use of continuous-wavelet transform (CWT). The voltage transient which was due to line faults was analyzed. Here, also the concept of

correlation that exists between the specified frequencies of the continuous-wavelet transformed signals and exact paths in the network was covered by the concept of travelling waves that was due to the fault. The method was not appropriate for frequencies lower than 200 Hz. The specified path for frequencies less than 200 Hz covered by the travelling waves did not yield proper result. This proved that the estimated fault location was inappropriate. The system considered for implemented was balanced and accuracy was unsatisfactory. It can be concluded that the most vital drawback of travelling wave and high frequency components methods are that they require measuring devices with a very high sampling rate (MHz).

2.3.3 Acquiring of Knowledge

The next category is methods which have been evolved by acquiring the knowledge. These methods can further be sub divided into three groups:

1. Artificial intelligence and statistical analysis
2. Distributed device based methods.
3. Hybrid based methods.

2.3.3.1 Artificial Intelligence (AI) and Statistical Analysis Based Methods:

With the development of technology, various artificial intelligent methods evolved. Artificial neural network, fuzzy logic, expert system and genetic algorithm are few examples of artificial intelligence. These reduce the laborious work of the engineers or researchers. Also, they reduce the time taken to attend the fault and the mistakes made by human being are drastically reduced. This has inclined the researchers to develop algorithms based on artificial intelligence for locating faults in distribution system. The author in [45] – [46] has used multi-way graph partitioning method. This method employs the concept of weighted minimum degree reordering. Using this, it divides a large -scale power network into several sub-networks. It can be used online since the speed at which the fault section is estimated is fast. The technique for fault location using neural network for multi-ring distribution systems can be seen in [47]. Several conditions linked with network such as faulted feeder voltage, the status of circuit breaker, real power of feeders during the normal condition, and real power of feeders during short circuit condition was taken into account to train the neural network. Wen in [48] gave a concept that constructed a probabilistic causality matrix that established the probabilistic relationship between faulted sections and the action of protective

device for these sections. The faulted section was estimated by the author using parsimonious set covering theory and it was treated as problem of integer-programming. Further, a refined genetic algorithm was used to resolve the problem. The genetic algorithm was based on the concept of "natural selection, best survival" theory. It evaluated the most reasonable hypothesis on the result obtained for each hypothesis using set covering theory. Thukaram et al. [49], proposed a method based on state estimation of the magnitude of the voltage and phase angle at all load buses. A threshold was calculated which detected the faulty path. The author in [50], utilized a cause-effect network that represented the causality between faults and the actions of protective devices. It had a high-speed inference and was easy to implement. These qualities made it effective to be used for on-line detection of the faulted section. Also, the knowledge given by the operation of protective devices, rapidly located the faulted section. Further, Mora et al [51] presented a solution for the problem of power service continuity arising due to fault location. Statistical based method which utilizes the finite mixtures was used. A statistical model was developed. This utilized the extraction of the magnitude of the voltage sag that was recorded during the fault along with the parameters of the network and its topology. A fault database was created where sag magnitude of the measurements of the voltage was stored and statistical model was developed. The groups were determined using the well-defined characteristics of the sag and gave an optimal classification result. It also ensured good accuracy. Another advantage of this method was it was financially viable since it had low cost of implementation. The author in [52] proposed an algorithm that was based on the utilization of the eigen value and learning based method using an artificial neural network. The neural network was trained in a manner that mapped the non-linear relationship between fault location and characteristic eigenvalue. Some of the highlights of these methods were that it reduced the number of input signals without the use of voltage detectors. This method was successful in detecting and identifying the faulted line Also, it was able to recognize the different type of faults and correct identification of different types of fault. Also, it fetched accuracy in fault location. Furthermore, it was independent from the effect of harmonics. The results obtained after simulation proved the effectiveness of the method for locating faults in distribution system. The author in [53] has developed a method for locating faults meant for parallel double-circuit distribution lines. This method was based on calculations of impedance and analysis of travelling-wave. The line currents were transformed into current components using the Clarke-Concordia transformation. After obtaining the current components, correlation matrix was constructed based on the sample data. The eigenvalue calculated for the current components had a non -linear

relationship with the distance of fault. Further, neural network was used to determine the relationship between eigenvalue and fault distance. Hence, the distance was calculated.

The author in [146] has presented a technique for fault diagnosis based on Fuzzy C-means (FCM) algorithm of the optimal number of clusters and probabilistic neural network. FCM is being widely used in pattern recognition and machine learning. An attempt has been made to detect the occurring fault in the system. Karwan in [147] has drawn a conclusion that clustering has found a wide application in classification of fault. In this regard, FCM has emerged as a suitable tool for classification. Further, the author in [148] has presented the diagnosis algorithm using FCM which has not only increased classification accuracy but have also reduced the computational load. Based on the above literature, an attempt has been made to use FCM for classification of faults.

2.3.3.2 Distribution Device Based Methods

Second type of technique for fault location that is based on acquiring of knowledge is distributed device based methods. Fault location on the concept of mathematical approach is defined in [54]. The approach needs the information about the voltage sensors installed in the network and its topological structure. Matrix representation is given for the relation of the voltage sensors with sections of the network. Second matrix was constructed keeping in mind the topological relation between sections and nodes of the distribution network. Faulted sections are calculated through some matrix operations. Mokhlis in [55] introduced a method for fault location by single measurement at the considered bus of the electrical network. A database was prepared in which the voltage magnitude and phase angle obtained from simulation of the network considered after fault analysis was created. Now, the actual magnitude of voltage and its phase angle was matched. This proposed technique had mainly two advantages that it was simple and easy to implement. Also, if there were any variations in the load or network configuration, then the database can be updated with new result. The effect of fault resistance was not incorporated. The author in [56]; proposed a technique by matching the measured data at the occurrence of fault with historical data. With the occurrence of fault in the distribution network, the waveform of voltage sags was measured at the substation. Now this measurement was recorded to create a database. This measurement was taken for different types of fault and its location. Further, in event of fault, the database was always updated. Now, when actual fault happened in the system, voltage sags waveforms collected at the substation were compared to the voltage sags waveforms available in the database. The most

corresponding waveform in the database gave the exact type of fault and its location. But, this method would not work for the actual occurrence of fault at some location, if it does not have the data available for that particular type of fault.

2.3.3.3 Hybrid Based Methods:

The methods discussed till now have taken into account the fault distance calculation and the status of the protective device available in the network with development of only one algorithm. With the advent of time, some researchers have emphasized to develop hybrid methods that may employ more than one algorithm in order to achieve more accuracy for location the faulty section and exact distance of occurrence of fault. The author in [32] has proposed a hybrid method where the fault distances was evaluated using the measurements available at the substation. In this approach, post-fault values of current or voltage was incorporated. This was done with the motive to get rid of the multiple estimation problems. This is due to the presence of numerous fault points in the network having similar impedance. Fault diagnosis procedure was adapted by creating a list for various fault locations points in the network. The effect of the change in load during different scenarios of fault and its effect on the operation of protective devices were obtained by extensive simulation. Now, when the actual fault occurred the measurements obtained were matched with that those available in database. This procedure was not appealing to the researchers since modeling and simulation of the circuit was required at different fault locations and for different types of fault. Also, with the change in network configuration, different set of modeling and simulation was required. It was indeed a time consuming procedure.

Järventausta et al. [57], has located faults by calculating the fault distance. It used the information of the fault detector and also the geographical knowledge of the distribution system was used. The author in [58], have located faults using the measurements of fault current. They were computed from the short circuit analysis, and the experience of system operator. The fault distance was computed in [59] by matching of current patterns. Also, interrupted analysis of load was also considered. The author in [60] developed a framework for detection of fault and modeling. Use of fault alarm was required in this approach. The alarm was blown, whenever there was a discrepancy between the behaviors of the system and the model. It should be kept in mind that the behavior of the faulty system was modeled using Adaptive Neuro Fuzzy Inference System. The model was also meant for fault location. Mora et al. in [61], had proposed a fault location technique which was based on the measurement of current waveforms at the substation end. It also required the

knowledge of setting of protective device installed in the network. Adaptive Neuro Fuzzy Inference System was also used. It was capable to locate the fault the specified zones of distribution system. Further, validation errors of less than 1% were reported in locating the zones of the network. It had an advantage of not using the electrical model of the system. Since, by not using them even the electrical parameters of the distribution system were neglected. Fuzzy inference system has been used in both the above approaches. Use of neural network can be found in [62].

The author in [63], has employed wavelet fuzzy neural network to locate fault. They have used use post-fault transient and steady-state measurements for the development of algorithm. Effect of fault resistance and load current has not been considered. Also, the distribution system has been considered to be a balanced system. This procedure has been a time taking procedure for computing the location.

2.4 SUMMARY

An attempt has been made in this chapter to give a brief review of the works carried out for identifying and locating faults in a distribution system. The techniques based on calculations of impedance, travelling wave and knowledge-based methods have been reviewed. Based on the literature reviewed the limitations of the location techniques can be summarized below:

a) Voltage and current measurements from all the nodes and branches are required to detect, identify and locate the fault in impedance based method.
b) The fault location algorithm which involves iterative procedure is time consuming and bears the risk of diverging from the solution.
c) Use of learning techniques reduces the model dependency because they are mainly based on information obtained from fault databases.
d) Heuristic procedure requires large amount of time and number of trials to be practically implemented in distribution system.

Based on the above review, It can be concluded that knowledge based method have more accuracy and speed as compared to other methods. Also, it involves less cost. Artificial intelligence method

such as ANN algorithm when used with features obtained from digital processing tools can result to be more fruitful in increasing the accuracy of identification classification and location.

Modern Tools and Techniques for Feature Extraction

Chapter 3

Feature extraction is the basic need for development of protection algorithms using digital signal processing tools. It transforms data of high dimension to a lower dimension. But at the same time, the embedded information content is kept intact. Also the dimensionality of data is reduced. Further, the complexity for the purpose classification or regression is decreased. This chapter presents a brief concept of the tools used for feature extraction. It covers a brief overview of the different signal processing tools involved in the development of algorithm. Wavelet Transform, Wavelet Packet Transform, Gabor Transform, M – Band Wavelet Transform and Complex Dual Tree Wavelet transform have been dealt. Also, it presents a brief overview of Artificial Neural Network meant for the classification and regression.

3. 1. NEED FOR WAVELET TRANSFORM

The periodicity of the time functions is present in Fourier series transform [64] - [65]. It means that the sine and cosine waves functions used in Fourier analysis are not only located in frequency but they are present for every time period. If one compute the frequency information of a signal by using the Fourier transform one gets an average of the signal over the complete duration of time. It means that suppose, if a local transient exists in a signal over small interval of time in the sampling duration of the signal, then the Fourier transformation will be contributed by this signal. But it will lose its location on the time axis. Thus, one can conclude that the Fourier analysis does not take into account the frequencies that change with time. It is worth mentioning that in order to get detail on transient signal, a windowed-fourier transformation approach should be applied with a series of windows of different widths. Hence, a wide window gives good frequency resolution but poor time

resolution. On the other hand, good time resolution but poor frequency resolution can be fetched by a narrow window.

Wavelet Transform conquers over the limitations of the Fourier methods since it analyzes functions both in time and frequency domain. It is well suited to non – periodic wideband signals. A power system transient signal may contain both sinusoidal and impulse components. Wavelets have the ability to concentrate on short - time intervals for high-frequency components and long-time intervals for low frequency components in the presence of fundamental and low-order harmonics. Hence, one can say that Wavelets have an adapting window in order to provide appropriate resolution.

3.2 WAVELET TRANSFORM

Electromagnetic transients' waveforms are naturally non-periodic in nature. It contains oscillations of high-frequency and have impulses of very short-duration. Further, These signals superimposed on signals of low power frequency. Due to this Fourier transform fails to analyze the given signal. Now, the signal requires a very high sampling rate as periodicity is assumed for the signal. It means if the signal is of large duration, good resolution can be maintained in the low-frequency range. Even though, Short - Term Fourier analysis has been able to resolve this problem up to certain extent but overall, Wavelet Transform finds edge over Fourier and Short Time Fourier Transform.

3. 2. 1 Continuous Wavelet Transform

The mother wavelet is a prototype function employed by the analysis of Wavelet. It has zero mean and decays sharply in an oscillations. It rapidly falls to zero on either side of its central path. Mathematically, the Continuous Wavelet Transform (CWT) of a given signal s (t) with respect to a mother wavelet g (t) is defined as:

$$\text{CWT (c, d)} = \frac{1}{\sqrt{c}}\int_{-\infty}^{\infty} s(t)\, p\left(\frac{t-d}{c}\right)dt \,. \qquad (3.1)$$

Where (c,d) denotes the dilation or scale factor and (d) is the translation factor. It should be noticed that these variables are continuous in nature. It can be seen from equation (3.1) that the

original one-dimensional time-domain signal *s (t)* is mapped to a new two-dimensional functional space across scale (c) and translation (d) by the wavelet transform (WT).

Coefficient of continuous wavelet transform (a,b) at particular scale and translation furnishes information about how the original signal s(t) are scaled and in which manner. It also provides information about its matching with the translated mother wavelet. Further, it can be concluded that the set of wavelet coefficients of Continuous Wavelet Transform of a particular signal are the wavelet representation of the original signal *s(t)* with respect to the mother wavelet *p(t).* The mother wavelet can be seen as a windowing function. It should be kept in mind that the scale factor (c) and the windowing function size are interdependent. It means that smaller window represents a smaller scale. The features of a particular signal can be captures by either narrow-band frequency components of the signal with a smaller scale factor. Also, wideband frequency components with a large scale factor can too give information about the signal.

For the purpose of multi-resolution, Wavelet transform includes an infinite set of wavelets due. For instance, by varying the scale and translation factors one can generate a very large family of wavelets. These are known as daughter wavelets and can be generated from one mother wavelet. A daughter wavelet can be distinguished from the family of other wavelets on the basis of number of coefficients and the number of iterations involved. Several types of mother wavelets can be used for analyzing the signal. The characteristics of the mother wavelet need to be considered for selecting the appropriate mother wavelets which can be used for the analysis. Haar, Symmlet, Daubechies, Morlet are the examples of mother wavelet Haar and Morlet are orthogonal in nature. Symmlet and Daubechies are non-orthogonal. It has been found that Daubechies Wavelet is preferred for detecting low amplitude signals. It is also helpful in short duration, fast decaying and oscillating type of signals can also be detected by Daubechies Wavelet.

3. 2. 2 Discrete Wavelet Transform

Similar to Continuous Fourier Transform and Discrete Fourier Transform, the Discrete Wavelet Transform is the counterpart of Continuous Wavelet Transform. It is defined by the following equation:

$$\text{DWT (l, q)} = \frac{1}{\sqrt{c_0^l}} \sum_r g\left(\frac{v - rd_0 c_0^l}{c_0^l} \right) \qquad (3.2)$$

Here, p (.) is the mother wavelet and the scaling and translation parameters (c) and (d) shown in equation (3. 2) are functions of an integer parameter m, i.e. c = c_0^l and d = $rd_0c_0^l$ which results into daughter wavelets. q is an integer variable which refers to a particular sample number in an input signal. The scaling parameter gives rise to geometric scaling, i.e. 1, $\frac{1}{c_0}, \frac{1}{c_0^2}$,…… The logarithmic frequency coverage of the discrete wavelet transform is given by the above scaling.

Rectangular time-bandwidths which are which are narrow at higher frequencies are the product of Discrete Wavelet Transform. The bandwidth increases with the decrease in the frequency. It successful isolates the highest frequency band at precisely. It takes less than the quarter cycle to distinguish the signal at the occurrence. It shows the multi-resolution attributes of the wavelet transform in the signal. Further, it analyzes a non-stationary transient signal that consists of high and low frequency components.

3. 3. Wavelet Multi-Resolution Analysis (MRA) of Fault Data

The multi- resolution analysis of the Wavelet Transform has established itself as a successful tool for evaluating and examining the disturbances present in the signal due to the presence of faults. Basically, it approximates the signal over a range of resolutions. A detail is defined as the difference of approximations for present and next resolutions of the signal can also be evaluated. Further, the information about the signal is given in terms of approximation and details. It has been designed in a manner that at high frequencies, good time resolution and poor frequency resolution is obtained. Similarly, at lower frequencies good frequency resolution and poor time resolution is calculated. The process for obtaining information about Wavelet - MRA analysis of the faulted data explained below. This can be helpful in extracting features for the purpose of development of algorithm.

3. 3. 1 Procedure for Obtaining Multi-Resolution Analysis of Fault Data

A signal can be decomposed up to a fixed resolution level, with the use of Discrete Wavelet Transform and Multi – Resolution Techniques. The DWT of discrete time sequence $o(v)$ of length R is essentially a multi resolution characterization of $o(q)$. The DWT of a signal is both limited

both in time as well as in resolution. A dyadic discrete wavelet transform is essentially a decomposition of the spectrum of $o(q), O(\omega)$ into orthogonal sub bands defined by,

$$\frac{1}{2^{l+1}T} \le \omega \le \frac{1}{2^{l}T}, l = 1, 2....I \qquad (3.3)$$

Where T is the sampling period associated with $o(q)$ and I gives the total number of resolution levels.

As seen in figure 3. 1, it is obvious that the Discrete Wavelet Transform is implemented by using a bank of high pass and low pass time discrete filters, g and h. The input sequence $o(q)$ propagates through the filter bank tree which consists of low pass and high pass filters. The signal is decomposed into low-pass and high-pass components through convolution (and subsequent decimation) with filters h and g, at each stage. Further, the bandwidth of both the filters is halved. The high half band width is associated with the high pass filter g and low half band width is connected with low pass filter h.The Discrete Wavelet Transform representation is comprises of scaling coefficients, $u_l(q)$, that represents low-pass signal information at level $l = i$, and wavelet coefficients, $y_l(v)$, provides signal detail at levels at $l = 1,.....I.$

Mathematically,

$$u_l(v) = \sum_r w(2q - r)u_{l-1}(r) \qquad (3.4)$$

$$y_l(q) = \sum_r p(2q - r)u_{l-1}(r) \qquad (3.5)$$

At level l, both $u_l(q)$ and $y_l(q)$ are composed of $2^{-l}R$ samples, forms a tree-like relationship between the coefficients at successive scales $y_l(q)$ is also called difference level m as it represents the difference in the signal between $u_{l-1}(v)$ and u_l. The resulting signal decomposition $[d_1, d_2, ..., d_j, c_j]$ is the Discrete Wavelet Transform representation of faulted signal $o(q)$.

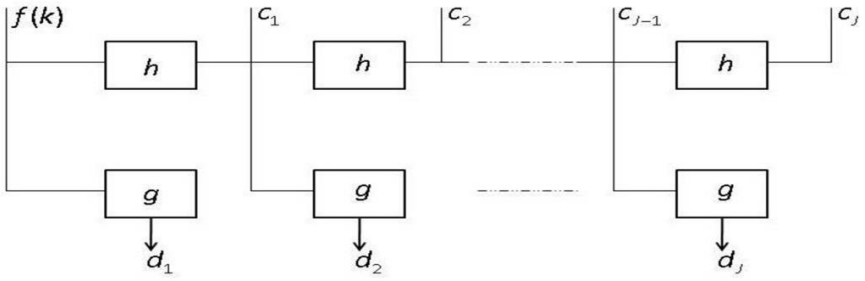

Figure 3.1: Wavelet multi resolution analysis of fault signal o(q)

Signal can be reconstructed by applying the inverse of Discrete Wavelet Transform. With the help of MRA, the sub-band information can be taken out from the original faulted signal. This is used for identification and location of the various types of faults that occurs in the distribution systems. Also, information content in sub-band has useful fault signatures that represent the faulted system. The output of the MRA is taken to detect, identify and classify the faults. It has been observed through simulation that the first-stage of MRA detail signal contains adequate information which can be very fruitful for the detection, identification, classification and location of the fault in distribution network. Also, exact information about the sampling frequency, the number of stages of the MRA filter banks and the type of wavelet to be used should be furnished in order to obtain proper result. One should not forget to keep the sampling frequency under permissible limit, simply because of the reason that it enhances the computation load of the algorithm.

3. 4 WAVELET PACKET TRANSFORM (WPT)

DWT gives flexible time frequency resolution. In the high frequency region, it experiences from a relatively low resolution. Due to which it is an uphill task to distinguish high frequency transient components. WPT is an extension of classical DWT [66]. For a given transient signal, wavelet analysis is better than the Fourier analysis. But, DWT is unsuccessful in taking out the high frequency information in signals. WPT represents high frequency information in a better manner when compared with DWT. In case of DWT a given signal is passed through high pass and low pass filters to obtain a detail and an approximation. The approximations are gathered from first level decomposition that splits into new detail and approximations. This process recurs to obtain the required level of decomposition. In case of DWT, only approximations of the signal are decomposed to next level. But this is not sufficient for few applications where the important high frequency components contain the required knowledge.

It can be concluded that WPT splits both approximations and details. But, DWT split only approximations. Hence, multi-layer division of the frequency band is obtained using the orthogonal WPT. It yields information about the high frequency content which was unable to fetch in the case of DWT. A three level WPT [67] gives a total of 8 sub bands. It should be observed that each sub band has the information of one-eighth of the signal frequency spectrum. The representation of time for the signal is given by top level of the WPT. Frequency resolution is seen in bottom level. Enhanced frequency resolution is obtained by using WPT. Further, more features are obtained using WPT as compared to DWT. Figure 3.2 shows the 3rd level wavelet packet decomposition.

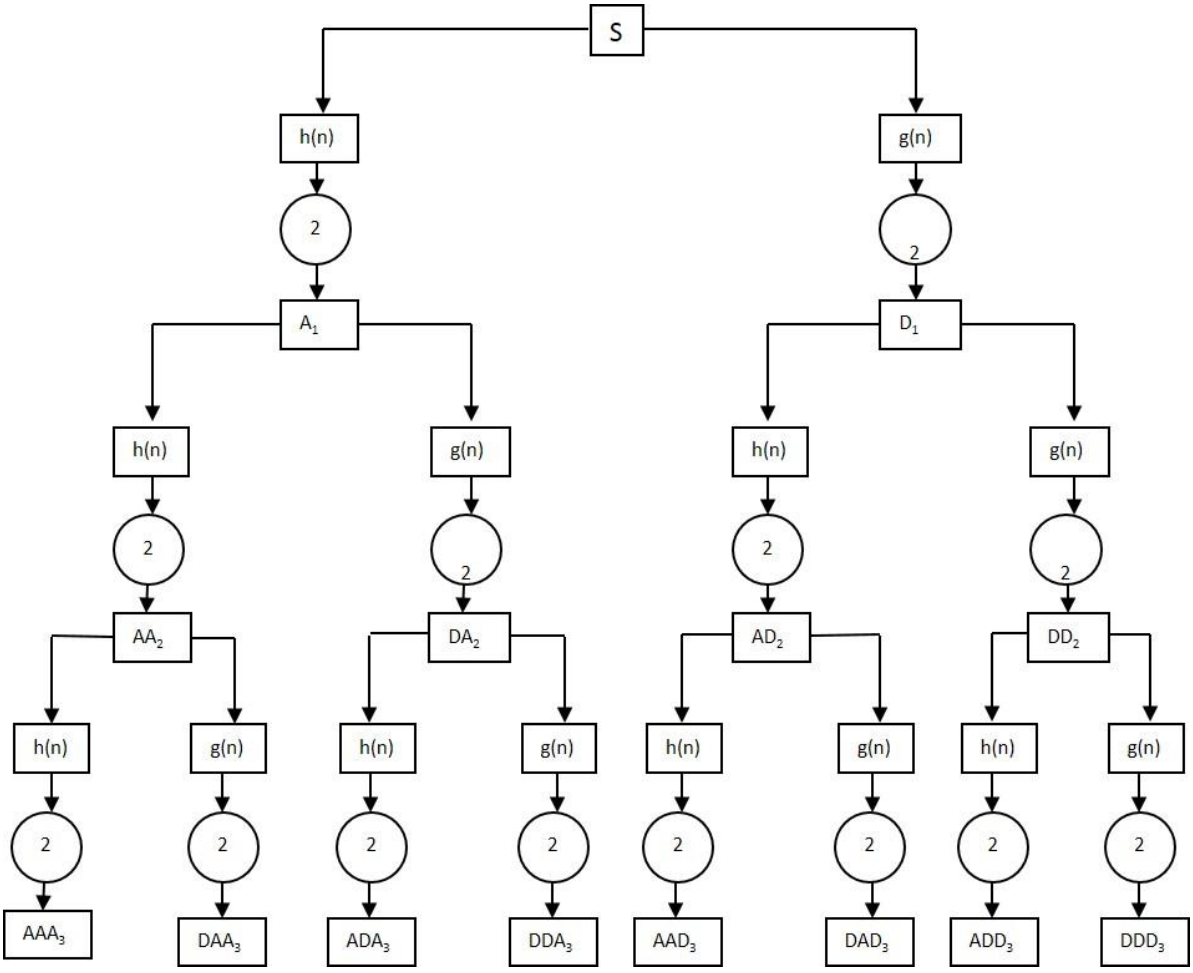

Figure 3.2: 3rd level Wavelet Packet Transform Decomposition Tree

If one talks about n levels of decomposition in the WPT, 2^n different sets of coefficients are obtained. In case of DWT (3n + 1) sets of coefficients were obtained. It should be observed that However,

number of coefficients is same in both the cases due to the process of down sampling. Also, there exists no redundancy. The sequence function P(x) is defined as,

$$P_{2r}(s) = 2^{j/2} \sum w_v P_r\left(2^{j/2}s - q\right) \quad (3.6)$$

$$P_{2r+1}(s) = 2^{j/2} \sum p_q P_r\left(2^{j/2}s - q\right) \quad (3.7)$$

Where i, q ϵ X, r ϵ R; $2^{j/2}$ $P_r(2^{j/2}$ s-q) is a WP function; j, q, r are the scale factor, time factor, oscillating factor respectively. P_0 (s) is a scaling function or a basis function; P_1 (s) is wavelet function; w_q, e_q are groups of conjugate mirror filter, that satisfies

$$\sum_{r\epsilon X} w_{r-2} w_{r-2u} = \delta_{vu}, \quad (3.8)$$

$$\sum_{r\epsilon X} w_r = \sqrt{2}, e_v = (-1)^v w_{1-v} \quad (3.9)$$

Signal s (t) is expressed by orthogonal wavelet packet basis function as follows:

$$U_{i,l}(q) = \sum_r U_{i+1,2l}(r) w_{q-2r} + \sum_n U_{i+1,2l+1}(r) e_{q-2r} \quad (3.10)$$

Here w_{v-2r}, p_{q-2r} is conjugate of w_{q-2r} and p_{q-2r}.

3.5 WAVELET ENERGY

The wavelet energy is defined as the sum of square of coefficients of the detailed WPT. There is a variation in the energy of wavelet coefficient over different scales. It depends on the input signals. The wavelet energy of coefficients p (t) is expressed as follows:

$$N(x(t)) = \sum_{i=1}^{U} abp_j^2 \quad (3.11)$$

Since, the faulted signals contain high frequency components, the energy of detail coefficients can be used to differentiate these signals. Hence, for a faulty signal one obtains seven features with three-levels WPT

3.6 WAVELET ENTROPY

A signal can be extended in various manners. Depending upon the extension, the size of number of binary sub trees may vary. Hence, it is mandatory to obtain a best decomposition by using a suitable algorithm. Entropy is defined as the amount of information contained in a signal. Several algorithms for entropy is available for WP. The entropy must be an additive cost function such that E (0) =0 and:

$$\mathrm{N}(\mathrm{x}) = \sum_i N(x_i) \tag{3.12}$$

The (non-normalized) Shannon entropy is given by,

$$N1(x_i) = x_i^2 \log(x_i^2) \tag{3.13}$$

Hence,

$$N1(x_{i,r}) = -\sum_i y_i^2 \log(x_i^2) \tag{3.14}$$

Where s_i is the probability distribution of the energy contained in the wavelet coefficients at the nth sub frequency band with the level j. The probability distribution function is defined as,

$$x_i = | b_{(j,u)}(i) |^2 / \| b_{(j,u)} \|^2 \tag{3.15}$$

With $\sum_{i=1}^{m} p_i = 1$, and $\log_2 p_i = 0$ if $\boldsymbol{\pi} = 0$ Upper limit 'm' represents the number of wavelet coefficients at the n^{th} sub frequency band with level j. When the value of the entropy is greater than one, then it is possible to furnish more information about the signal which needs to be decomposed so that simple frequency component of the signal can be obtained. It provides distinguish features about the signal. With the use of node coefficients, it reduces the size of feature vector. The entropy of the wavelet coefficients is bordered by,

$$0 \le N_{entropy}(b_{j,u}) \le log_2 f \tag{3.16}$$

If the energy content in a signal is spread out across the constituent wavelet coefficients within the sub frequency band, then the Shannon entropy would have a large value. On the other hand, it presumes that some amount of the energy is concentrated on a few dominant components contained in a signal.

Several entropy algorithms like ‘log energy’, ‘threshold’, ‘sure’, ‘norm’ and ‘user’ entropies are available. But these entropies require the optional parameter depending on the entropy type. Algorithms meant for ‘Shannon’ and ‘log energy’ entropy does not require them. Figure 3.3 shows the faulted phase current under fault condition. The corresponding colored coefficients for terminal nodes after applying wavelet packet transform are shown in figure 3.4. The initial purple color corresponds to coefficients obtained from normal decomposition of approximations and blue color gives the coefficients obtained from the decomposition of details.

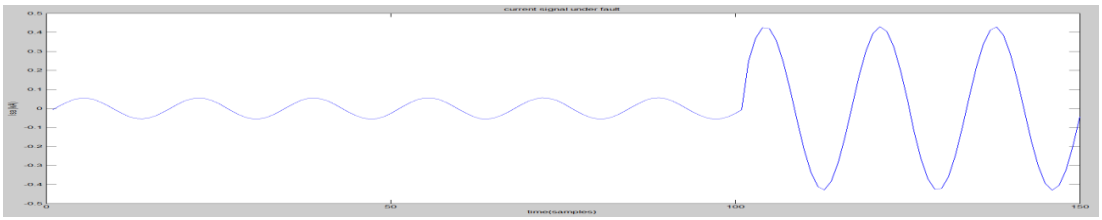

Figure 3.3: Faulted Phase Current Waveform

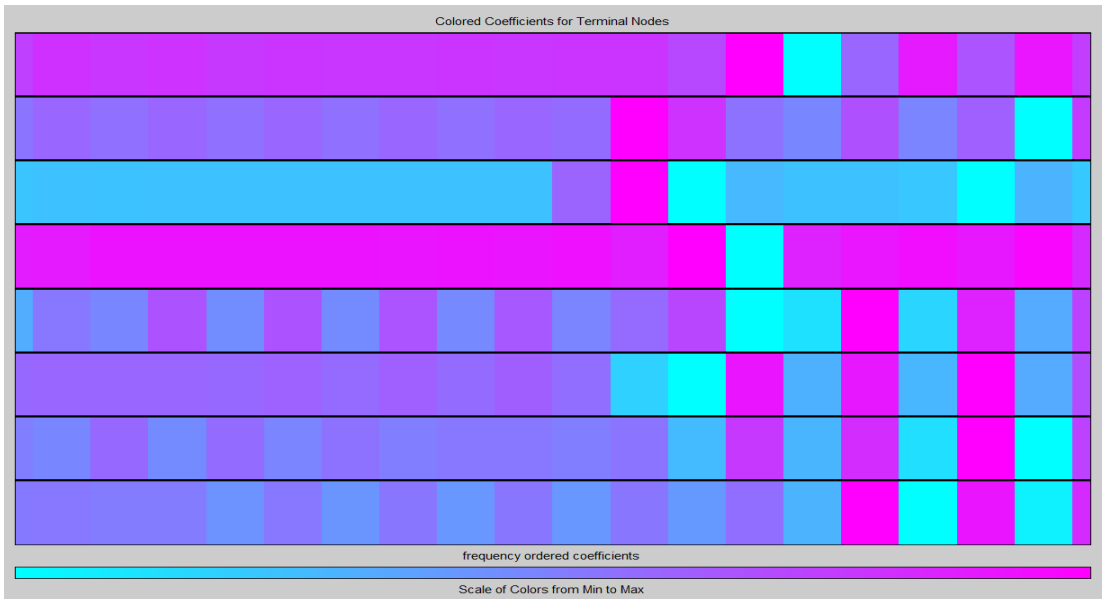

Figure 3.4: Colored coefficients for Terminal Nodes with WPT up to 3rd level Decomposition

3.7 GABOR TRANSFORM

Dennis Gabor [68] introduced the Gabor filter in 1946. It is developed from the short – time Fourier transform. It contains a Gaussian window. It can be observed as a particular case of the Short-Time Fourier Transform. Further, the frequency and its phase content of a signal can be determined throughout the time period. There are some reasons that justify the use of this transform. First and foremost, it presents a best example of localization in combined spatial and frequency domains. This further helps in taking our information from the signals. Another important aspect of the Gabor transform lower order of entropy is also reduced. It helps in applications meant for data reduction. These properties make it useful for power system protection applications. The function which has to be transformed is first multiplied by a Gaussian function. This is considered as the window. The time-frequency analysis is done by transforming the resultant function with Fourier transform. The Gaussian window used is as follows:

$$a_{t_0,\omega_0}(t) = p(t - t_0).\exp(jf_0 t) \tag{3.17}$$

Here $p(t)$ is the window function:

$$p(t) = \left(\sqrt{2\lambda}\right)^{\frac{1}{2}} \exp\left(-\prod \lambda^2 t^2\right) \tag{3.18}$$

λ : Window Width

χ : Phase constant of the changing oscillations

f_0 : Frequency of these oscillations

t_0 : Window function Centre

The Fourier Transform of this basis function has similar analytical concept which is as follows:

$$A_{t_0,\omega_0}(f) = P(p - p_0).e^{(2\prod j t_0 (f - f_0)} \tag{3.19}$$

Where,

$$P(f)=\left(\frac{\sqrt{2}}{\lambda}\right)^{\frac{1}{2}} e^{\frac{f^2}{4\Pi\lambda^2}} \tag{3.20}$$

In order to get the accurate time and frequency resolutions, the window function should be selected properly in time-frequency analysis. As one knows that the Heisenberg inequality principle restricts the existence of window with arbitrary small duration, both in time as well as bandwidth in frequency. It implies that a trade -off exists between both time and the frequency resolutions. For a function $p(t)$, width is calculated by the root mean square value of the second moment of its energy distribution. Hence, time resolution is denoted by the following equation:

$$\Delta(t)=\frac{\int_{-\infty}^{\infty} t^2 \left|p(t)\right|^2 dt}{\int_{-\infty}^{\infty} \left|P(t)\right|^2 dt} \tag{3.21}$$

Where:

$\Delta(t)$: Resolution of Time

$\left|p(t)\right|^2$: Distribution of Energy

The resolution of the frequency also known as the useful bandwidth is computed from $P(p)$ and is given by:

$$\Delta(f)=\frac{\int_{-\infty}^{\infty} f^2 \left|P(f)\right|^2 df}{\int_{-\infty}^{\infty} \left|P(f)\right|^2 df} \tag{3.22}$$

Where, $\Delta(f)$ is the resolution of frequency. The uncertainty principle states that the product of resolution of time and frequency is lower surrounded by the Heisenberg inequality which is expressed below:

$$\Delta(f)\times\Delta(t)\geq\frac{1}{2} \tag{3.23}$$

Gabor transform meets the lower boundary in the Heisenberg inequality =1/2. Perfect time resolution is achieved when $p(t) = \sigma(t)$ condition is satisfied; this is the expression for unit impulse function $\sigma(t)$. Window function $p(t)$ can also be selected by a unit step function $o(t)$. It may result into ideal frequency resolution with no time resolution. Gabor has established that the when the window is of Gaussian shape, lower bound of the inequality is achieved [69]. Using Gabor Transform, the frequency and time resolution is represented by:

$$\Delta(t) = \frac{1}{2\lambda\sqrt{\Pi}} \tag{3.24}$$

$$\Delta(f) = \lambda\sqrt{\Pi} \tag{3.25}$$

Two conditions of "λ" is taken into account. When $\lambda = 0$, the Gabor elementary function (GEF) turns into a sinusoidal of infinite duration. It reduces to traditional Fourier transform with ideal frequency resolution. For $\lambda = \infty$, the window function turn into a delta function. An outstanding time resolution is achieved with no frequency resolution. Therefore, in order to get the required frequency and time resolutions "λ" should be selected properly. The amount of effective overlap of the GEF across the neighboring windows can also be computed. The GEF for one – dimensional discrete-time signals is given by:

$$a_{nk}(t) = p(t - nN).e^{j\frac{2\Pi kt}{N}} \tag{3.26}$$

Here, n and k integers represents the temporal and frequency sampling indices. Also, $p(t)$ represents the Gaussian window function,

$$p(t) = \left(\sqrt{2\lambda}\right)^{\frac{1}{2}} e^{\left(-\Pi\lambda^2 t^2\right)} \tag{3.27}$$

The (GEFs) is regarded as a set of shifted and modulated window functions with specific effective width and shift parameter "N" which in turn controls the discrete time shift along time axis. These windows concentrate on window intervals $[-N/2 + nN, N/2 + nN]$ with centers at point nN. The convergence of the solution is affected by the selection of λ and N. The Gabor representation for any signal $s(t)$, in order to find out a set of coefficients is given by:

$$s(t) = \sum_{n=-\infty}^{\infty} \sum_{k=-\infty}^{\infty} b_{nk} a_{nk} \tag{3.28}$$

Here, a_{mr} is the basis function. For 1- D a finite extent $s(t), t \in [0, L-1]$ with $L \prec \infty$, only finite number of windows intervals shall be present. When $L = dN$, where d is a positive integer that represents the number of windows covering the whole signal $s(t)$, the GEFs' can be translated so that they are centered at central point of each window as follows:

$$a_{mr}(t) = p(q(t) - nN).ee^{j\frac{2\Pi\Pi q(k)q(t)}{N}} \tag{3.29}$$

Where,

$$q(y) = y - \frac{N-1}{2} \tag{3.30}$$

Gabor Transform is redrafted as:

$$s(t) = \sum_{n=0}^{d-1}\sum_{k=0}^{n-1} b_{nk} a_{nk} \tag{3.31}$$

The coefficients b_{nk} constitute one dimensional Gabor transform.

3.8 MULTI BAND WAVELET TRANSFORMS (M - BAND WT)

M - Band Wavelets are simplification of the conventional wavelets [70]. Signals with high frequency content having relatively narrow bandwidth cannot be analyzed by standard wavelets. Their decomposition yields a logarithmic frequency resolution. But, logarithmic and linear frequency resolution decomposition is obtained using M-band. Also, a large number of sub bands are available by its decomposition which further gives more information about the signal. It also performs multi scale, multi directional filtering of the signal. It is used a tool to view signals at different scales. Decomposition of a signal is achieved by exposing it to the family of functions which are produced from wavelet through its dilations and translations.

M-band orthonormal wavelets were introduced as direct simplification of the two band Daubechies orthogonal wavelets [71]. It is able to zoom in onto narrowband high-frequency components of a signal. When compared with two band wavelets energy compactness is better in case of M – Band [72].

An M-Band wavelet is defined as a tight frame for the set of square integrable functions over the set of real numbers $P^2(N)$ [73]. There are $K-1$, wavelets, $\xi_a(s)$, $a=1,.....,K-1$ are connected with the scaling function. For function $y(s)\in P^2(N)$, it is perceived that

$$y(s)=\sum_{a=1}^{a=K-1}\sum_{b\in D}\sum_{c\in D}\langle y(s),\xi_{a,b,c}(s)\rangle\xi_{a,b,c}(s) \tag{3.32}$$

Here, D stands for the set of integers while the inner product operator is denoted by $\langle,\rangle$. By scaling and shifting the corresponding wavelets $\xi_a(s)$:, the $\xi_{a,b,c}(s)$ functions are derived

$$\begin{aligned}&\xi_{a,b,c}(s)=K^{b/2}\xi_a(K^b s-c)\\&a=1,.....,K-1,c\in D,b\in D\end{aligned} \tag{3.33}$$

For the scaling function $\xi_0(s)$ in $P^2(N)$, the wavelet functions are defined as follows

$$\begin{aligned}&\xi_a(s)=\sqrt{K}\sum_{c-0}^{c=F-1}g_a(c)\xi_0(Ks-m)\\&a=1,.....,K-1\end{aligned} \tag{3.34}$$

The recursive equation is satisfied by the scaling. It is compactly supported in $[0.(F-1)/(K-1)]$,

$$\xi_o(s)=\sqrt{K}\sum_{c=0}^{c=F-1}g_0(c)\xi_0(Ks-m) \tag{3.35}$$

Here, the sequence g_0 is the scaling filters of length $\mathrm{F=KC}$ where C gives the regularity of scaling function and fulfils the following equation:

$$\sum_{c=0}^{c=F-1}g_0(c)=\sqrt{K} \tag{3.36}$$

$$\sum_{c=0}^{c=F-1}g_0(c)g_0(c+Kq)=\sigma q \tag{3.37}$$

The $(K-1)ga$ vectors are known as the wavelet filters that satisfies the following equation

$$\sum_{c=0}^{c=F-1}g_0(c)g_0(c+Kq)=\sigma(q)\sigma(a-b) \tag{3.38}$$

3.8.1 Multi Resolution Analysis:

The study of multi resolution concept is given by the scaling and the $K-1$ wavelet functions. It is a sequence of approximation spaces for $P^2(N)$. If the space spanned by translates of $\xi_a(s)$ for fixed b and $c \in D$, then it is defined by $W_{a,b} = Span\{\xi_{a,b,c}\}$, It can be observed that

$$W_{0,b} = \bigoplus_{a=0}^{K-1} W_{a,b-1} \tag{3.39}$$

$$\lim_{b\to\infty} W_{0,b} P^2(N) \tag{3.40}$$

Thus, the $W_{0,a}$ spaces from a multi resolution for $P^2(N)$. A significant feature of M-Band wavelet is that scaling factor g_0 specifies a unique $\xi_o(s)$ and hence a unique multi resolution analysis. For example, with $K = 4$,

$$\begin{aligned} V_1 &= V_0 \oplus W_{10} \oplus W_{20} \oplus W_{30}, \\ V_2 &= V_1 \oplus W_{11} \oplus W_{21} \oplus W_{31}, \end{aligned} \tag{3.41}$$

Where V_b and W_b are the spaces spanned by the scaling and wavelet functions different resolution. It can be observed in figure 3.5.

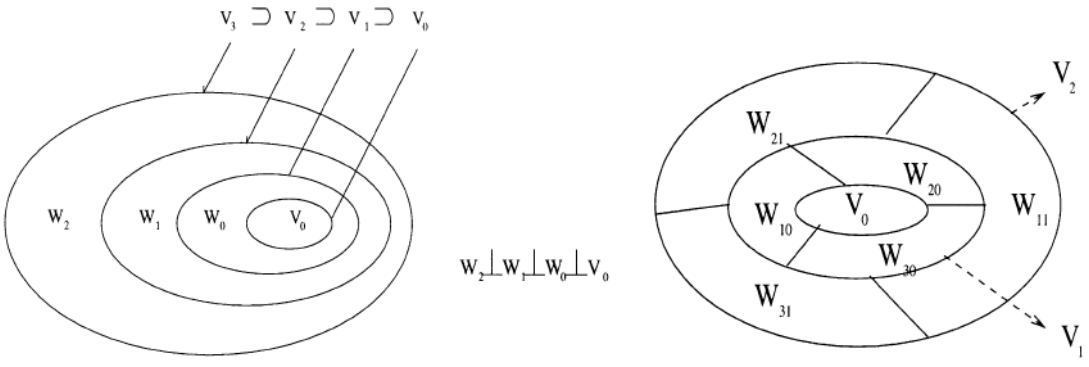

Figure 3.5: Spanned Nested vector spaces functions in standard and M- Band wavelet

The scale – space tiling for standard wavelet M=2 and M band wavelet (M=4) can be seen in figure 3.6. From the figure shown below it is quite evident the frequency tiling in the standard wavelet decompositions are logarithmic , while in case of M-Band decomposition a mixture of logarithmic as well as linear frequency tiling is observed.

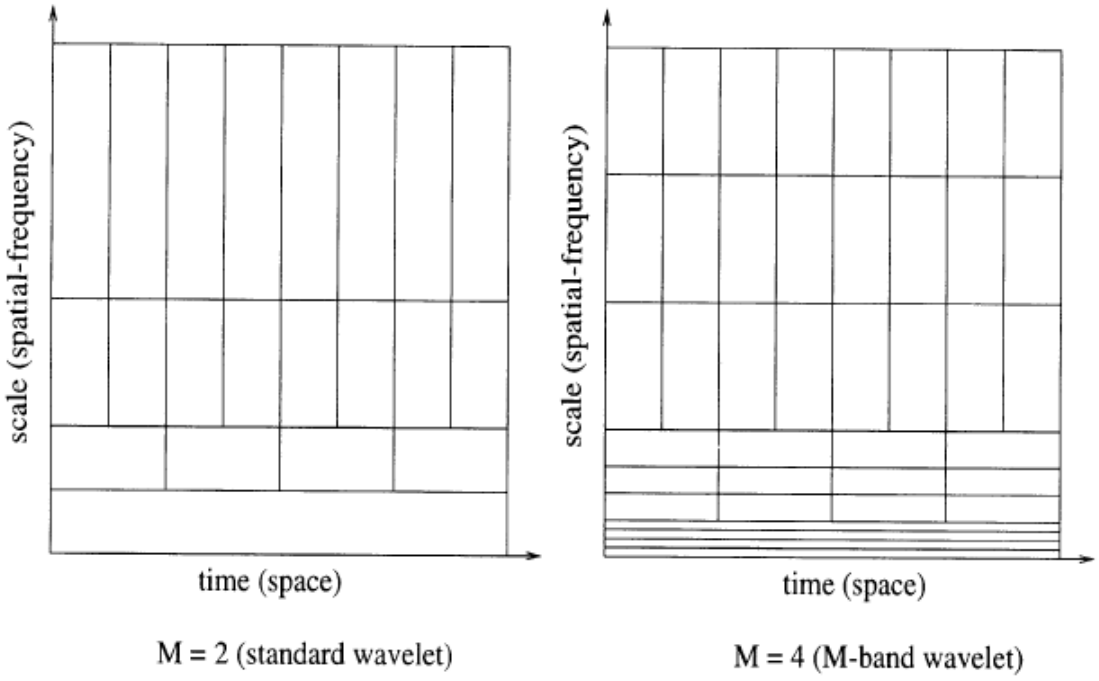

Figure 3.6: Tiling in 2-band and 4-band

3.8.2 M - Band Wavelet Filters

A close relation exists between M-Band wavelets and M-channel filter banks. The filter bank is a set of band pass filters that has both the property of frequency and orientation selection. In the stage of filtering, orthogonal and linear M-band wavelet transform decompose signals into $K \times K$ channels. This corresponds to different direction and resolutions. A typical M-channel filter bank is shown below in figure 3.7.

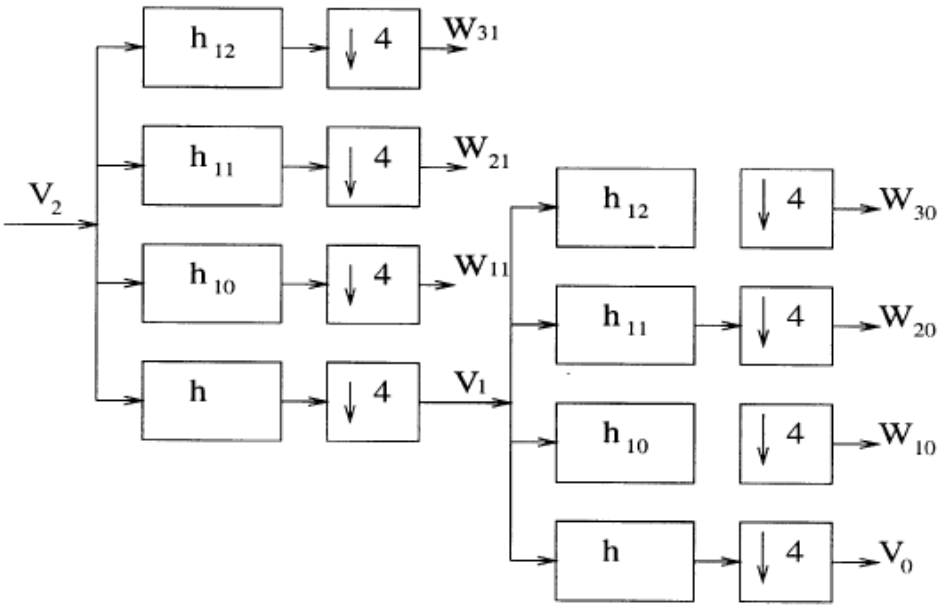

Figure 3.7: Structure of an M-channel filter bank (M=4)

3.9 THE DUAL TREE COMPLEX WAVELET TRANSFORM (DTCWT)

Wavelet based transform are successfully applied in the field of pattern recognition. The major problem of the common decimated Discrete Wavelet Transform (DWT) is its lack of shift invariance. The wavelet coefficients vary substantially when there are shifts of the input signal. Complex Wavelet Transform does not suffer from this problem. But, they generally lack in speed in calculating the coefficients. They also have poor inversion properties [74]. Kingsbury [75, 76] developed Dual-Tree Complex Wavelet Transform (DTCWT) to find the solution for the above problem. It retained the properties of nearly shift invariance as well as directionally selectivity. It consists of a dual tree structure of the wavelet transform. The author has introduced a delay of one sample between level one filter in each tree. Also, linear-phase filters with alternate odd-length and even-length have been employed. The odd/even filter approach has its own problem which is discussed later. A new Q-shift dual-tree is shown in figure 3.8.

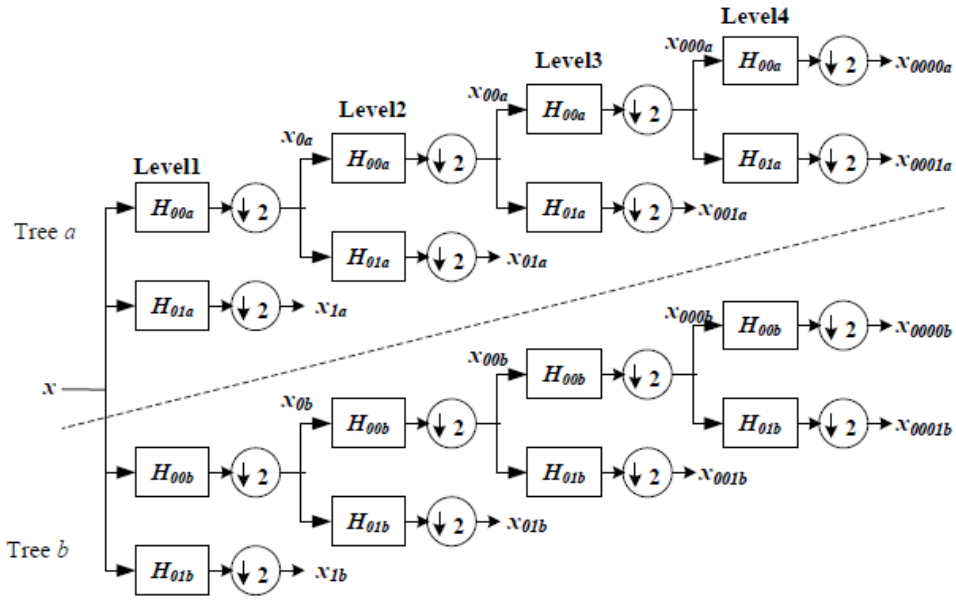

Figure 3.8: The 1-D Q-Shift Dual Tree Structure

Two sets of filters are used for implementation of DT-CWT. One set of filters is used at first level. At higher levels, the other set of filters are employed. The filters beyond level one have even length. It may not be a longer linear phase. A group delay of ¼ samples is present. The necessary difference in delay of 1/2 samples is obtained by using the time reverse of the tree and filters in tree b. At each scale, the real part of the complex wavelet coefficients can found at one tree. The other tree gives the imaginary part. DT-CWT employs two real DWTs in essence. When the two trees are joined, the complex coefficients appear. The properties are summarized below:

(i) It has nearly shift invariance;

(ii) They have good selectivity and directionality in 2D (or higher dimension) like Gabor filters

(iii)It can be perfectly reconstructed by using short linear phase filters

(iv)Redundancy is limited It is not governed by the presence of the number of scales.

(v) It has an efficient order N computation: 2^m times the simple real DWT for m-dimensional signal.

The real wavelet transform suffers mainly from the following four problems:

1. **Oscillations**: It is a band pass function. Wavelet-based processing is complex because the coefficients oscillate around positive and negative singularities. Hence, singularity extraction and modeling of the signal is a daunting task [77]. Since an oscillating function

often passes through zero, singularities give way for large wavelet coefficients which is not correct. This means that a wavelet overlapping a singularity can have a small or even zero wavelet coefficient.

2. **Shift variance:** A small shift of the signal greatly disturbs the wavelet coefficient oscillation pattern around singularities. Wavelet-domain processing is made complex by this procedure. Algorithm should be developed in a manner that it should be capable of handling a broad range of wavelet coefficient patterns [78], [79], [80], [81], and [82].
3. **Aliasing:** There exists wide spacing between the samples of the wavelet coefficient. The wavelet coefficients are computed via iterated discrete-time down sampling operations. These are mixed together with non ideal low-pass and high-pass filters that result into substantial aliasing. When the wavelet and scaling coefficients are not changed the inverse of DWT cancels the aliasing. Artifacts are present in the reconstructed signal during the wavelet coefficient processing. It also disturbs the delicate balance between the forward and inverse transforms.
4. **Deficient of Directionality:** Sinusoidal signals in Fourier transform corresponds to higher dimensions in highly directional plane waves. A checkerboard pattern is created by the construction of multi dimension wavelets. It has orientation along several directions and hence lacks the sense of directional selectivity.

DTCWT [83], [84], [85] was introduced in 1983. The first part gives information about the real part while the second gives the imaginary part.

The condition of proper reconstruction for WT is satisfied by the use of two different sets of filter. They are designed jointly in order to get an analytical transform. If it is presumed that $h_0(n), h_1(n)$ indicates the low-pass/high-pass filter pair for the upper filter bank, and let $b_0(m), b_1(m)$ is the low-pass/high-pass filter pair for the lower filter bank. It indicates that the two real wavelets associated with each of the two real wavelet transforms as $\phi_a(t), \phi_b(t)$. The filters are designed in such a manner that the complex wavelet $\phi(t) := \phi_a(t) + j\phi_b(t)$ is approximately analytic. Equivalently, they are designed so that $\phi_b(t)$ is approximately the Hilbert transform of $\phi_a(t)$. Filters are themselves real. One of the advantages of DTCWT is that it does not involve complex arithmetic.

In order to obtain the inverse of the transform, the real part and the imaginary part are both inverted. The inverse of each of the two real DWTs are used to get two real signals. Final output is obtained by averaging the two real signals. The original signal $x(n)$ can be recovered alone from either the real part or the imaginary part. If the two real DWTs are represented by the square matrices P_a and P_b then the dual-tree CWT can be represented by the rectangular matrix

$$P = \begin{bmatrix} P_a \\ P_b \end{bmatrix} \tag{3.42}$$

If the vector s denotes a real signal, then $n_a = P_a s$ gives the real part and $n_b = P_b s$ is the imaginary part of the dual-tree CWT. The complex coefficients are known by $n_a + jn_b$. Inverse of P is then given by

$$P^{-1} = \frac{1}{2}\begin{bmatrix} P_a^{-1} & P_b^{-1} \end{bmatrix} \tag{3.43}$$

This is verified by:

$$P^{-1}.P = \frac{1}{2}\begin{bmatrix} P_a^{-1} & P_b^{-1} \end{bmatrix}.\begin{bmatrix} P_a \\ P_b \end{bmatrix} = \frac{1}{2}[1+1] = 1 \tag{3.44}$$

One half factor between the forward and inverse transforms is shared to get the

$$P := \frac{1}{\sqrt{2}}\begin{bmatrix} P_a \\ P_b \end{bmatrix}, P^{-1} := \frac{1}{\sqrt{2}}\begin{bmatrix} P_a^{-1} & P_b^{-1} \end{bmatrix} \tag{3.45}$$

If the two real DWTs are orthonormal transforms, then the transpose of P_a is its inverse $P_a^t.P_a = 1$. In the similar manner, for P_b, the transpose of the rectangular matrix P is a left inverse $P^t.P = 1$. The inverse of the DTCWT can be performed using the transpose of the forward dual-tree CWT. It also has the self-inverting [86] property.

The dual-tree wavelet transform manages to separate the real and imaginary parts of the complex wavelet coefficients. However, the complex coefficients can be calculated using the following form:

$$P_d = \frac{1}{2}\begin{bmatrix} 1 & j1 \\ 1 & -j1 \end{bmatrix}.\begin{bmatrix} P_a \\ P_b \end{bmatrix}$$
$$P_d^{-1} := \frac{1}{2}\begin{bmatrix} P_a^{-1} & P_b^{-1} \end{bmatrix}.\begin{bmatrix} 1 & 1 \\ -j1 & j1 \end{bmatrix} \quad (3.46)$$

It is worth mentioning that the complex sum or difference of the matrix has unit value:

$$\frac{1}{\sqrt{2}}\begin{bmatrix} I & jI \\ I & -jI \end{bmatrix}.\frac{1}{\sqrt{2}}\begin{bmatrix} I & I \\ -jI & jI \end{bmatrix} = I \quad (3.47)$$

It is observed that the identity matrix on the right-hand side is twice the size of those on the left-hand side. Therefore, if the two real DWTs are orthonormal transforms, then the dual-tree CWT satisfies

$$P_d^*.P_d = I \quad (3.48)$$

Where $*$ denotes conjugate transpose. If

$$\begin{bmatrix} r \\ q \end{bmatrix} = P_d.s \quad (3.49)$$

When x is real, then $q = r^*$ so v need not be computed when the input signal x is complex, then $q \neq r^*$ so both r and q need to be computed. When the DTCWT is applied to a real signal, the output of the upper and lower filter banks will be the real and imaginary parts of the complex coefficients. They can be collected separately. If the DTCWT is applied to a complex signal, then the output of both the upper and lower filter banks will also be complex. Hence, it cannot be labeled as the real and imaginary.

When the two real DWTs are orthonormal and the $1/\sqrt{2}$ factor is included, the DTCWT gains Parseval's energy theorem: the energy of the input signal is equal to the energy in the wavelet domain

$$\sum_{j.n}(|e_a(j.m)|^2 + |e_b(j.m)|^2) = \sum_m |s(m)|^2 \quad (3.50)$$

The DTCWT is easy to implement. In addition, because the dual-tree DTCWT is implemented using two real wavelet transforms, the use of the DTCWT can be informed by the existing theory and practice of real wavelet transforms.

3.10 ARTIFICIAL NEURAL NETWORK (ANN)

A neural network [87] is defined as the set of organized elements better known as neurons. Each connection has weight associated with it. The neurons are usually arranged in a series of layers. It can give the desired output based on the adjustment of weights and trial and error method. It basically consists of three or more layers [88]. The first layer is the input layer which feds data into the network. The intermediate layer also knows as the hidden layer has weights associated with it. The neurons in the hidden layer collect the weighted inputs and compute the outputs by the given transfer function hidden layer is fed to the subsequent layer until the desired output is achieved. No rule defines the selection of hidden layer. It is basically selected on hit and trial method. Artificial Neural Network (ANN) is a powerful tool [89] which can effectively solve the existing protection problems such as identifying classifying and locating faults. Based on the training with the simulation/field data, the fault and no fault conditions can be differentiated.

Data can be classified in neural network. The technique of classification involves two main steps the first one is learning and other one is recall. In the process of learning the network weights are adjusted in such a manner that the data become accustomed to the patterns of the training data. On the other hand, in the process of the recall, this trained network gives the responses of the test data. Several training algorithms are available for feed-forward networks. They employ the gradient of the performance function in order to optimize the performance. The gradient is computed back propagation technique. It performs computational backwards through the network. Back propagation artificial neural networks (BP-ANN) are highly effective for the purpose of pattern recognition. They find their effective use in detection, identification and location of faults in both distribution and transmission system.

3.11 LEARNING IN ARTIFICIAL NEURAL NETWORK

For the purpose of learning in neural network, the nature of data sets needs to be described. These data sets are input vectors, outputs vector and target vector. The neural network is always trained to get the desired output. The algorithms for learning in ANN can easily be classified into three categories.

3.11.1 Supervised Learning

During the training a neural network, input vectors are fed to network in order to get the output. The received output is now compared matched until the resulting output is achieved. Whenever there exists a difference between obtained output and preferred output an error signal is generated. This error modifies the network weights till the point when the actual output equals the desired output. Multi-Layer Perceptron (MLP) is based on the concept of supervised learning.

3.11.2 Unsupervised Learning

In case of unsupervised learning, the network receives inputs but does not obtain supervised target outputs. It refers to the difficulty of finding the hidden structure. During the training process, the network is fed with different input vectors. It randomly systematizes the input vectors into clusters. Now, when an input vector is fed during the course of testing the network matches the output with the input vector. The self-organizing map (SOM) and adaptive resonance theory (ART) are the example of unsupervised learning algorithms.

3.11.3. Self-Supervised Learning

In this process learning occurs by a knowledge component without having a training system providing feedback on correctness. The system generates the error signal is fed back. Several iterations are required to obtain the correct target.

3.12 MULTI-LAYER PERCEPTRON (MLP)

A Multi-Layer Perceptron (MLP) [90] is an example of feed forward artificial neural network. It consists of several layers. Each layer is connected to the next layer. Each node consists of a neuron with a nonlinear activation function. MLP works on the concept of a supervised learning. As usual it consists of input hidden and output layer. Hidden layer is the link between the inputs and the output. It extracts useful features from the input data so that the output values can be predicted. It is sometimes known as Back Propagation Network (BPN). Since, the training is done by error back propagation.

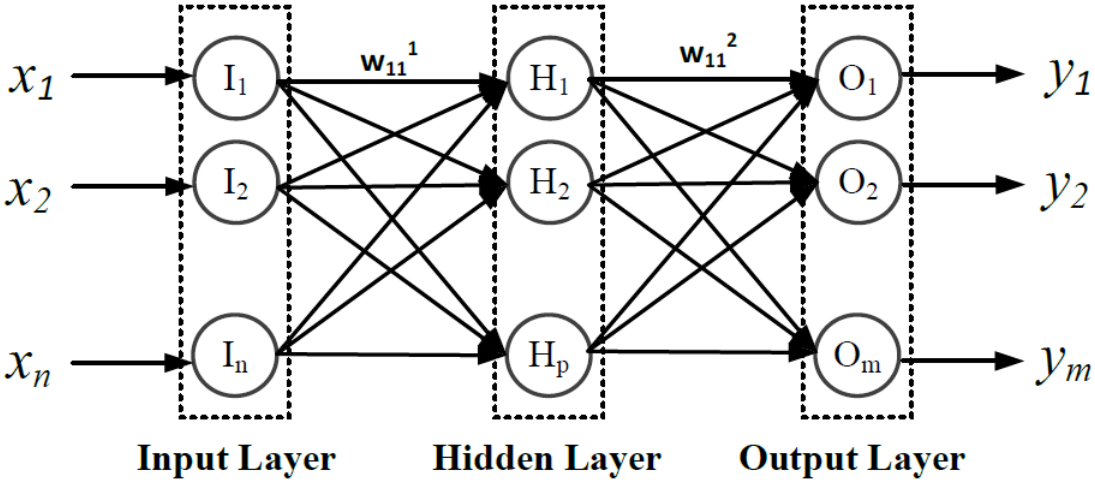

Figure 3.9: Multi-Layer Perceptron (MLP)

When an input pattern is applied to the input layer of network, it propagates through each next layer of the network until an output is generated. Now, the obtained output is compared with desired target. An error signal is calculated for each output. This error signal then propagates backward from the output layer to each node in the intermediate layer in order to obtain the output. The weights are updated by the error signal that is received. Back propagation algorithm is an iterative gradient search algorithm that minimizes the cost function equal to the mean square error/mean squared error with regularization between the desired and actual output of MLP. Multi-Layer Perceptron can be seen in figure 3.9.

3.12.1 Performance Function

Selection of performance function plays a vital role while training a neural network. Usually, the performance function selected for training feed forward neural networks is the mean sum of squares of errors.

$$\text{Pf} = \text{mse} = \frac{1}{N}\sum_{i=1}^{N}(e_i)^2 = \frac{1}{N}\sum_{i=1}^{N}(t_i - a_i)^2 \tag{3.51}$$

Here, “t” and “a” represents the “N” dimensional vector of the input model. In order to improve the simplification process, the performance function is modified by adding a term that consists of the mean of the sum of the squares of the network weights and biases.

$$\text{msereg} = \Upsilon\text{mse} + (1-\Upsilon)\,\text{msw} \tag{3.52}$$

Where Υ is the performance ratio and

$$msw = \frac{1}{n}\sum_{j=1}^{n} w_j^{\,2} \tag{3.53}$$

It leads the network to have smaller weights and biases. On the same hand, it asserts that the response of the network is smooth.

3.12.2 Activation Function

To add layers one need to do one more thing other than just connecting some new weights. By using a sigmoidal activation function, efficient output layer is obtained. It tends to get rid of mathematical values that are in the middle. They may force values to become from low to even lower and high to be even higher. It should be noted that there are two basic commonly used sigmoidal activation functions.

The Logistic Sigmoid which is also called as the *logsig*.

$$g(a) \equiv \frac{1}{1+e^{-a}} \tag{3.54}$$

The tangential sigmoid also called as the *tansig*, is derived from the hyperbolic tangent. It is able to handle negative numbers.

$$g(a) \equiv \tanh(a) \equiv \frac{e^{a}-e^{-a}}{e^{a}+e^{-a}} \tag{3.55}$$

The author in [149] and [150] has used very less data for training in neural network and more than 60% data have been tested. The same concept is employed in the present thesis while training and testing the neural network.

3.13 SUMMARY

A brief description of the various digital signal processing tools have been discussed in this chapter. Features are extracted by the use of these tools which has been used for development of algorithm for detection, identification and location of fault in distribution system. The literature has been given in terms of the tools used for extracting the features and the improvement of the result. The brief literature is available so that in the subsequent chapters only governing equations are given. The transforms have been given in the order in which they have been used. At last, theory is given about the Back Propagation Neural Network which has been used throughout the work to classify and locate the fault.

Wavelet Transform and Wavelet Packet Transform Based Features

Chapter 4

During the past five decades, there has been a rapid growth in electric power systems. Due to which, there has been an increase in length of the line and its operation. The lines experience regular faults. This causes rise in line currents. In the present scenario of digital protection, protective relays can be operated well in time, if one has the appropriate knowledge of the type of fault. Due to unavailability of adequate system information, detection, identification and classification of faults in a electrical distribution system is a challenging task for power system engineers. Whenever fault occurs in the system, proper information about the fault type and its exact location is required for restoration of power supply. Faults has also been identified by use of fuzzy logic [12] which utilizes the angle and magnitude comparison was successful in identification and classification of faults but it needs exact determination of threshold. This method is a tedious method since it involves an iterative procedure. With the introduction of application of digital signal processing tools in the field of power system, accurate results are approachable.

Wavelet Transform [91] – [92] has been able to capture the information of high frequency signals. It has a wide application in content based image retrieval, image compression, image segmentation, image encryption [93] – [94]. It had also found its application in detecting faults in transmission [95] – [100] and distribution system. Successful algorithms have been developed identifying and locating different types of faults. The author in [101] has been successful in identifying faults in a non –linear system by using Wavelet Transform. The author in [102] – [104] has been successful in detecting high impedance fault in distribution system.

When WT fails to capture the information content in the signal WPT is employed to develop the algorithm. Several works [105] – [106] have been carried out for combination of WPT and artificial intelligence.

In the present chapter, current and voltage measurement have been collected at the substation end for both the sample distribution system as discussed in the previous chapter. Current samples are used for the purpose of identification and classification, whereas voltage samples are used for locating faults. Features are collected using wavelet and wavelet packet decomposition. These features are then fed to artificial neural network. This is for classifying and locating all ten types of fault with perfection. A comparative analysis of the result between wavelet and wavelet packet transform over different "*daubechies"* is presented. Further, feature extraction time, training time per sample and testing time per sample is also provided.

4.1 SAMPLE DISTRIBUTION SYSTEM

In order to overcome the multiple estimation problems, due to the existence of multiple locations (usually far away, one from each other) in the power distribution network, the sample 1 has been divided into 7 zones and sample 2 has been divided into 04 zones as discussed earlier in chapter -1. Table 1 gives a complete overview of the number of current and voltage samples collected at each zones respectively:

Table: 4.1- Number of current and voltage samples collected

Name	**SD 1**	**SD 2**
No of Zones	7	4
Fault Resistance (Ω)	0.05, 10, 20, 30, 40, 50	0.05, 10, 20, 30, 40, 50
Fault Inception Angle (°)	0, 60, 90, 180	0, 60, 90, 180
Fault Types	10	10
Total Samples	3107	768

In the first distribution system considered for simulation zone 1, zone 2 and zone 3 consists of all ten types of faults. Zone 4 and zone 5 consists of only one fault since it involves only phase –b. Similarly, Zone 6 and zone 7 consists of only one fault since it involves only phase –c. On the other hand, in the second distribution system considered zone 1 and zone 3 comprises of all ten types of fault. While, zone 2 involves 4 types as it involves phase – b and phase – c. Also, zone 4 involves 4 types as it involves phase – a and phase – c respectively.

The sampling frequency considered for the present work is 15.360 kHz. The duration of run for the present simulation in both the cases is 0.5 sec. Fault has been incepted according to the various inception angle. The solution time step is 25 μs. It is the EMTDC simulation time step. The channel plot step is 65.104 μs which in turn determines the sampling frequency. It should be kept in mind that more is the sampling frequency; more is the information content in a signal. In the present work and in the consequent chapters effort has been made that the algorithm effectively works with minimum information content.

4.2 FEATURE EXTRACTION

Feature extraction is the basic need for development of protection algorithms using digital signal processing tools. It transforms data of high dimension to a lower dimension. But at the same time, the embedded information content is kept intact. Also the dimensionality of data is reduced. Further, the complexity for the purpose classification or regression is decreased. The signal is analyzed by multi – resolution approach. It has been designed in a manner that at high frequencies, good time resolution and poor frequency resolution is obtained. Similarly, at lower frequencies good frequency resolution and poor time resolution is calculated. In the present work wavelet and wavelet packet transform is used to extract the features of current and voltage samples.

4.2.1 Wavelet Transform (WT)

Wavelet Transform conquers over the limitations of the Fourier methods since it analyzes functions both in time and frequency domain. It is well suited to non – periodic wideband signals. It is defined by the following equation:

$$\text{DWT}(l, q) = \frac{1}{\sqrt{c_0^l}} \sum_r g\left(\frac{v - rd_0 c_0^l}{c_0^l}\right) \tag{4.1}$$

Here, p (.) is the mother wavelet and the scaling and translation parameters (c) and (d) shown in equation (3. 2) are functions of an integer parameter m, i.e. $c = c_0^l$ and $d = rd_0c_0^l$ which results into daughter wavelets. q is an integer variable which refers to a particular sample number in an input signal. The scaling parameter gives rise to geometric scaling, i.e. $1, \frac{1}{c_0}, \frac{1}{c_0^2}, \ldots\ldots\ldots$ The logarithmic frequency coverage of the discrete wavelet transform is given by the above scaling.

The logarithmic frequency coverage of the discrete wavelet transform is given by the above scaling. In case of DWT, only approximations of the signal are decomposed to next level. In the present work, third level decomposition has been carried out for the voltage and current signals. Figure 4.1 gives third level decomposition of the current signals.

4.2.2 Wavelet Packet Transform (WPT)

WPT represents high frequency information in a better manner when compared with DWT. In case of DWT, only approximations of the signal are decomposed to next level. WPT splits both approximations and details. Figure 4.2 gives third level decomposition of the current signals.

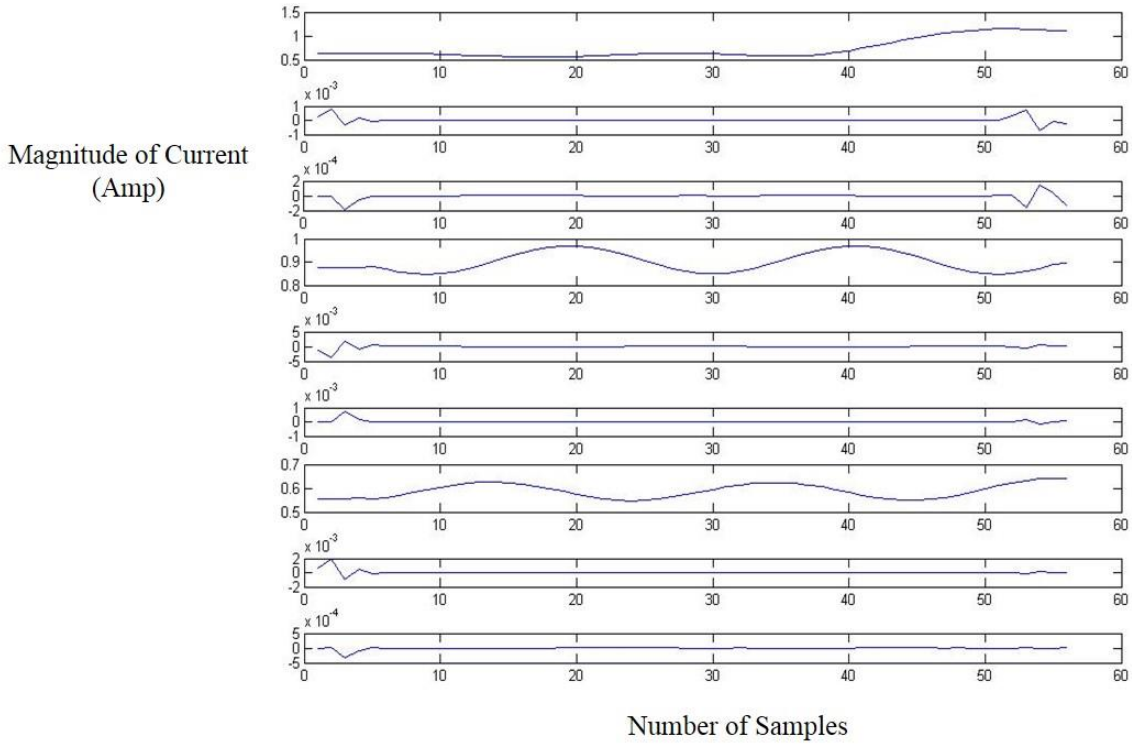

Figure 4.1: Third level decomposition of current signal using DWT

If one talks about n levels of decomposition in the WPT, 2^n different sets of coefficients are obtained. In case of DWT (3n + 1) sets of coefficients were obtained. It should be observed that However, number of coefficients is same in both the cases due to the process of down sampling. Also, there exists no redundancy. The sequence function P(x) is defined as,

$$P_{2r}(s) = 2^{j/2} \sum w_v P_r\left(2^{j/2}s - q\right) \qquad (4.2)$$

$$P_{2r+1}(s) = 2^{j/2} \sum p_q P_r\left(2^{j/2}s - q\right) \tag{4.3}$$

Where i, q ϵ X, r ϵ R; $2^{j/2}$ $P_r(2^{j/2}$ s-q) is a WP function; j, q, r are the scale factor, time factor, oscillating factor respectively. P_0 (s) is a scaling function or a basis function; P_1 (s) is wavelet function; w_q, e_q are groups of conjugate mirror filter, that satisfies

$$\sum_{r\epsilon x} w_{r-2} w_{r-2u} = \delta_{vu}, \tag{4.4}$$

$$\sum_{r\epsilon X} w_r = \sqrt{2}, e_v = (-1)^v w_{l-v} \tag{4.5}$$

Signal s (t) is expressed by orthogonal wavelet packet basis function as follows:

$$U_{i,l}(q) = \sum_r U_{i+1,2l}(r) w_{q-2r} + \sum_n U_{i+1,2l+1}(r) e_{q-2r} \tag{4.6}$$

Here $w_{v-2r,}$ p_{q-2r} is conjugate of w_{q-2r} and p_{q-2r}.

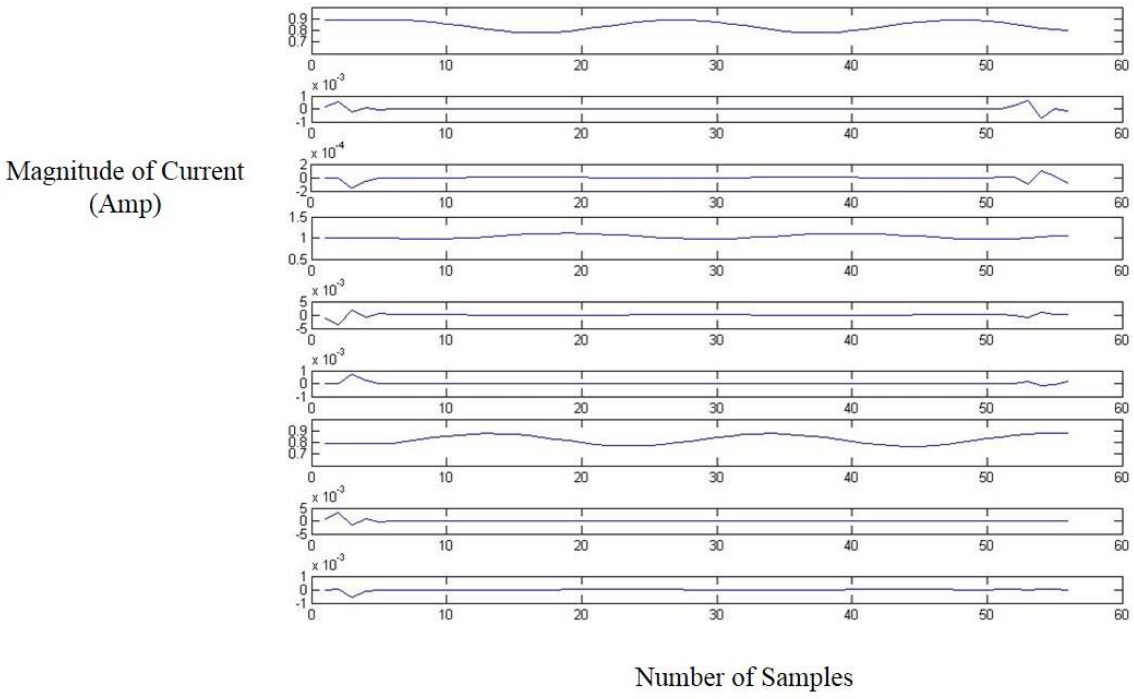

Figure 4.2: Third level decomposition of current signal using WPT

The different frequency distributions used in wavelet transform and wavelet packet transform for three level decomposition of current signal is seen in Table 4.2:

Table 4.2: Frequency Distribution for different levels of decomposition

Decomposition Level	Frequency in Hz
Initial Frequency	15360
1st	7680
2nd	3840
3rd	1920

4.3 NEURAL NETWORK

A neural network [87] is defined as the set of organized elements better known as neurons. Each connection has weight associated with it. It basically consists of three or more layers [88]. The first layer is the input layer which feds data into the network. The intermediate layer also knows as the hidden layer has weights associated with it. The neurons in the hidden layer collect the weighted inputs and compute the outputs by the given transfer function hidden layer is fed to the subsequent layer until the desired output is achieved In the present work, Levenberg–Marquardt algorithm is employed. The network performance parameters mean square error "mse" was used for the purpose of classification and mean square error with regularization "msereg" was used for the purpose of location.

For the purpose of classification, the current samples features collected from WT and WPT are fed to the neural network. In the present work, the network stops learning, at the instant when the mean square error (MSE) or number of iterations reaches a predetermined target value of 0.000001 and the number of epochs considered was 2000. The purpose of training is to reduce mse to reasonably low value in few epochs. A maximum of 2000 epochs was considered since as per the configuration of the sample system some samples required approximately 1800 – 1950 epochs to obtain accuracy. Similarly, for the purpose of location maximum of epoch considered was 3000. Another feature of the algorithm is that it only involves 33% of the samples for training and rest 77% for testing. It has been observed in the literature almost 50% - 70% of samples are used for training the neural network and rest data is used for testing.

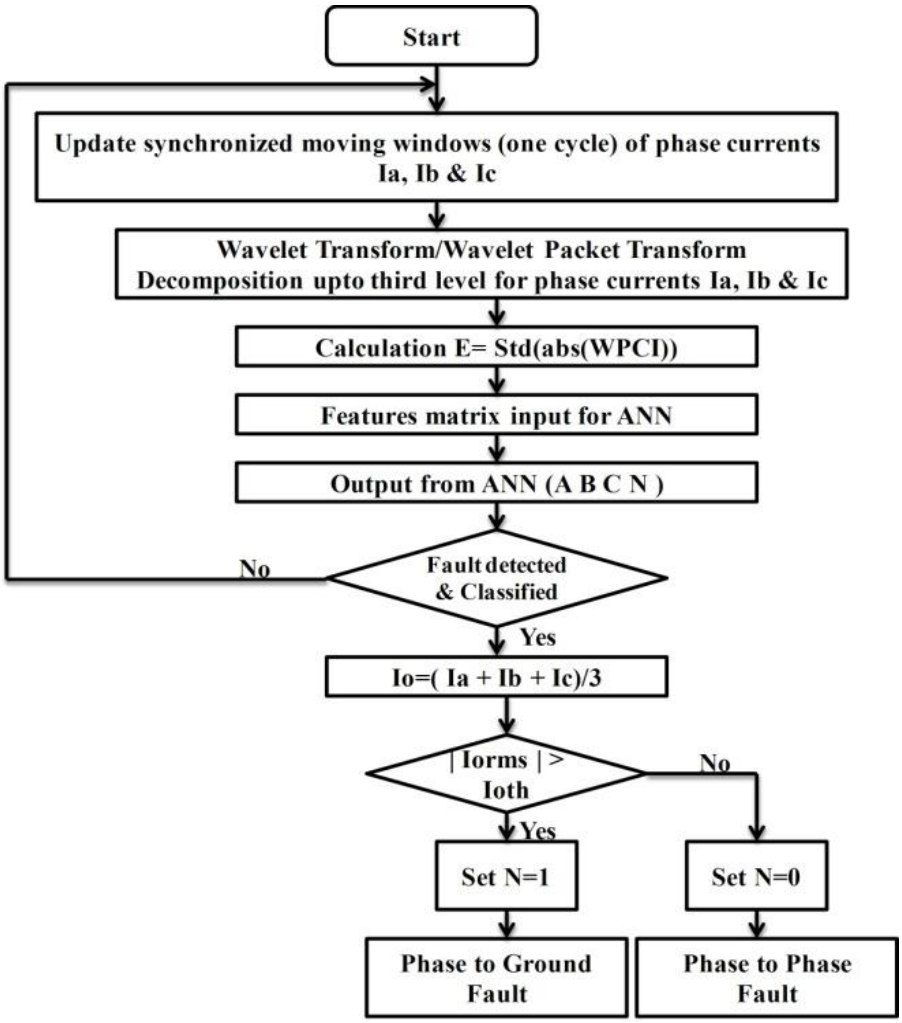

Figure 4.3: Algorithm for Fault Classification

4.4 ALGORITHM

Separate algorithm has been developed for classifying and locating faults in distribution system. The algorithm is effective in giving results by employing less than quarter of full cycle data of the sample collected. The algorithm for classification of fault is given in flowchart as shown in figure 4. 3.

4.5 EXPERIMENTAL RESULTS AND DISCUSSION

4.5.1 Classification Result for SD1

The results are presented below in terms of total classification error; classification error for all sections for both sample 1 and sample 2. The results are compared for different daubechies family *"db1, db2, db4* and *db8*" respectively. Total Classification Error is determined as:

$$\text{Total Classification Error } (\%\text{age}) = \frac{\text{Number of Misclassified Samples}}{\text{Total number of samples in that particular zone}} \times 100$$

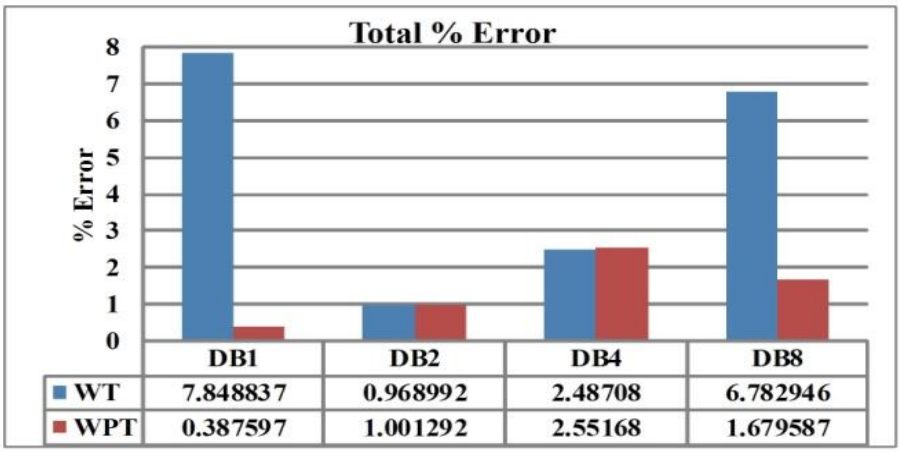

Figure 4.4: Total Classification Error for SD1

It is observed from the above figure that 99.61% of the samples have been classified accurately by using mother wavelet "db1" WPT features. At the same time, db1 of WT gives a maximum error of 7.848837%. Even though "db2" of WT gives a slightly better result (0.0323%) than db2 of WPT, overall WPT outperforms the WT features. Based on the above figure it is concluded that current features obtained from WPT yield better classification result.

Fig. 4.5 depicts the classification error for four different types of daubechies considered in WT and WPT for all the seven sections of SD1. As seen from the above figure: section 1, section 2 does not give any error for both the features. WT db1 of section 3, section 4, and section 5 gives a maximum error of 10. 4166%, 95.833% and 100% as compared with db2, db4 and db8 respectively. One thing should be kept in mind that section 1, 2 and 3 consists of 2880 samples whereas section 4, 5, 6 and 7 constitutes only 216 samples. WT db1 in section 4 and section 5 gives a maximum error of 95.83%

and 100% respectively whereas WPT db1 gives 0% error for the same section. WT db1, db2, db4 and db8 fail to classify the sections 4, 5, 6 and 7 accurately. It might be due to the fact that very less samples were considered for training.

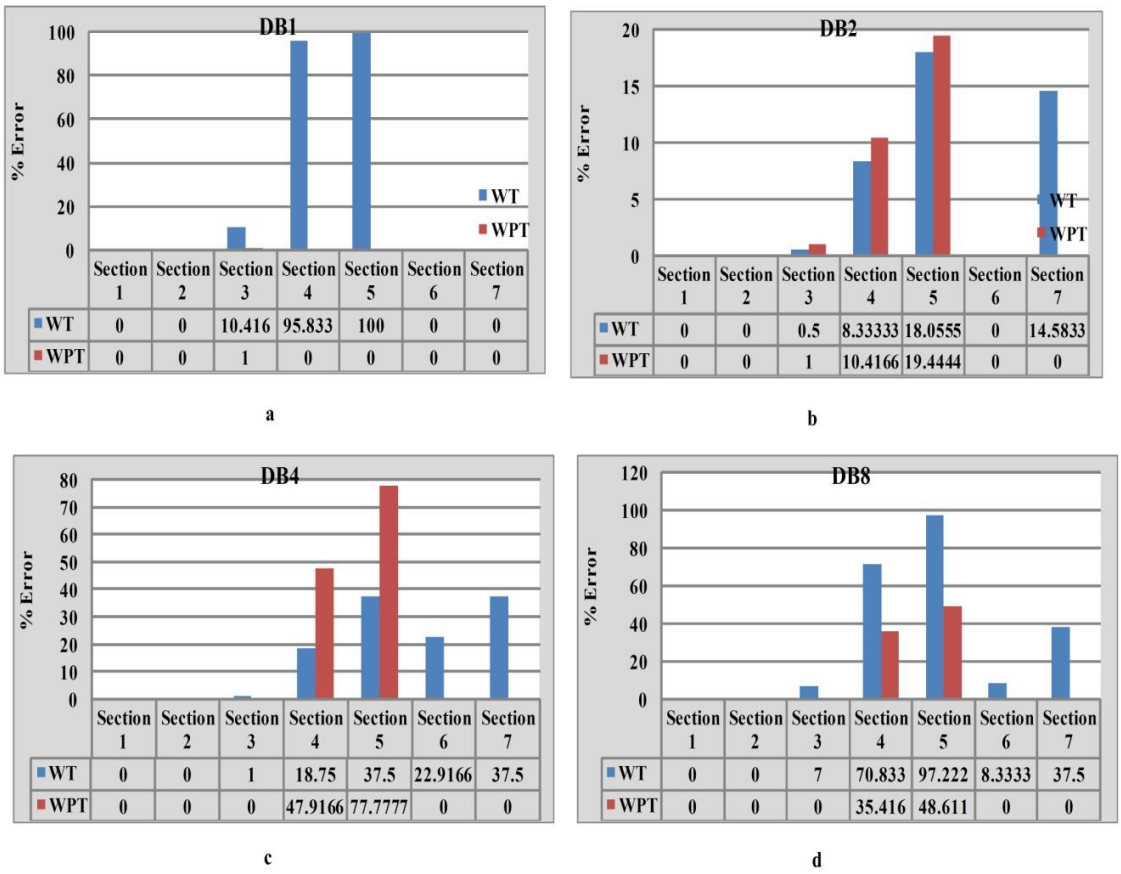

Figure 4.5: Classification Error for all Sections for SD1

It is evident from the above figure that section 1 and section 2 are classified properly and both WPT and WT give better result. In section 3, db4 and db8 of WPT gives no error as compared to db1 and db2 of WPT. But for section 4 and section 5 db1 of WPT outperforms completely with no error over db2, db4 and db8 where the error is (10.416%, 19.444%) for db2, (47.9166%, 77.777%) for db4, and (35.416%, 48.611%) for db8 respectively. Based on the other results it is therefore concluded that db1 of WPT provides best result for classification.

4.5.2 Classification Result for SD2

It is seen from the 4.6 figure that 99.158% of the samples have been classified accurately by using“db1” WPT features. On the same time db1, db2, db4 and db8 of WT gives a maximum error

of 9.864%, 7.321%, 3.465% and 10.621% respectively. Whereas db1 (0.842%) of WPT have an edge over db2, db4 and db8 where the error are 1.962%, 3.132%, 2.216% respectively.

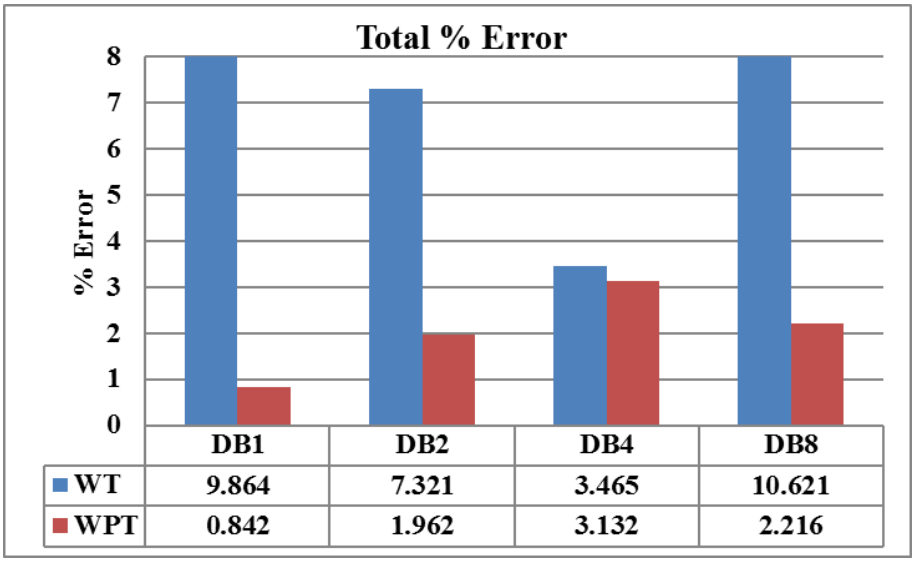

Figure 4.6: Total Classification Error for SD2

The classification error for four different types of daubechies considered in WT and WPT for all the four sections of SD2 can be observed in Fig. 4.7. It is obvious from the above figure that WT does not performs well to classify the faults. Db4 of WT gives better result than “db1”, “db2” and “db8” respectively. But for more accuracy, WPT performs far better than db1, db2 db4 and db8 of WPT. Using db1 of WPT, section 1 has an error of 1.612% as compared to the results of section 2, 3 and 4 which has an error of 0.913%, 0.324% and 0.889% respectively. Still, mother wavelet db1 of WPT yields accurate result.

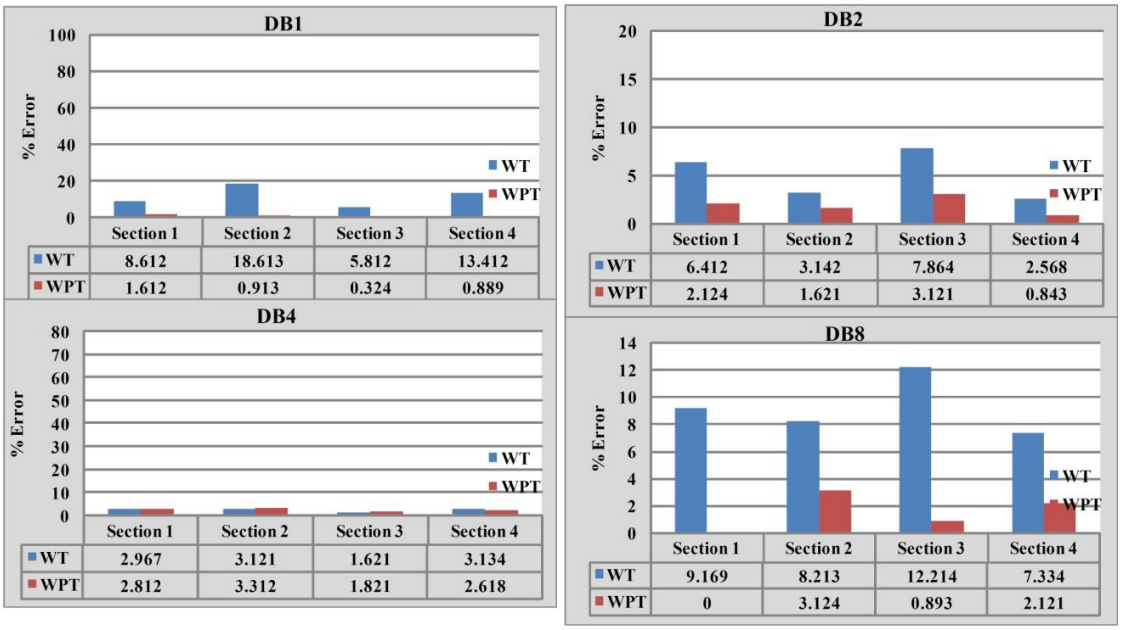

Figure 4.7: Classification Error for all Sections for SD2

4.5.3 Location Result for SD1

Fig. 4.8 depicts the location error obtained from using features obtained from WPT for all the seven sections of SD1. It is seen from the results obtained in zone - 1 that the maximum error is 0. 2468% and average error is 0.0161% for AG fault which is very good. The maximum and average error for double – phase to ground BCG fault in this zone is 0.2752% and 0.0206% respectively. Further, improvement in results can be noticed in zone - 2 where maximum and average error is 0.515 and 0.2% respectively for double – phase to ground fault (ACG fault) which proves the effectiveness of the algorithm. Similarly, the maximum error and average error in section – 3 is 3.5065% and 0.3288 respectively for AG fault. The maximum error is due to the fact that laterals are present. The results presented in the other sections are almost negligible and are in the range which would not disturb the effectiveness of the algorithm.

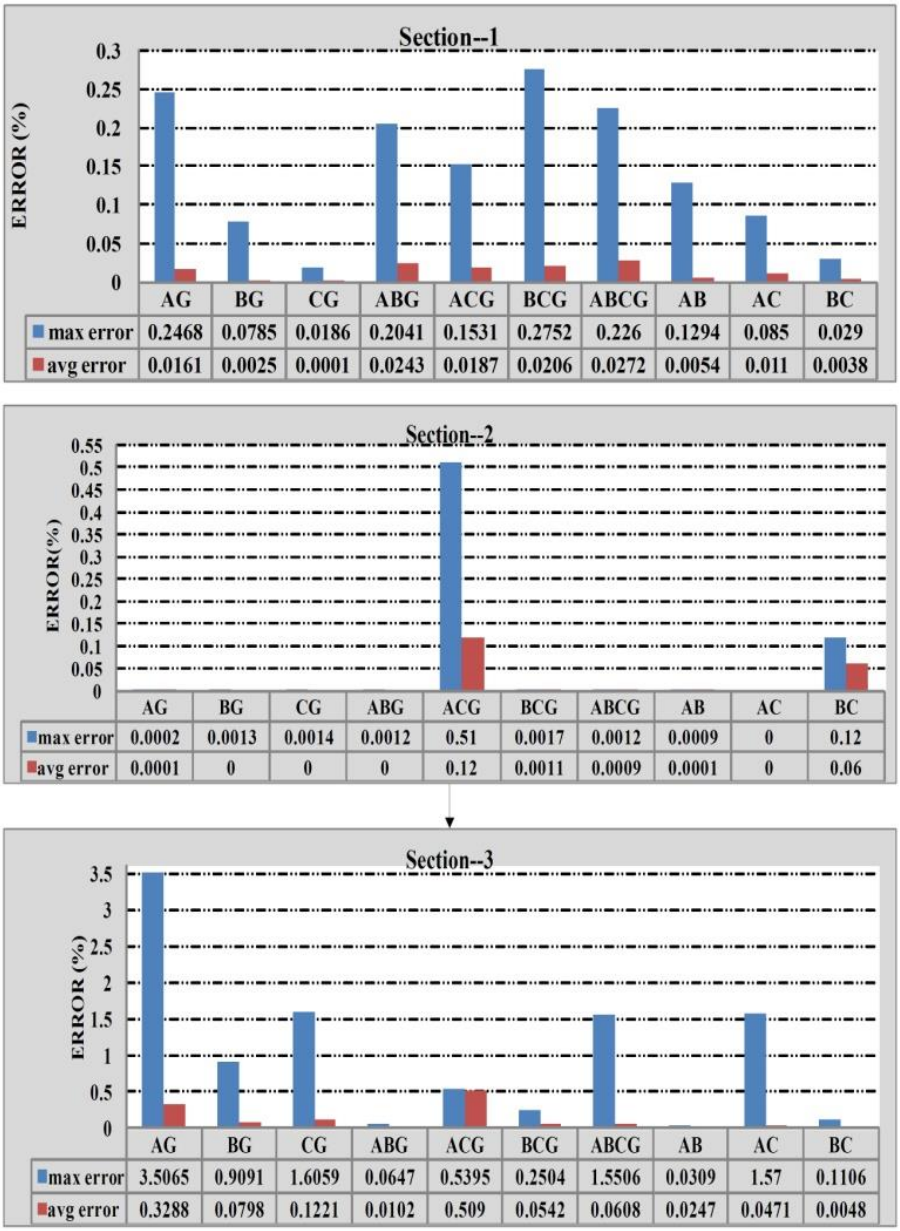

Figure 4.8: Location Error for all Sections for SD1

Table 4.3: Maximum and Average Error

Section	Maximum Error	Average Error
Section - 4	0.341	0.211
Section - 5	0.132	0.111
Section – 6	0.4001	0.121
Section - 74	0.352	0.310

Table 4.3 gives a detail description of the results obtained for section 4, 5, 6 and 7 respectively. As discussed earlier in chapter 2, these sections consist of only one phase. Similar appealing results are also observed in section 4, 5 and 6 respectively. It should also be kept in mind that the results have been compared with the impedance based method as adopted in [6] and [107].

4.5.4 Location Result for SD2

Fig. 4.9 depicts the location error obtained from using features obtained from WPT for all the four sections of SD1.

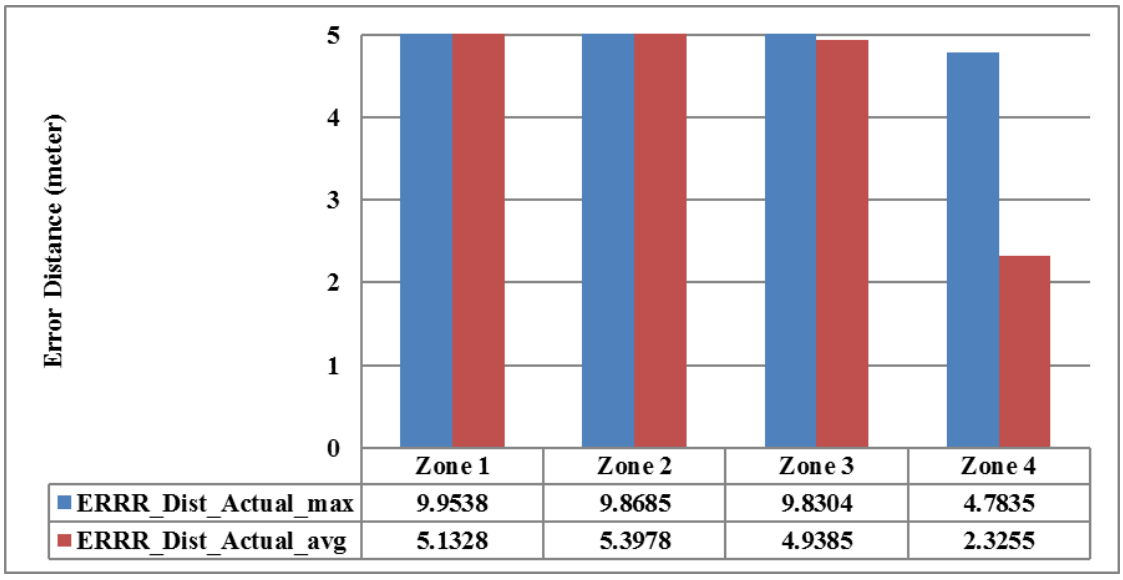

Figure 4.9: Location Error for all Sections for SD2

The location error are represented as maximum error and average error. As seen from the above figure the maximum error is 9.9538 metres in zone1 , 9.865 mts in zone 2 , 98304 mts in zone 3 and 4.7835mts. The average error is 5.1328 m, 5.39 m, 4.93 m, and 2.32m which is very promising. The results have not been compared with any other results since for this particular system since in any literature fault location has not been carried out. Further, zone wise error % age is presented below.

In order to introspect the result obtained and to get a better picture of the error obtained zone wise error is demonstrated for all the ten types of fault. As mentioned in chapter-1, 1to 10 represents the ten different types of faults involving different phases. Fig. 4.10 depicts the location error for zone 1. Results have been presented as maximum error and average error respectively. Here, the maximum error is 0.985% for AG fault. The average error is same 0.586% for AG and CG fault. The maximum error for all types of fault lies in between 0.7% to 0.9% respectively. Overall, the

error result is less than 1% which is very promising. The average error lies in between 0.402% to 0.586%.

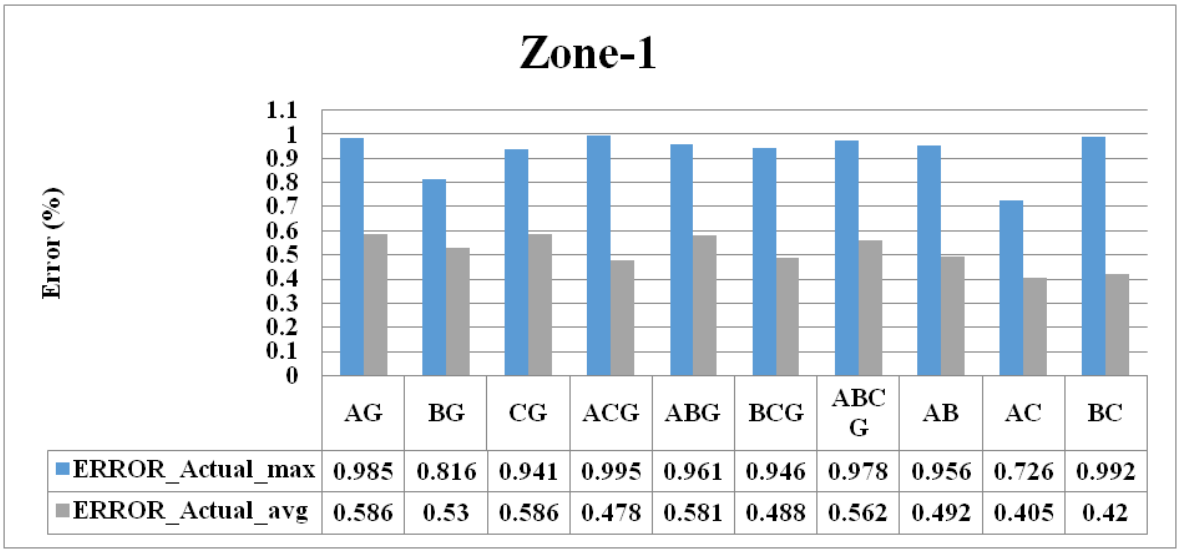

Figure 4.10: Location Error for Zone 1 for SD2

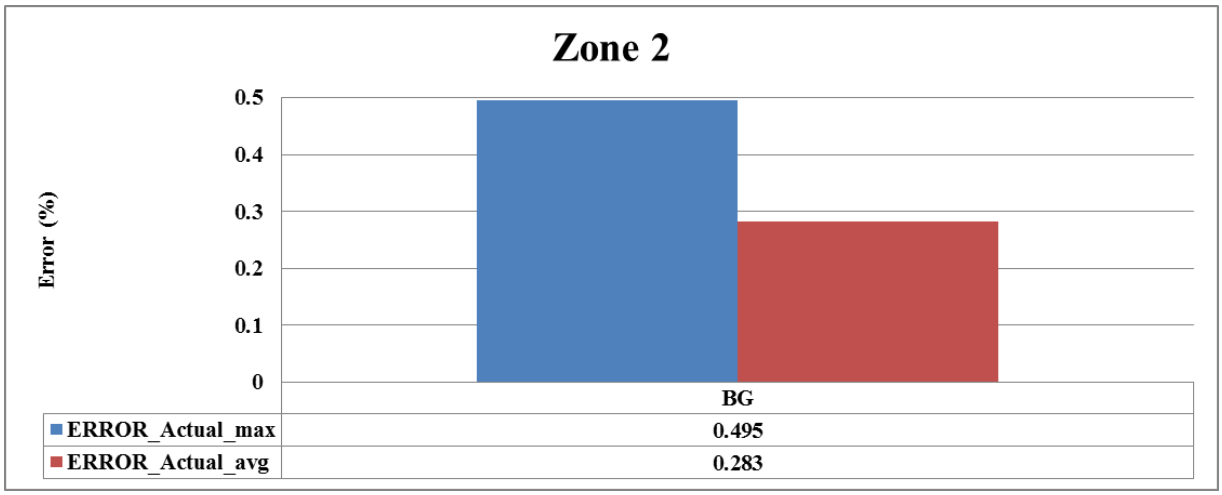

Figure 4.11: Location Error for Zone 1 for SD2

Fig. 4.11 depicts the location error for zone 2. Results have been presented as maximum error and average error respectively. Here, the maximum error is 0.495% .Average error for BG fault is more i. e. 0.283%. Zone 2 also demonstrates better result.

Fig. 4.12 presents the location error for zone 3. Results have been presented as maximum error and average error respectively. Here, the maximum error is 0.986% for BC fault and average error is 0.572% for ABG fault. Excluding ABCG fault, all other types of fault are in between 0.51% to

0.55%. It may be due to the fact that it involves all three phases and ground. In zone 3 also the results for all the ten types of fault are under 1%. Overall, the error result is very promising.

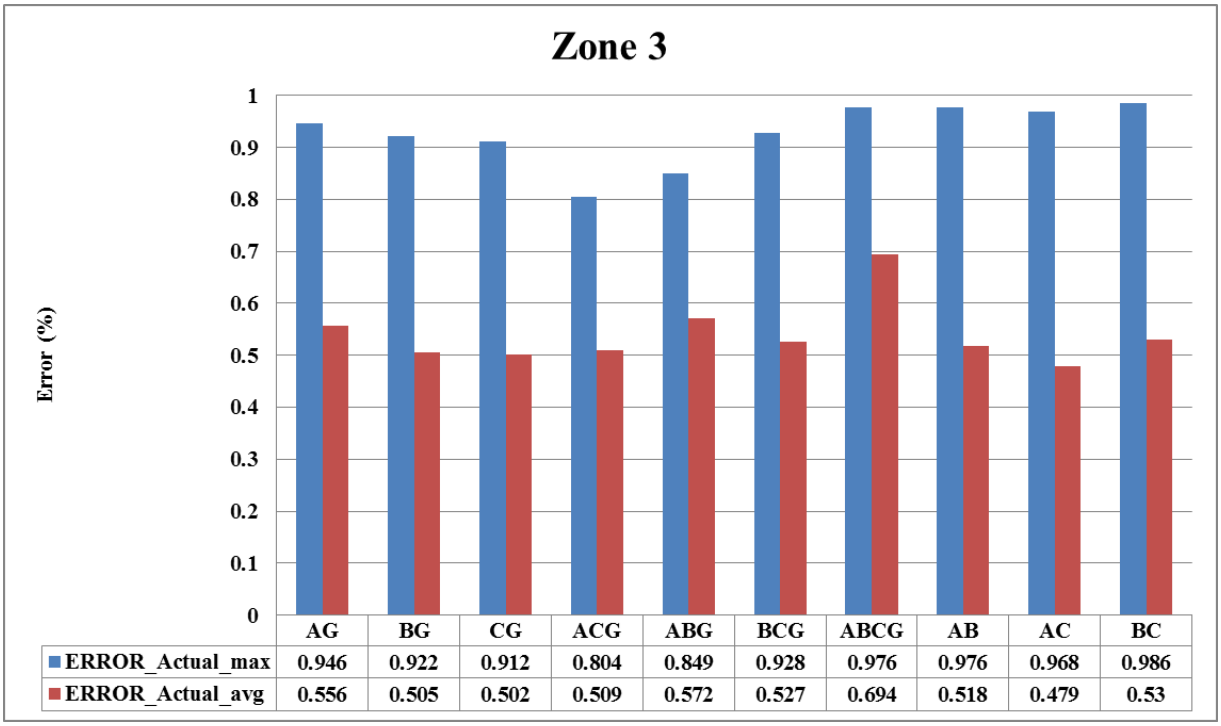

	AG	BG	CG	ACG	ABG	BCG	ABCG	AB	AC	BC
ERROR_Actual_max	0.946	0.922	0.912	0.804	0.849	0.928	0.976	0.976	0.968	0.986
ERROR_Actual_avg	0.556	0.505	0.502	0.509	0.572	0.527	0.694	0.518	0.479	0.53

Figure 4.12: Location Error for Zone 3 for SD2

Fig. 4.13 depicts the location error for zone 4. Results have been presented as maximum error and average error respectively. Here, the maximum error is 1.003% for AG fault; rest CG and AC are with 0.917% and 0.964% respectively .Average error for AG, CG and AC fault is. 0.544%., 0.519% and 0485% respectively. Zone 4 also demonstrates better result but has the maximum slightly error more than 1% which does not make any difference.

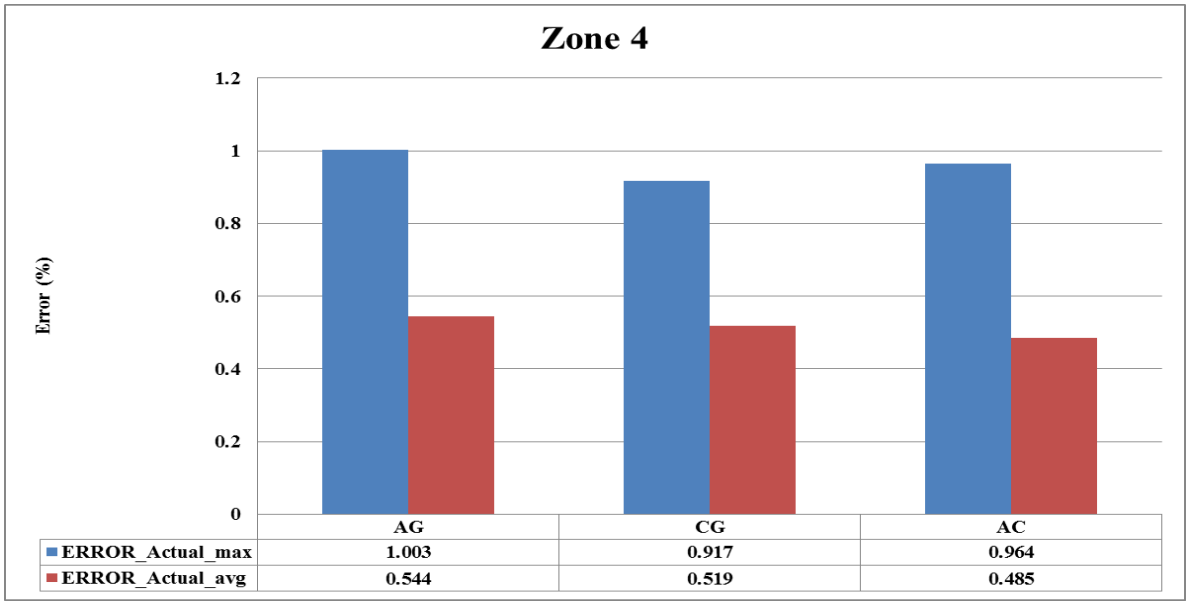

Figure 4.13: Location Error for Zone 4 for SD2

4.6 COMPUTATIONAL TIME

In the figure 4.14, computation time taken for various processes involved for development of algorithm using WT has been presented. The computational time for WPT is presented in figure 4.15. It should be noted that all these times were evaluated after calculating the total time taken for each process divided by total no of samples considered. The configuration of the computer on which the algorithm for fault classification and fault location was tested is as: Core*i7* processor, 3.2GHz speed, 12 GB Ram memory.

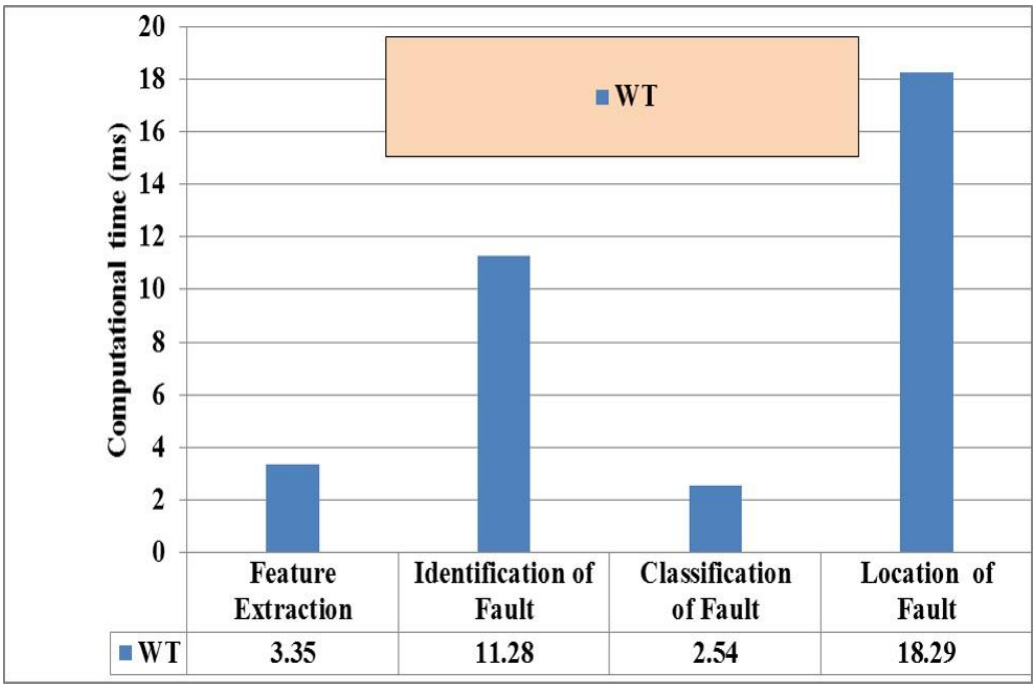

Figure 4.14: Computational Time for Different Evolutionary Process using WT

The feature extraction time is 3.35 ms which is very low as compared with other signal processing tools. The time taken for identification of faults is 11.28ms, classification of faults is 2.54 ms and for location of fault is 18.29 ms respectively.

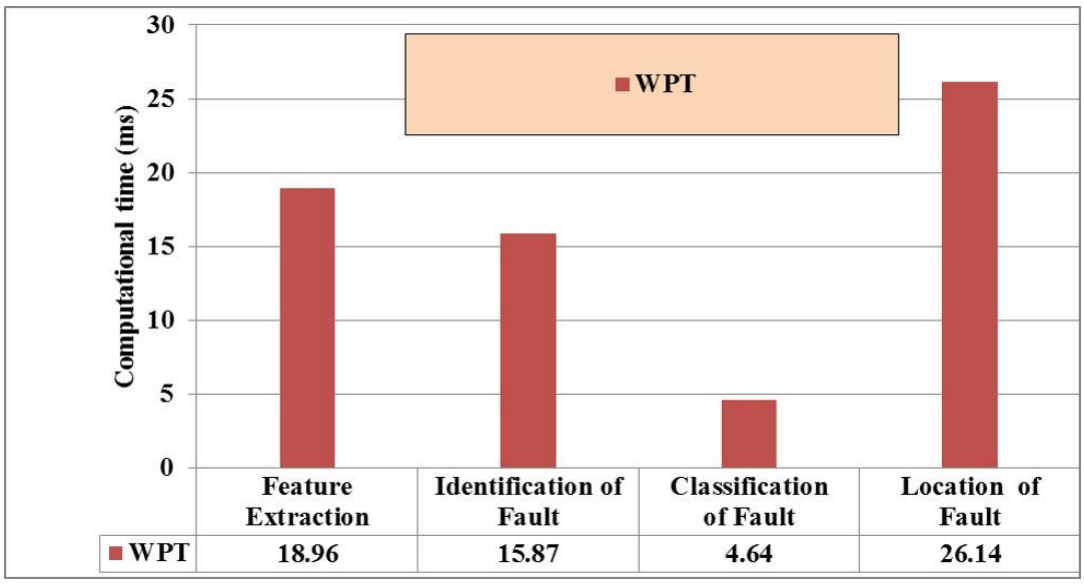

Figure 4.15: Computational Time for Different Evolutionary Process using WPT

The feature extraction time is 18.96 ms which is very low as compared with other signal processing tools. The time taken for identification of faults is 15.87 ms, classification of faults is 4.64 ms and for location of fault is 26.14 ms respectively.

4.7 SUMMARY

A comparative analysis of the result between wavelet and wavelet packet transform over different "*daubechies"* has been presented for the purpose of classification. As per the result obtained even though the classification accuracy is 99.61% in case of WPT and 99.03% in case of WT for SD1, the location accuracy obtained is more in case of WPT. It is quite evident from the results obtained that the feature extracted from WPT yield better result as compared to WT. It should be kept in mind that since WPT gives better classification result in both SD1 and SD2, hence these features were used for the purpose of location. The WPT results are promising but the computation time taken to obtain the result is high. This is proved due to the fact that both approximations and details are decomposed in WPT.

Gabor Transform Based Features

Chapter 5

Electric Power Distribution System is a complicated network of electrical power system. This is due to its complex configuration and extended lines. Now, these are subjected to faults which results in high value of current. Fast and exact location of fault plays a pivotal role in speeding up system restoration which is the need of modern day. Unlike transmission system which involves relatively a simple connection, distribution system has a very complicated structure thereby making it a herculean task to design the network for computational analysis. Transmission system had been a broad area for engineers due to its simplified structure. It carries major portion of power over long distances. But at present, the network of distribution system has expanded, the amount of power carried by the distribution grids has also enhanced quite considerably. Due to insufficient information about the network, and sometimes occurrence of high impedance faults, detection, identification and location of faults in a distribution system is indeed challenge. Further, in present scenario of digital protective relays, for correct operation of protective relays, there should be correct and fast determination of fault.

As already discussed, the methods adopted for locating faults in transmission lines cannot be easily applied to distribution system. Modern day trend recommends the use of algorithms developed by employing features extracted from digital signal processing tools. The author in [108] has defined an approach for detecting fault in transmission line using time – frequency analysis. Wavelet transform came into play for extraction of current features that can be subjected to algorithm meant for appropriate location of faults but yet an errorless fault location could not be achieved. Data structure based on N-ary trees has been proposed for locating faults. It contains all the information about the parameter of the network in compact manner. Further, it is helpful in development of algorithm for locating faults. Since, the uses of WT and WPT have already been discussed in the previous chapter. Now, Gabor Transform has also found its use in some of algorithms developed for identifying and classifying faults in transmission system. The author in [109] – [110] has introduced a concept of detecting, identifying and classifying faults in transmission system using

the features extracted from Gabor Transform and feeding it to ANN for the above said purpose. Recently, the features extracted from Gabor Transform were fed to ANN for detecting arcing faults in transmission lines [111]. The results obtained are good and hence, the combinations of features of GT and ANN have proved to be worth. The features of GT have not been used till date for detecting, identifying, classifying and locating faults in distribution system.

In the present chapter Gabor transform are used for fault identification and location in distribution system. Current and voltage samples have been measured at the substation end for both the sample distribution system as discussed in the Chapter 1. Current samples are used in the purpose of fault identification and classification, whereas voltage samples are used for locating faults. Also, discrimination between load current and fault current has been made.

Henceforth, current and voltage features are collected using Gabor decomposition. These features are provided as an input to artificial neural network for the purpose of fault classification and location of all ten types of fault with perfection. Further, feature extraction time, time taken for identification, classification and location of fault, is also provided.

5.1 SAMPLE DISTRIBUTION SYSTEM

Two sample distribution systems have been considered as already described in section 1.3.1 and 1.3.2 of Chapter 1. The problem of the multiple estimation of location of faults has also been tackled. It arises due to presence of laterals at the same distance in the power distribution network by dividing the network into various zones.

The sample distribution (SD 1) has been divided into 7 zones and sample distribution (SD 2) has been divided into 04 zones. In the first distribution system considered for simulation, zone 1, zone 2 and zone 3 consists of all ten types of faults. Zone 4 and zone 5 consists of only one fault since it involves only phase –b. Similarly, Zone 6 and zone 7 consists of only one fault since it involves only phase –c.

On the other hand, in the second distribution system considered zone 1 and zone 3 comprises of all ten types of fault. While, zone 2 involves 4 types as it involves phase – b and phase – c. Also, zone 4 involves 4 types as it involves phase – a and phase – c respectively. Also, the current and voltage database have been made by increasing the load present in the particular zone to 25%.

In total 7750 samples have been used for evaluating the effectiveness of the algorithm developed. A total of 6214 current and voltage samples for zone 1 and 1536 samples for zone 2 have been collected for preparing the database and used for testing the algorithm. Table 5.1 gives a complete overview of the number of current and voltage samples collected at each zones respectively:

Table: 5 1- Number of current and voltage samples collected

Name	**SD 1**	**SD 2**
No of Zones	7	4
Fault Resistance (Ω)	0.05, 10, 20, 30, 40, 50	0.05, 10, 20, 30, 40, 50
Fault Inception Angle (°)	0, 60, 90, 180	0, 60, 90, 180
Fault Types	10	10
Load (+)	25%	25%
Total Samples	**6214**	**1536**

The sampling frequency considered for the present work is 12.000 kHz. The duration of run for the present simulation in both the cases is 0.5 sec. Fault has been simulated at various inception angles as mentioned in Table 5.1. The solution time step is 42 µs. This is the EMTDC simulation time step. The channel plot step is 83.333 µs which in turn determines the sampling frequency. This is the time interval at which EMTDC sends data to PSCAD for plotting as well as writing data to output files. It should be kept in mind that more is the sampling frequency; more is the information content in a signal.

5.2 DISCRIMINATION BETWEEN LOAD CURRENT AND FAULT CURRENT

Sometimes, there is a similarity between load data and fault data. Due to which one may consider the load data to be classified as fault. This leads to wrong estimation of fault. In order to overcome this difficulty, current and voltage samples collected at 100% and 25% increased load has been distinguished from fault data by calculating mean and standard deviation and then subjecting it to ANN.

5.2.1 Mean

It is the average of current and voltage signal. For a normal signal without fault, its value is zero. During the presence of faults, transients present in the signal makes the value of mean other than zero. Mathematically, it is represented as:

$$\overline{y} = \frac{1}{t_2 - t_1}\int_{t_1}^{t_2} y(t)dt \qquad (5.1)$$

$y(t)$ represent the signal and $\overline{y}$ is its average.

5.2.2 Standard Deviation:

It is the computation of deviation from its mean value. Mathematically, it is given as: $\gamma(t_1, t_2) = (\int_{t_1}^{t_2} (y(t) - \overline{y})^2 dt)^{\frac{1}{2}}$

(5.2)

γ: Standard deviation. Standard deviation for a normal signal without fault is one. While, for a transient signal the value deviates from one. Figure 5.1 gives the method adopted to distinguish between load data and fault data.

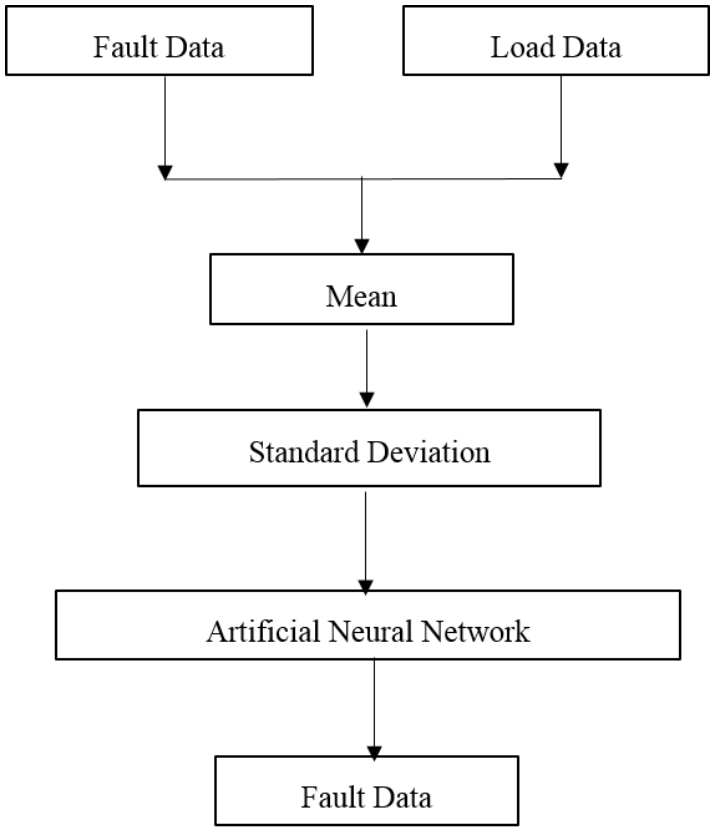

Figure 5.1: Algorithm for Fault and Load Discrimination

At first, about 40% of fault data comprising of different phases voltages and current were fed to artificial neural network along with the load data which consists of load voltage and load current for training. Rest 60 % of the data was used for testing. In zone 1 of SD1 out of 6214 samples, only 65 samples were found out to be mismatching i.e. 98.95% of fault data were correctly classified. In zone 2 of SD1 out of 1536 samples, 28 samples were misclassified i.e. 98.15% of fault data were correctly classified. Now, these samples were considered for classification into ten types of faults as well as its location.

5.3 FEATURE EXTRACTION

Feature extraction transforms data of high dimension to a lower dimension. But at the same time, the embedded information content is kept intact. In the previous chapter wavelet and wavelet packet transform were used for feature extraction. As already discussed in Chapter 3 under section 3.2.2 wavelet transform suffers from mainly two disadvantages in order to analyze the signal. It

lacks in shift invariance. It means even when there is a small shift in the input signal, major difference in the distribution of energy between DWT coefficients at different scales is observed. Also, the frequency resolution of the decomposition filter may not be able to extract necessary information from the fault signal. Wavelet packet transform too suffers from the problem of shift – invariance since it is difficult to determine "the best basis" i.e. the one which provides the representation of input signal minimizing a cost function.

As mentioned earlier in the present algorithm, Gabor transform is used as a tool to extract the features of current and voltage samples.

5.3.1 Gabor Transform (GT)

As discussed in the Chapter 3, under section Gabor filter was originally introduced by Dennis Gabor. It is developed from the short – time Fourier transform. It contains a Gaussian window. There are some reasons that justify the use of this transform.

- It presents a best example of localization in combined spatial and frequency domains. This further helps in taking our information from the signals.
- Lower order of entropy is also reduced. It helps in applications meant for data reduction.

The Gaussian window used is as follows:

$$a_{t_0,\omega_0}(t) = p(t - t_0).\exp(jf_0 t) \tag{5.3}$$

Here $p(t)$ is the window function:

$$p(t) = \left(\sqrt{2\lambda}\right)^{\frac{1}{2}} \exp\left(-\prod \lambda^2 t^2\right) \tag{5.4}$$

λ : Window Width

χ : Phase constant of the changing oscillations

f_0 : Frequency of these oscillations

t_0 : Window function Centre

The Gabor representation for any signal $s(t)$, in order to find out a set of coefficients is given by:

$$s(t) = \sum_{n=-\infty}^{\infty} \sum_{k=-\infty}^{\infty} b_{nk} a_{nk} \tag{5.5}$$

Here, a_{mr} is the basis function. For 1- D a finite extent $s(t), t \in [0, L-1]$ with $L \prec \infty$, only finite number of windows intervals shall be present. When $L = dN$, where d is a positive integer that represents the number of windows covering the whole signal $s(t)$, the GEFs' can be translated so that they are centered at central point of each window as follows:

$$a_{mr}(t) = p(q(t) - nN).ee^{j\frac{2\Pi\Pi q(k) q(t)}{N}} \tag{5.6}$$

Where,

$$q(y) = y - \frac{N-1}{2} \tag{5.7}$$

Gabor Transform is redrafted as:

$$s(t) = \sum_{n=0}^{d-1} \sum_{k=0}^{n-1} b_{nk} a_{nk} \tag{5.8}$$

The coefficients b_{nk} constitute one dimensional Gabor transform.

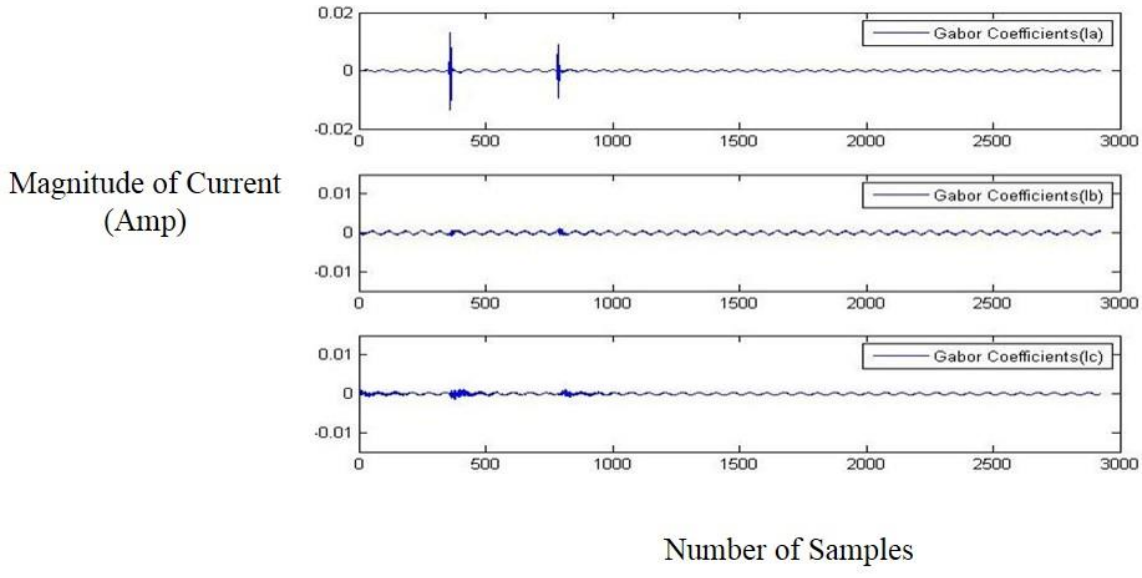

Figure 5.2: 1 Level Decomposition for Fault Classification.

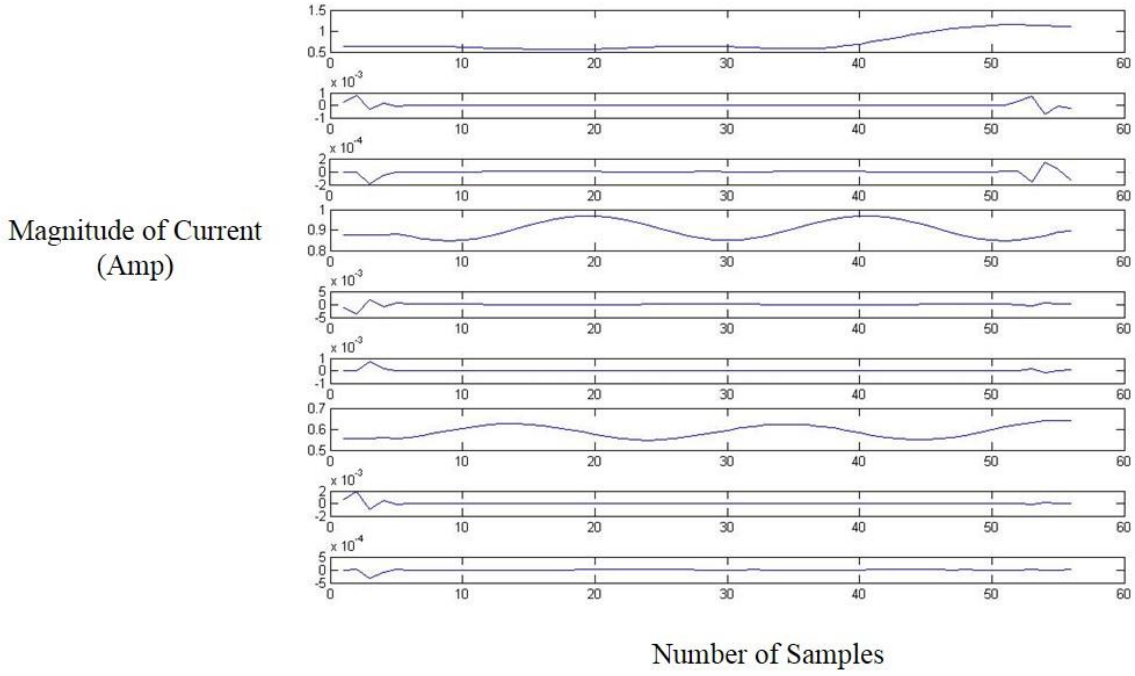

Figure 5.3: 4 level decomposition of current signal using Gabor transform

In Gabor Transform, one obtains the coefficients through high pass filter only. It gives detail information which is required to trap the sudden changes in the fault signal. In the present work, the signals are decomposed by one level as shown in figure 5.2 and are used for fault classification. Further, they are decomposed by four levels as shown in figure 5.3 and have been used for fault location.

The different frequency distributions used in Gabor Transform for up to four level decomposition of current signal is seen in Table 5.2:

Table 5.2: Frequency Distribution for different levels of decomposition

Decomposition Level	Frequency in Hz
Initial Frequency	12000
1st	6000
2nd	3000
3rd	1500
4th	750

5.4 NEURAL NETWORK

In the present work, Levenberg–Marquardt algorithm is employed. The network performance parameters mean square error “mse” was used for the purpose of fault classification and mean square error with regularization “msereg” has been employed for the purpose of location of faults.

In case of fault classification, the features of current samples collected from GT are fed to the neural network. In the present work, the network stops learning when either the mean square error (mse) or number of iterations have reached a predetermined target value which was set to 0.000001 and the number of epochs considered was 1500. The purpose of training is to reduce mse to reasonably low value in few epochs. A maximum of 1500 epochs was considered since as per the configuration of the sample system some samples required approximately 1800 – 1950 epochs to obtain accuracy. Similarly, for the purpose of fault location maximum value of 4000 epoch was considered. Another feature of the algorithm is that it only involves 25% of the samples for training and rest 75% for testing.

5.5 ALGORITHM

Separate algorithm has been developed for classification and location of faults. The algorithm is effective in giving results by employing less than quarter of full cycle data of the sample collected. The algorithm for classification of fault is given in flowchart shown in figure 5.4.

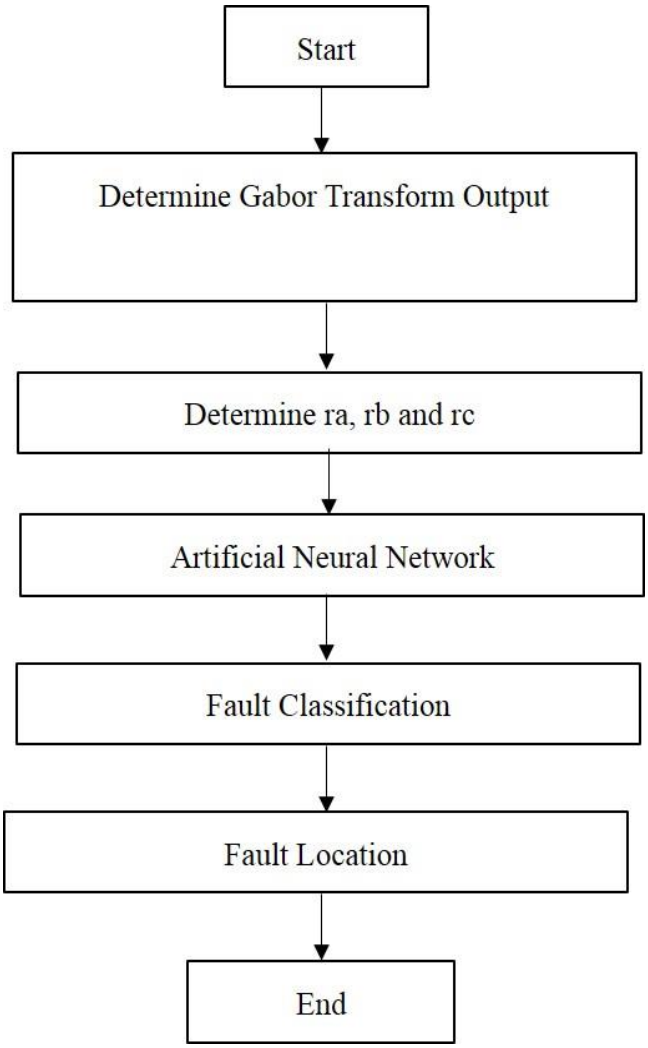

Figure 5.4: Algorithm for Fault Classification and Location

The following notations are required for preparing the algorithm:

G_a : Absolute values of Gabor transform components in phase "a".

G_b : Absolute values of Gabor transform components in phase "b"

G_c : Absolute values of Gabor transform components in phase "c"

M_a : Peak absolute value of Gabor transform component G_a

M_b : Peak absolute value of Gabor transform component G_b

M_c : Peak absolute value of Gabor transform component G_c

$$S_a = \sum |I_a|, S_b = \sum |I_b|, S_c = \sum |I_c| \quad (5.9)$$

Where

S_a : refers to summation of current in phase "a"

S_b : refers to summation of current in phase "b"

S_c : refers to summation of current in phase "c"

The values of S_a, S_b, S_c has been calculated using equation. (5.9). The system kept for observation is an unbalanced system which in turn provides variation in the magnitude of current for all the ten types of faults considered for different resistances. Hence, there exists a need for converting the values under similar benchmark for the purpose of computation. Thus, these values are subjected to normalization using equation (5.10).

Further, r_a, r_b, r_c values are calculated.

$$\begin{aligned} r_a &= 10 * M_a * S_a \\ r_b &= 10 * M_b * S_b \\ r_c &= 10 * M_c * S_c \end{aligned} \quad (5.10)$$

5.6 EXPERIMENTAL RESULTS AND DISCUSSION

5. 6. 1 Classification Result for SD1

The results are presented below in terms of total classification error; classification error for all sections for both sample 1 and sample 2.Total Classification Error is determined as:

$$\text{Total Classification Error } (\%\text{age}) = \frac{\text{Number of Misclassified Samples}}{\text{Total number of samples in that particular zone}} \times 100$$

It is depicted that 99.94% of faults have been accurately classified from the features obtained from Gabor Transform as compared to Wavelet Packet Transform where 97.294% of faults have been classified accurately. Table 5.3 gives the classification error for all the seven zones of sample distribution system 1 (SD1). Since, in the chapter – 4, WPT has given better result as compared to WT hence, the results of WPT has been compared with GT.

Table 5.3: Classification Error for Zones for SD1

S. No	Zones	WPT	GT
1	Zone 1	0.57	0.033
2	Zone 2	1.97	0.077
3	Zone 3	0.045	0
4	Zone 4	0.121	0.028
5	Zone 5	0	0
6	Zone 6	0	0
7	Zone 7	0	0

It can be seen from the above figure that the errors obtained are very less. With GT features Zone 1 and zone 2 has an error of 0.0333% and 0.0778% only as compared to 0.57% and 1.97% of WPT. Zone 3 of WPT gives error of 0.045% as compared to negligible error in case of GT. Zone 4 has an error of 0.28% which is also minimal. It is worth mentioning that zone 3, zone 5, zone 6 and zone 7 are errorless.

5. 6. 2 Classification Result for SD1

Table 5.4: Classification Error for Zones for SD2

S. No	Zones	WPT	GT
1	Zone 1	0.32	0
2	Zone 2	0.08	0
3	Zone 3	0.04	0
4	Zone 4	0.87	0.263

When the algorithm is applied to the features collected from the Gabor transform for SD2, the classification accuracy is 99.73% while the features extracted from Wavelet Packet Transform gives the classification accuracy of 98.69%. It is obvious that Gabor Transform fetches better result as compared to Wavelet Packet Transform. From table 5.4, it is obvious that errors are found in almost all zones for the features collected from WPT. It is observed that only zone 4 has an error of 0.263% while other zones are errorless for the features collected from GT while WPT gives the error of 0.87%. The result obtained from GT turns out to be promising as already discussed that zone 1 and zone 3 have maximum samples and zone 4 has very less sample.

5. 6. 3 Location Result for SD1

Table 5.6 depicts the location error for SD1 for all sections with a comparison between WPT and GT. The location errors are compared with the work of G. Morales Espana [121] where only average error has been demonstrated as shown in Table 2. Zone 4, zone 5, zone 6 and zone 7 results have not been reported owing to less number of samples.

Table 5.5: Average Error for all zones [112]

Zones	Average Error
Zone 1	1.483
Zone2	1.437
Zone 3	1.642

Table 5.6: Fault Location Error for Zones for SD1

S. No	Zones	WPT		GT	
		Maximum Error	Average Error	Maximum Error	Average Error
1	Zone 1	85.89	-6.23	43.61	-4.19
2	Zone 2	248.76	20.146	139.276	10.057
3	Zone 3	498.34	7.89	256.89	2.091
4	Zone 4	3.45	0.86	0.088	0.006
5	Zone 5	2.45	-0.57	0.557	-0.081
6	Zone 6	3.56	-1.34	1.52	-0.945
7	Zone 7	86.23	2.34	45.141	1.86

In the table shown above, the results obtained from Gabor features are very promising as compared to the results obtained from Wavelet Packet Transform. As discussed earlier, zone 1, 2 and 3 constitute the maximum number of samples, so the average error is just -4.190, 10.057, 2.091 m only which is negligible in case of GT while it is -6.23, 20.146 and 7.89 m respectively in case of WPT. It should be noted clearly that the negative sign indicates that the fault was under reached. It is obvious from the above table that the fault was under reached at zone 1, 5 and 6. The maximum error in zone 1, 2 and 3 is just 43.61, 139.276, 256.89 m as compared to 85.89, 248.76, 498.34 m in WPT. This again shows that the results obtained from GT are better than WPT. But that is not at all the problem since as per the details of the distance given zone 1 is in kilometers and few meters does not make any operational difference.

Table 5.7: Fault Location Error for Zone 1 for SD1

S. No	Faults	WPT		GT	
		Maximum Error	Average Error	Maximum Error	Average Error
1	**AG**	5.97	-1.245	3.162	-0.775
2	**BG**	5.632	-0.887	3.101	-0.667
3	**CG**	5.234	-1.456	3.2759	-0.810
4	**ABG**	5.567	-2.345	3.4326	-0.162
5	**ACG**	5.212	-1.008	3.3875	-0.187
6	**BCG**	4.987	-0.986	3.1218	-0.544
7	**ABCG**	6.234	1.763	4.3618	0.3045
8	**AB**	6.487	-0.258	3.4938	-0.125
9	**AC**	3.879	-0.348	3.3984	-0.300
10	**BC**	3.97	-0.987	3.1013	-0.920

Table 5.7 illustrates the location error of zone 1 in % age for all the ten types of fault. It is quite obvious that except ABCG fault all faults were under reached. BC has the maximum average error of 0.920% in GT while WPT has 0.987% error as compared to other phase faults. The maximum error in terms of WPT is found in the case of AB fault with 6.487% while in case of GT, AB has the minimum fault average with 0.125%. ABCG fault has the maximum average of 4.36% in case of GT while it is 6.234% in case of WPT. The results obtained in WPT gives more error as compared to GT as obvious from the above table It should be kept in mind that the average error results when compared with [112] as shown in Table 5.5, is promising since the error is less than 1% as compared to 1.48%.

Table 5.8 gives the location error of zone 2. It is seen that all faults over reach. The average error is almost around 1% which is far superior 1.437% as compared with [112] in the case of GT. In case of WPT the average error is in between the range of 2.00% to 2.9%. The maximum error in terms of GT, that too for just one case, is also around 13.9%. While in case of WPT, the maximum error goes up to 24.89%. In zone 2 also the results turned out to be good.

Table 5.8: Fault Location Error for Zone 2 for SD1

S. No	Faults	WPT		GT	
		Maximum Error	Average Error	Maximum Error	Average Error
1	**AG**	23.48	2.56	13.926	1.009
2	**BG**	24.84	2.58	13.924	1.0097
3	**CG**	25.60	2.19	13.913	1.0037
4	**ABG**	23.46	2.45	13.927	1.0095
5	**ACG**	23.59	2.62	13.913	1.0031
6	**BCG**	24.89	2.87	13.912	1.0031
7	**ABCG**	24.67	2.76	13.913	1.0031
8	**AB**	24.87	2.82	13.926	1.0092
9	**AC**	21.32	2.56	13.911	1.0022
10	**BC**	19.89	2.01	13.914	1.0040

The results of zone 3 are presented in Table 5.9. Here, except AG, BG, CG and ACG, all faults were under reach. The average error per fault is even less than the average error of zone 3 as presented in [111] if compared with the features obtained from GT. In case of GT, ACG fault has an average error of 1.5578% while the maximum error is 25.350%. Only, AG, CG and ACG faults have average value of more than 1% while rest all are under 1%. If one observes the result obtained from WPT, the maximum error is 53. 45% in case of CG fault. The average error is 6.67% for this particular case.

Table 5.9: Fault Location Error for Zone 3 for SD1

S. No	Faults	WPT		GT	
		Maximum Error	Average Error	Maximum Error	Average Error
1	**AG**	43.28	6.65	24.798	1.2396
2	**BG**	48.35	3.56	20.062	0.9267
3	**CG**	53.45	6.67	25.689	1.3255
4	**ABG**	49.23	1.25	3.385	-0.249
5	**ACG**	32.31	3.67	25.350	1.5578
6	**BCG**	6.24	-1.789	3.8761	-1.167
7	**ABCG**	5.234	-2.213	4.991	-0.175
8	**AB**	14.567	-1.458	7.481	-0.257
9	**AC**	46.89	-2.345	24.859	-0.492
10	**BC**	29.87	-1.345	10.614	-0.615

Table 5.10 depicts the location error of zone 4. In case of GT, the maximum error is 0.008% while the average error is 0.0006% which is almost negligible. While, WPT have 2.452% as the maximum error and 1.23% as the average error. Zone 4 consists of only CG fault.

Table 5.10: Fault Location Error for Zone 4 for SD1

S. No	Faults	WPT		GT	
		Maximum Error	Average Error	Maximum Error	Average Error
1	**CG**	2.452	1.23	0.0088	0.0006

It is seen from table 5.11 the location error of zone 5. The maximum error calculated is 0.3178% while the average error is -0.321% which is almost negligible by the use of GT feature. When WPT feature is employed the maximum error is 1.452% and average error is -1.008%. Zone 4 consists of only BG fault. It is seen that the fault was located beyond the fault point.

Table 5.11: Fault Location Error for Zone 5 for SD1

S. No	Faults	WPT		GT	
		Maximum Error	Average Error	Maximum Error	Average Error
1	**BG**	1.452	-1.008	0.317	-0.0321

It is obvious from table 5.12 the fault location error for zone 6 is very less. The maximum error reported is 0.817% while the average error is -0.953% which is also very good as obtained from GT. In case of WPT, the maximum error was 2.345% and the average error was -1.458%. The error shows that the fault was under reach.

Table 5.12: Fault Location Error for Zone 6 for SD1

S. No	Faults	WPT		GT	
		Maximum Error	Average Error	Maximum Error	Average Error
1	**CG**	2.345	-1.458	0.817	-0.95321

Table 5.13 gives the fault location error of zone 7. The average error is 1.15% while the maximum error is 6.45%. When GT features are employed. When WPT features are used the maximum error is 1.365% and average error is -2.458%. It should be noted down that the author in [111] has not given the results for zone 4, 5, 6 and 7 due to very small number of sample used in that work.

Table 5.13: Fault Location Error for Zone 7 for SD1

S. No	Faults	WPT		GT	
		Maximum Error	Average Error	Maximum Error	Average Error
1	**CG**	1.365	-2.458	0.817	-0.95321

5. 6. 4 Location Result for SD2

It can be seen from table 5. 14 the fault location error for all the sections are presented.

Table 5.14: Location Error for Zones for SD2

S. No	Zones	WPT		GT	
		Maximum Error	Average Error	Maximum Error	Average Error
1	Zone 1	7.346	4.562	4.9921	2.508
2	Zone 2	8.456	7.321	4.9393	2.4815
3	Zone 3	6.224	5.865	4.9766	2.4264
4	Zone 4	6.543	5.641	4.720	2.4832

In case of GT, zone 1 has the maximum average error of 2.50 m as compared with other zones. Zone 2 and zone 4 has almost similar average error of 2.5 and 2.48 m. It should be kept in mind that no literature is available for locating faults in IEEE 13 node system since the distances are very small. The results are very promising as it constitutes very negligible error. The maximum error is all between 4.9 and 5 m, but still they are very promising. When WPT is used the zone 2 has the maximum error of 8.456 m while zone 1 has the minimum average error of 5.641m.

Table 5.15: Fault Location Error for Zone 1 for SD2

S. No	Faults	WPT		GT	
		Maximum Error	Average Error	Maximum Error	Average Error
1	AG	6.23	2.34	0.4939	0.2757
2	BG	5.67	2.21	0.4825	0.2815
3	CG	6.78	2.14	0.462	0.2335
4	ABG	8.76	2.46	0.4866	0.2995
5	ACG	9.23	3.45	0.4579	0.2736
6	BCG	7.86	2.45	0.4800	0.2799
7	ABCG	6.76	2.21	0.4851	0.2104
8	AB	4.56	1.98	0.4992	0.2190
9	AC	3.67	1.67	0.4937	0.2072
10	BC	5.78	1.87	0.4919	0.2273

Table 5.15 depicts the fault location error for zone 1 of SD2. Here, it is found that ACG fault has the maximum average error of 0.299% as compared with other faults. All the error for these faults is in the range of 0.2% to 0.3%, which is very promising. The maximum error for ACG is 0.4866% while the maximum error for AB fault is more i. e. 0.499% .The results obtained are very promising in case of GT. If we observe the result obtained for WPT, it is found that the maximum error is 9.23% which is far more than GT. Also, the average error is 3.45% for ACG fault which is gain more as compared to the results obtained by GT features.

Table 5.16: Fault Location Error for Zone 2 for SD2

S. No	Faults	WPT		GT	
		Maximum Error	Average Error	Maximum Error	Average Error
1	BG	2.252	1.008	0.49908	0.3023

It can be seen from table 5.16, that the results for fault location error for zone 2 of SD 2 that it involves only phase b. The maximum error in this zone is 0.499% and average error is 0.3023% in case of GT while in WPT the maximum error is 2.252% and average error is 1.008%.

Table 5.17: Fault Location Error for Zone 3 for SD2

S. No	Faults	WPT		GT	
		Maximum Error	Average Error	Maximum Error	Average Error
1	**AG**	5.45	1.45	0.4976	0.2711
2	**BG**	6.23	1.21	0.4507	0.2390
3	**CG**	4.48	1.64	0.3599	0.1464
4	**ABG**	4.98	1.32	0.4688	0.2402
5	**ACG**	4.63	1.31	0.4534	0.2801
6	**BCG**	3.48	1.28	0.4963	0.2680
7	**ABCG**	3.98	1.86	0.4973	0.2634
8	**AB**	2.87	1.43	0.4900	0.2504
9	**AC**	3.98	1.32	0.4770	0.1992
10	**BC**	2.86	1.33	0.4545	0.2683

It is seen from table 5.17, the fault location error for zone 3 of SD2. Zone 3 comprises of all ten types of fault. Here, AG fault has the maximum average error of 0.2711% and AC fault has minimum average error of 0.199%. The maximum error reported is that of AG and BCG with 0.4976% and 0.4963% respectively. It can be concluded that the results are very promising since the error is almost less than 0.5% in case of GT. Similarly, in case of WPT the maximum error of 6.23% is observed in BG fault and the maximum average error is seen in ABCG fault with 1.86%.

Table 5.18: Fault Location Error for Zone 4 for SD2

S. No	Faults	WPT		GT	
		Maximum Error	Average Error	Maximum Error	Average Error
1	**AG**	3.45	1.01	0.440	0.244
2	**CG**	2.48	1.23	0.463	0.245
3	**AC**	4.98	1.11	0.469	0.292

Zone- 4 involves two phases A and phase C as seen from table 5.18. Here AC fault 0.292% has more average error than AG and CG fault i.e. 0.244% and 0.245% respectively. AG and CG faults have similar average fault %age. CG and AC fault have the maximum error of 0.463% and 0.469% respectively when the features are taken from GT. In case of WPT, the maximum error for AC is 4.98% and minimum average error is 1.01%. Based on the above results, it is therefore concluded that the results obtained from GT are very promising.

5.7 COMPUTATIONAL TIME

In the figure 5.5, computation time taken for various processes involved for development of algorithm has been presented. It should be noted that all these times were evaluated after calculating the total time taken for each process divided by total no of samples considered. The configuration of the computer on which the algorithm for fault classification and fault location was tested is as: Core*i7* processor, 3.2GHz speed, 12 GB Ram memory.

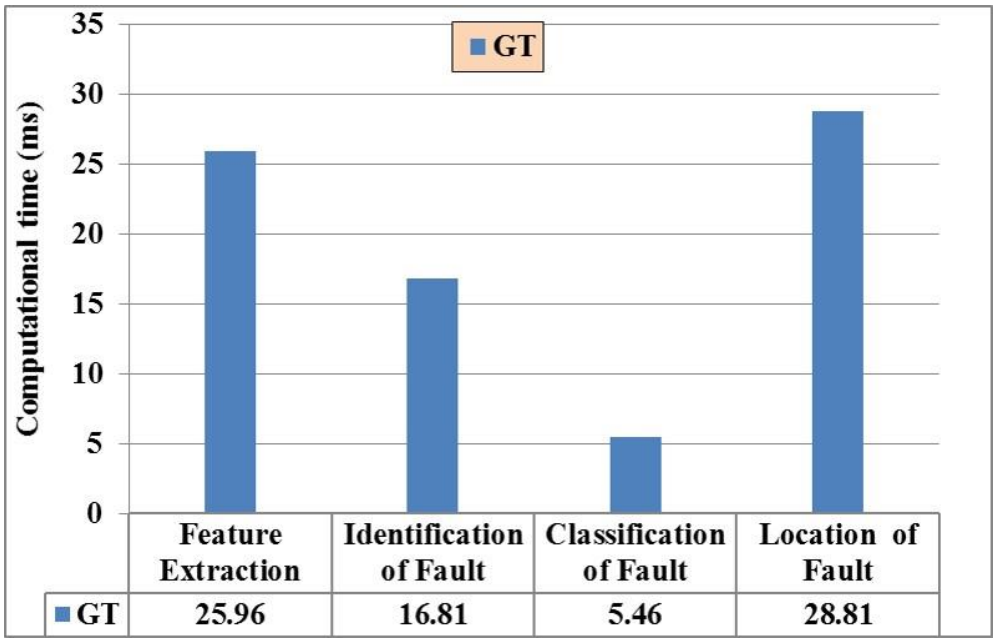

Figure 5.5: Computational Time for Different Evolutionary Process

The feature extraction time is 25.96 ms which is quite high as compared with other signal processing tools. The time taken for identification of faults is 16.81ms, classification of faults is 5.46 ms and for location of fault is 28.81 ms respectively.

5.8 SUMMARY

An algorithm for detection, identification, classification and location of faults is presented in this chapter. Discrimination between load signals and fault signals have also been presented. Gabor Transform has not found its use in any other literature for algorithms meant for locating faults in distribution system. The features extracted are basically decomposition of high frequency content in the signal. The results are very promising when the features of GT are combined with ANN. In the case of GT classification an accuracy of 99.94% is obtained in comparison to 97.294% in case of WPT for SD1. Similarly, the maximum error attained by using GT features is equal to 139.27 m as compared with WPT where the error in location is 248.76m. For SD2, the classification accuracy is 99.73% for GT as compared to 98.69% in case of WPT. Similarly, the location error in terms of WPT is almost approximately double when compared with GT features where the maximum error is 8.456 m as compared to 4.99 m. Thus, it proves that GT provides optimal feature extraction signal for ANN. The results which have been obtained are very promising giving less error in both sample distribution system 1 and sample distribution system 2. The results have been compared with WPT and it has been proved that GT yields better result. The time taken for different evolutionary processes has been given which shows that the feature extraction takes more time.

M – Band Transform Based Features

Chapter 6

There exists a need for uninterrupted supply in power transmission and distribution systems. An uninterrupted supply is required. The service continuity is measured by these parameters known as the system average interruption frequency index (SAIFI) and system average interruption duration index (SAIDI). When the faults occur in the system, these indices get affected. If the faults are diagnosed and located properly, then the

It is broadly established that by locating faults, one can reduce the impact of such faults on the SAIFI and SAIDI indexes in some ways such as: With the proper location of fault, the service can be brought back into the service. When the zone which is affected by the fault is detected and the exact distance is located, one can perform sectionalized switching operations in order to minimize the affected area; and by locating non -permanent faults, one can take fruitful preventive steps in ascertaining that the fault does not occur in future.

As already discussed, many algorithms have been developed to locate faults in power transmission systems. But they are not useful for locating faults in distribution systems, due to reasons addressed in Chapter 2 under section 2.2.1. Several methods have been proposed for locating faults in power distribution systems. Previously, Impedance-based methods were developed that estimates the distance of fault but gave uncertain locations if some distances were similar. Also, while developing algorithms, economics have to be considered so that the cost of implementation does not rise.

On the other hand, many researchers have recently addressed the problem of fault location by using knowledge-based techniques but due to the inadequacy of availability of information the technique fails. Further, it is not economically viable. With the advent of time, methods based on soft computing [113] were employed. In the previous chapters, WT and WPT and GT had been utilized to extract features for detection, identification and location of faults in electrical

distribution system. Each had its own limitations and advantages. Now, for the work carried out in the present chapter, the sampling frequency was decreased and also the database was increased. There was a need for another transform to extract the features so that whatever error remains should be decreased.

The author in [114] – [116] has used M – Band transform for detection of transient signals. Also, it had thrown light on the design of filters. Now, the author in [117] has given the decomposition of M – Band Wavelet.

In the present chapter, M - Band transform is used for fault identification and location in distribution system. Current and voltage samples have been measured at the substation end for both the sample distribution system as discussed in the Chapter 1. Current samples are used in the purpose of fault identification and classification, whereas voltage samples are used for locating faults. Also, discrimination between load current and fault current has been made.

Further, current and voltage features are collected using M - Band Transform decomposition. These extracted features are then subjected to ANN for the purpose of fault classification and location of all ten types of fault with perfection. Further, feature extraction time, time taken for identification, classification and location of fault, is also provided. It is worth mentioning that till date M – Band transform has not been found for detecting, identifying and locating faults in either transmission or distribution network.

6. 1 SAMPLE DISTRIBUTION SYSTEM

Two sample distribution systems have been considered as already described in section 1.3.1 and 1.3.2 of Chapter 1. The problem of the multiple estimation of location of faults has also been tackled. It arises due to presence of laterals at the same distance in the power distribution network by dividing the network into various zones.

The sample distribution (SD 1) has been divided into 7 zones and sample distribution (SD 2) has been divided into 04 zones. In the first distribution system considered for simulation, zone 1, zone 2 and zone 3 consists of all ten types of faults. Zone 4 and zone 5 consists of only one fault since it

involves only phase –b. Similarly, Zone 6 and zone 7 consists of only one fault since it involves only phase –c.

On the other hand, in the second distribution system considered zone 1 and zone 3 comprises of all ten types of fault. While, zone 2 involves 4 types as it involves phase – b and phase – c. Also, zone 4 involves 4 types as it involves phase – a and phase – c respectively. Also, the current and voltage database have been made by increasing the load present in the particular zone to 50%.

In total 7750 samples have been used for evaluating the effectiveness of the algorithm developed. A total of 6214 current and voltage samples for zone 1 and 1536 samples for zone 2 have been collected for preparing the database and used for testing the algorithm. Table 6.1 gives a complete overview of the number of current and voltage samples collected at each zones respectively:

Table: 6 1- Number of current and voltage samples collected

Name	SD 1	SD 2
No of Zones	7	4
Fault Resistance (Ω)	0.05, 10, 20, 30, 40, 50	0.05, 10, 20, 30, 40, 50
Fault Inception Angle (°)	0, 60, 90, 180	0, 60, 90, 180
Fault Types	10	10
Load (+)	50%	50%
Total Samples	**6214**	**1536**

The sampling frequency considered for the present work is 8.00 kHz. The duration of run for the present simulation in both the cases is 0.5 sec. Fault has been simulated at various inception angles as mentioned in Table 6.1. The solution time step is 62 µs. This is the EMTDC simulation time step. The channel plot step is 125 µs which in turn determines the sampling frequency. This is the time interval at which EMTDC sends data to PSCAD for plotting as well as writing data to output files. It should be kept in mind that more is the sampling frequency; more is the information content in a signal.

6.2 DISCRIMINATION BETWEEN LOAD CURRENT AND FAULT CURRENT

Sometimes, there is a similarity between load data and fault data. Due to which one may consider the load data to be classified as fault. This leads to wrong estimation of fault. In order to overcome this difficulty, current and voltage samples collected at 100% and 50% increased load has been distinguished from fault data by calculating mean and standard deviation and then subjecting it to ANN.

6.2.1 Mean

It is the average of current and voltage signal. For a normal signal without fault, its value is zero. During the presence of faults, transients present in the signal makes the value of mean other than zero. Mathematically, it is represented as:

$$\overline{y} = \frac{1}{t_2 - t_1}\int_{t_1}^{t_2} y(t)dt \qquad (6.1)$$

$y(t)$ represent the signal and $\overline{y}$ is its average.

6.2.2 Standard Deviation:

It is the computation of deviation from its mean value. Mathematically, it is given as: $\gamma(t_1, t_2) = (\int_{t_1}^{t_2} (y(t) - \overline{y})^2 dt)^{\frac{1}{2}}$

(6.2)

γ: Standard deviation. Standard deviation for a normal signal without fault is one. While, for a transient signal the value deviates from one. Figure 6.1 gives the method adopted to distinguish between load data and fault data.

At first, about 40% of fault data comprising of different phases voltages and current were fed to artificial neural network along with the load data which consists of load voltage and load current for training. Rest 60 % of the data was used for testing. In zone 1 out of 6214 samples only 127 samples were found out to be mismatching i.e. 97.95% of fault data were correctly classified. In zone 2 out of 1536 samples, 18 samples were misclassified i.e. 98.82% of fault data were correctly

classified. Now, these samples were considered for classification into ten types of faults as well as its location.

6.3 FEATURE EXTRACTION

Feature extraction transforms data of high dimension to a lower dimension. But at the same time, the embedded information content is kept intact. In the previous chapter wavelet and wavelet packet transform were used for feature extraction.

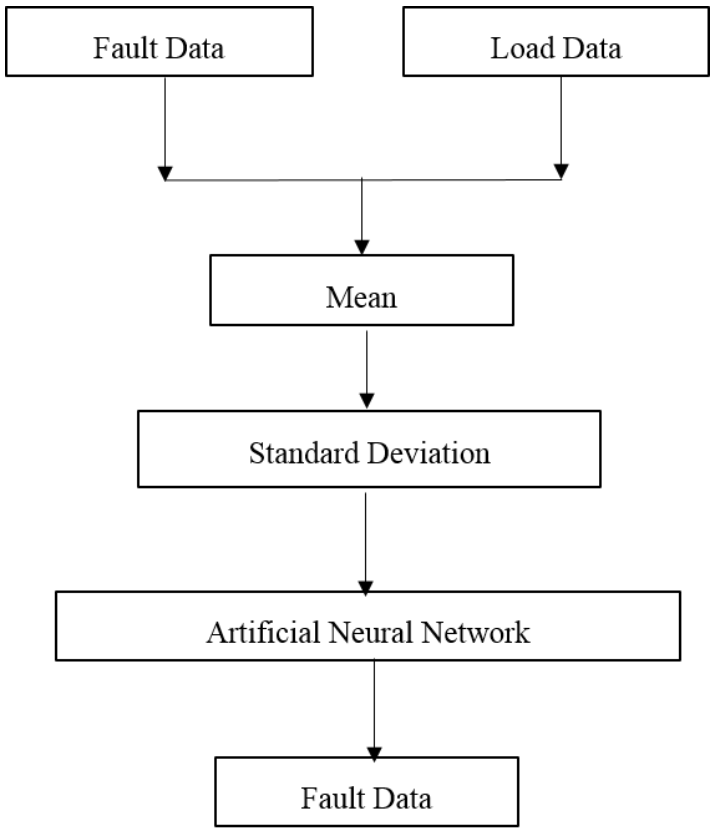

Figure 6.1: Algorithm for Fault and Load Discrimination

In the previous chapter, GT were used for feature extraction. The Gabor wavelet is used as discrete wavelet transform with either continuous or discrete input signal. But it suffers from the disadvantage that it does not have orthonormal bases. That means the inverse of transform could not be easily constructed. Also, since Gabor transform involves numerous parameters for feature

extraction, hence it is computationally expensive. As mentioned earlier in the present algorithm, M - Band transform is used as a tool to extract the features of current and voltage samples. Needless to mention that M - Band Transform has not been used earlier for classifying and locating faults in a distribution system as per the literature reported. It also reduces computational requirements as compared to Gabor Transform.

6.3.1 M - Band Transform (MBT)

M - Band Wavelets are simplification of the conventional wavelets [70]. Signals with high frequency content having relatively narrow bandwidth cannot be analyzed by standard wavelets. Their decomposition yields a logarithmic frequency resolution. But, logarithmic and linear frequency resolution decomposition is obtained using M-band. Also, a large number of sub bands are available by its decomposition which further gives more information about the signal. It also performs multi scale, multi directional filtering of the signal. It is used a tool to view signals at different scales. Decomposition of a signal is achieved by exposing it to the family of functions which are produced from wavelet through its dilations and translations.

M-band orthonormal wavelets were introduced as direct simplification of the two band Daubechies orthogonal wavelets [71]. It is able to zoom in onto narrowband high-frequency components of a signal. When compared with two band wavelets energy compactness is better in case of M – Band [72].

An M-Band wavelet is defined as a tight frame for the set of square integral functions over the set of real numbers $P^2(N)$ [73]. There are $K-1$, wavelets, $\xi_a(s)$, $a=1,.....,K-1$ are connected with the scaling function. For function $y(s)\in P^2(N)$, it is perceived that

$$y(s)=\sum_{a=1}^{a=K-1}\sum_{b\in D}\sum_{c\in D}\langle y(s),\xi_{a,b,c}(s)\rangle\xi_{a,b,c}(s) \tag{6.3}$$

Here, D stands for the set of integers while the inner product operator is denoted by $\langle,\rangle$. By scaling and shifting the corresponding wavelets $\xi_a(s)$:, the $\xi_{a,b,c}(s)$ functions are derived

$$\begin{aligned}&\xi_{a,b,c}(s)=K^{b/2}\xi_a(K^b s-c)\\&a=1,.....,K-1,c\in D,b\in D\end{aligned} \tag{6.4}$$

For the scaling function $\xi_0(s)$ in $P^2(N)$, the wavelet functions are defined as follows

$$\xi_a(s) = \sqrt{K} \sum_{c-0}^{c=F-1} g_a(c)\xi_0(Ks-m) \tag{6.5}$$
$$a = 1,.....,K-1$$

The recursive equation is satisfied by the scaling. It is compactly supported in $[0.(F-1)/(K-1)]$,

$$\xi_o(s) = \sqrt{K} \sum_{c=0}^{c=F-1} g_0(c)\xi_0(Ks-m) \tag{6.6}$$

Here, the sequence g_0 is the scaling filters of length $\mathrm{F = K\,C}$ where C gives the regularity of scaling function and fulfils the following equation:

$$\sum_{c=0}^{c=F-1} g_0(c) = \sqrt{K} \tag{6.7}$$

$$\sum_{c=0}^{c=F-1} g_0(c)g_0(c+Kq) = \sigma q \tag{6.8}$$

The $(K-1)ga$ vectors are known as the wavelet filter that satisfies the following equation:

$$\sum_{c=0}^{c=F-1} g_0(c)g_0(c+Kq) = \sigma(q)\sigma(a-b) \tag{6.9}$$

In the present work, decomposition up to two levels is used for fault classification and decomposition up to four levels has been used for fault location. In M- Band transform for a level decomposition one obtains the one low pass filter decomposition and two high pass filter decomposition. Figure 6.2 gives decomposition up to two levels for fault classification. Ia (phase a) refer to current in phase a. Figure 6.3 gives the decomposition of current signal in phase b (Ib).

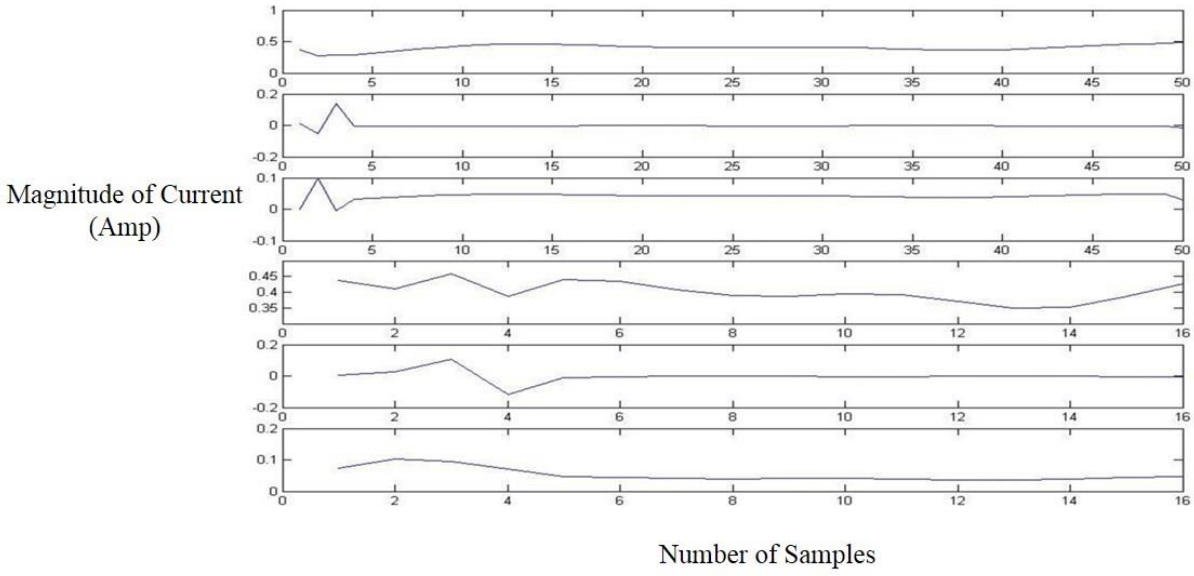

Figure 6.2: Two level decomposition of Current Signal (Ia) using M - Band Transform

The different frequency distributions used in M – Band transform for four level decomposition of current signal is seen in Table 6.2:

Table 6.2: Frequency Distribution for different levels of decomposition

Decomposition Level	Frequency in Hz Approximations	Frequency in Hz Detail
Initial Frequency	8000	
1st	2666	2667, 2667
1st	889	889, 889
2nd	296	296, 296
3rd	99	99, 99

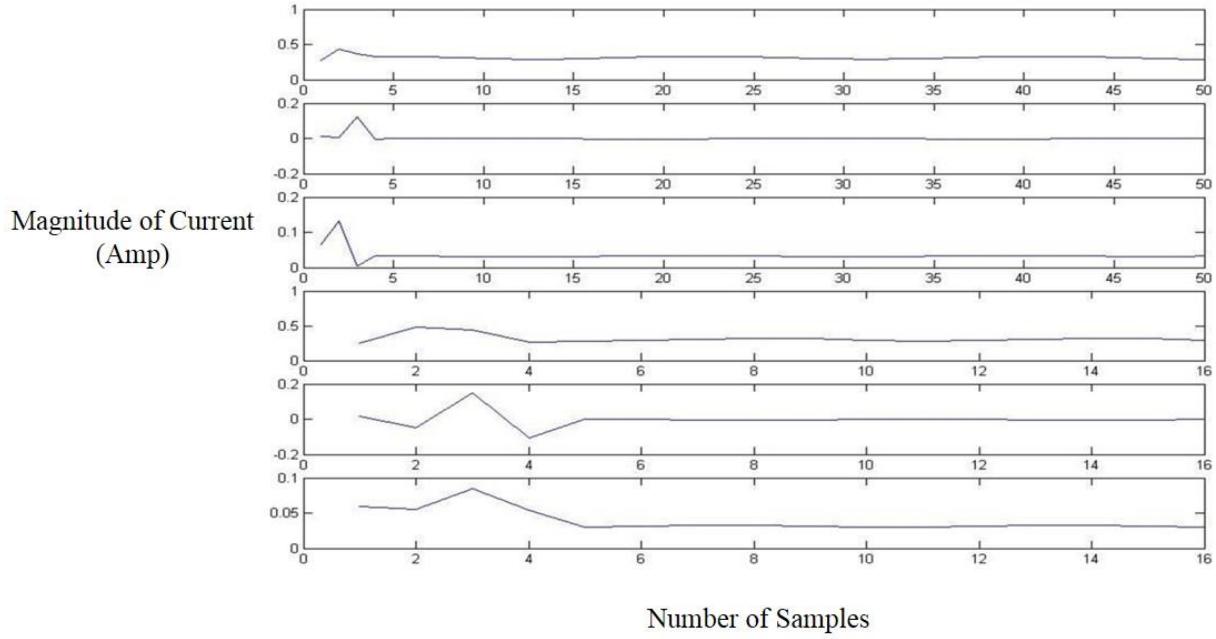

Figure 6.3: Two level decomposition of Current Signal (Ib) using M - Band Transform

6.4 NEURAL NETWORK

In the present work,; Levenberg–Marquardt algorithm is employed. The network performance parameters mean square error "mse" was used for the purpose of fault classification and mean square error with regularization "msereg" has been employed for the purpose of location of faults.
In case of fault classification, the features of current samples collected from MBT are subjected to the neural network. In the present work, the network stops learning when either the mean square error (mse) or number of iterations have reached a predetermined target value which was set to 0.000001 and the number of epochs considered was 3000. The purpose of training is to reduce mse to reasonably low value in few epochs. A maximum of 3000 epochs was considered since as per the configuration of the sample system some samples required approximately 2400 – 2800 epochs to obtain accuracy. Similarly, for the purpose of fault location maximum value of 4000 epoch was considered. Another feature of the algorithm is that it only involves 20% of the samples for training and rest 80% for testing.

6.5 ALGORITHM

Separate algorithm has been developed for classification and location of faults. The algorithm is effective in giving results by employing less than quarter of full cycle data of the sample collected. Mean and Standard deviation is calculated after feature extraction. They are calculated using equation 6.1 and 6.2 respectively. It is evident from the flowchart that features are extracted from M- band transform. Hence forth, mean and standard deviation are evaluated of the extracted features and are subjected to ANN for fault classification and location.

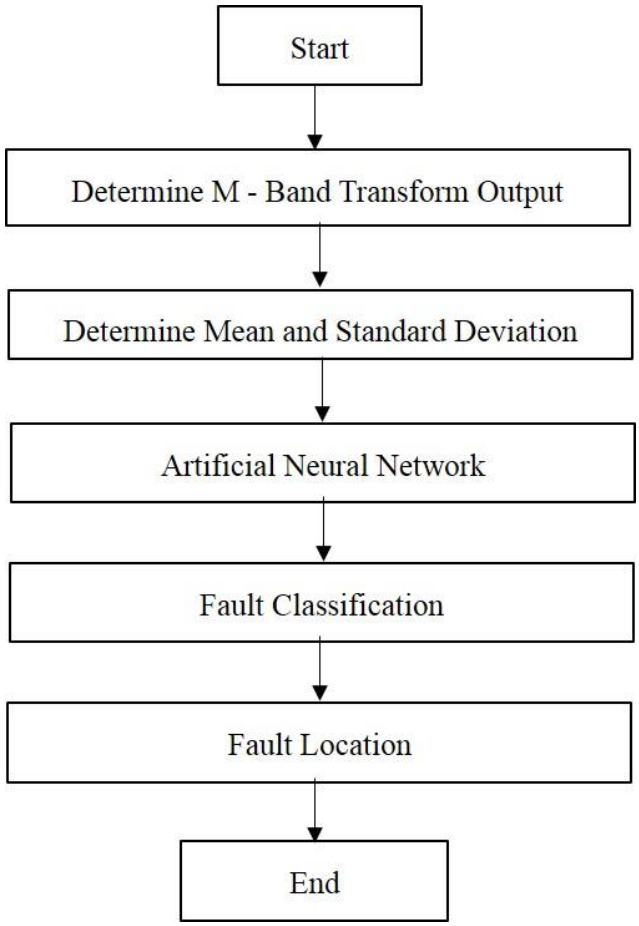

Figure 6.4: Algorithm for Fault Classification and Location

6.6 EXPERIMENTAL RESULTS AND DISCUSSION

6.6.1 Classification Result for SD1

The results are presented below in terms of total classification error; classification error for all sections for both sample 1 and sample 2. Total Classification Error is determined using the same mathematical relationship given by equation (1.1). The same is given below for ready reference.

$$\text{Total Classification Error } (\%\text{age}) = \frac{\text{Number of Misclassified Samples}}{\text{Total number of samples in that particular zone}} \times 100$$

It is depicted that 99.76% of faults have been accurately classified from the features obtained from M - Band Transform while Gabor Transform gives 97.56% accuracy. Table 6.3 gives the classification error for all the seven zones of sample distribution system 1 (SD 1).

Table 6.3: Classification Error for Zones for SD1

S. No	Zones	GT	MBT
1	Zone 1	1.086	0.0416
2	Zone 2	0.875	0.0185
3	Zone 3	0.113	0
4	Zone 4	0.232	0.176
5	Zone 5	0.012	0
6	Zone 6	0.112	0
7	Zone 7	0.014	0

In case of MBT features, it can be seen from the above table that the errors obtained are very less. Zone 1 and zone 2 has an error of 0.4166% and 01851% only. Zone 4 has an error of 0.176% which is also very low. It is worth mentioning that zone 3, zone 5, zone 6 and zone 7 are errorless. If the GBT features are considered zone 1 has the maximum error of 1.086% while zone 7 has the minimum error of 0.014%. Zone 2 has an error of 0.875% while other zones 3,4,5,6 and 7 has very less error beyond 0.25%.

6.6.2 Classification Result for SD2

When the algorithm is applied to the features collected from the M - Band Transform for SD 2, the classification accuracy is 99.82%. While using Gabor Transform the classification accuracy turns out to be 98.68%. Table 6.4 gives the zone wise classification error for SD 2. It is observed that only zone 4 has an error of 0.176% while other zones are errorless. The result turns out to be promising, as already discussed, zone 1 and zone 3 have maximum samples and zone 4 has very less sample in case of MBT features. It is observed that the maximum error of 0.87% is reported using GT

Table 6.4: Classification Error for Zones for SD2

S. No	Zones	GT	MBT
1	Zone 1	0.32	0
2	Zone 2	0.08	0
3	Zone 3	0.04	0
4	Zone 4	0.87	0.176

6. 6. 3 Location Result for SD1

Table 6.6 depicts the location error for SD1 for all sections. The location error are compare with the work of G. Morales Espana [118] where only average error has been demonstrated as shown in Table 2. Zone 4, zone 5, zone 6 and zone 7 results have not been reported owing to less number of samples. The results have been compared with this paper as at the initial stage in chapter 4; the results have been compared with [31]. The results obtained thereafter have shown improvement. Also, varieties of conditions have been adapted.

Table 6.5: Average Error for all zones [118]

Faults	Average Error
Single - Phase	1.75
Phase to Phase	1.04
Double Phase to Ground	0.72
Three Phase	1.45

Table 6.6: Fault Location Error for All Zones for SD1

S. No	Zones	GT		MBT	
		Maximum Error	Average Error	Maximum Error	Average Error
1	Zone 1	56.87	-39.897	46.274	-23.0502
2	Zone 2	234.578	15.673	139.260	10.05
3	Zone 3	14.568	6.23	4.980	2.3546
4	Zone 4	1.87	0.987	0.0272	0.0014
5	Zone 5	2.34	0.875	0.0272	0.0014
6	Zone 6	3.453	-0.453	0.4172	-0.0212
7	Zone 7	69.786	2.453	45.1412	1.86

In the figure shown above, the results obtained from M - Band Transform features are very promising. As discussed earlier, zone 1, 2 and 3 constitute the maximum number of samples, so the average error is just -23.05, 10.057, 2.3546 m only which is significantly low. It should be noted clearly that negative sign indicates that the fault was under reach from the actual fault location. It is obvious from the above figure that the fault was under reach from the exact location at zone 1, and 6. The average error determines that some of the faults may be positive but when the average is taken on the whole the faults are under reach from the exact location of fault. The maximum error in zone 1 is just 46.27 m. But that is not at all the problem since as per the details of the distance given zone 1 is in kilometer and few meters does not make any operational difference. When the results are further compared with Gabor Transform, it is observed that the maximum error obtained is 234.578 m for zone 2 which is far worse as compared with MBT. The minimum average error for GT is for zone 6 with -0.453m. The average error in zone 1 and zone 6 gives an indication that it was under reach from the exact location of fault The results obtained are much better than the results reported in [118], thereby making the algorithm more robust.

Table 6.7: Fault Location Error for Zone 1 for SD1

S. No	Faults	GT		MBT	
		Maximum Error	Average Error	Maximum Error	Average Error
1	**AG**	7.654	-4.234	4.1648	-2.241
2	**BG**	7.348	-4.112	3.6497	-2.2467
3	**CG**	8.018	-3.976	4.2637	-2.2484
4	**ABG**	5.467	-2.897	0.9735	-2.3828
5	**ACG**	6.346	-3.113	4.5623	-2.0891
6	**BCG**	5.876	-3.124	4.6279	-2.2295
7	**ABCG**	5.112	-2.765	4.2124	-2.2758
8	**AB**	3.214	-2.674	0.3313	-2.53
9	**AC**	3.876	-2.546	3.7009	-2.316
10	**BC**	2.231	-2.879	0.7612	-2.4909

Table 6.7 illustrates the location error of zone 1 in % age for all the ten types of fault. It is quite obvious all faults were estimated before the fault point. BCG has the maximum average error of 4.620% as compared to other phase faults. AB has the minimum fault average with 0.331%. BC fault has the maximum average of – 2.49% when MBT features are considered. When the results are compared with GT it is obvious from the above table that the maximum error is 7.348% for AG fault and least for BC fault with 2.231%. In terms of average error, the maximum average error for AG fault is 4.234%. Needless to mention all the faults have been under reach from exact occurrence of fault.

Table 6.8 gives the location error of zone 2. It is seen that all faults were located after the location. The average error is almost around 1% which is far superior to 1.437% as reported in [118]. The maximum error, that too for just one case, is also around 13.925%. In zone 2 also, the results have turned out to be better when MBT features are considered. When GT features are employed for the algorithm. The maximum error is for ABCG fault with 18.987% and the average error is 2.456% for AG fault. It is also observed that average error range is between 2.456% to 1.011% which is more than the features obtained for MBT.

Table 6.8: Fault Location Error for Zone 2 for SD1

S. No	Faults	GT		MBT	
		Maximum Error	Average Error	Maximum Error	Average Error
1	**AG**	18.543	2.456	13.9258	1.0217
2	**BG**	17.678	2.211	13.9144	1.0197
3	**CG**	17.986	1.865	13.8783	0.9972
4	**ABG**	14.567	1.347	13.9261	1.0219
5	**ACG**	14.234	1.321	13.8862	0.9952
6	**BCG**	16.891	1.112	13.8672	0.9916
7	**ABCG**	18.987	1.568	13.8775	0.9905
8	**AB**	16.342	1.082	13.9245	1.0233
9	**AC**	14.567	1.089	13.8976	1.0008
10	**BC**	13.998	1.011	13.8726	0.9955

The results of zone 3 are presented in table 6.9. Here, except AG, BG, CG, AC and ABCG, all faults were under reach from the exact location. The average error per fault is even less than the average error of zone 3 as presented in [118]. AG fault has the maximum average error of 0.923% while the maximum error is 10.687% using MBT features. When GT features are considered, the maximum error is for AG fault with 14.354% and the average error is 2.321%. For BC fault only 0.335% error is reported.

Table 6.9: Fault Location Error for Zone 3 for SD1

S. No	Faults	GT		MBT	
		Maximum Error	Average Error	Maximum Error	Average Error
1	AG	14.354	2.321	10.6871	0.9213
2	BG	7.654	0.998	6.7241	0.3054
3	CG	13.546	0.885	11.1156	0.4726
4	ABG	8.834	-0.654	5.458	-0.228
5	ACG	9.823	-0.458	7.7461	-0.0125
6	BCG	6.785	-0.865	4.4713	-0.4274
7	ABCG	9.834	0.564	6.1743	0.1292
8	AB	8.835	-0.546	7.6037	-0.177
9	AC	8.457	0.248	7.2232	0.0133
10	BC	9.487	0.335	7.1096	-0.0573

Table 6.10: Fault Location Error for Zone 4 for SD1

S. No	Faults	GT		MBT	
		Maximum Error	Average Error	Maximum Error	Average Error
1	CG	1.003	0.554	0.0027	0

Table 6.10 depicts the location error of zone 4. The maximum error obtained is 0.027%, while the average error computed is 0.0001% which is almost negligible using MBT. While, GT gave the maximum error of 1.003% and average error of 0.554% respectively. Zone 4 consists of only CG fault.

Table 6.11: Fault Location Error for Zone 5 for SD1

S. No	Faults	GT		MBT	
		Maximum Error	Average Error	Maximum Error	Average Error
1	BG	3.994	0.553	3.7668	0.112

It is seen from table 6.11 the location error of zone 5. The maximum error calculated is 3.7688% while the average error is -0.112% which is almost negligible for MBT. GT fetched the maximum error of 3.994% and average error of 0.553% respectively. Zone 4 consists of only BG fault. It is seen that the fault was over reached from the fault point.

Table 6.12: Fault Location Error for Zone 6 for SD1

S. No	Faults	GT		MBT	
		Maximum Error	Average Error	Maximum Error	Average Error
1	**CG**	1.345	-0.458	0.0417	-0.0021

It is obvious from table 6.12 that the fault location error for zone 6 is very less. The maximum error reported is 0.0417% while the average error is -0.0021% which is also very good in case of MBT. The error shows that the fault was under reach from the exact point of fault. In case of GT, the maximum error was 1.345% and -0.458% respectively.

Table 6.13: Fault Location Error for Zone 7 for SD1

S. No	Faults	GT		MBT	
		Maximum Error	Average Error	Maximum Error	Average Error
1	**CG**	6.548	0.458	4.5141	0.1861

Table 6.13 gives the fault location error of zone 7. The average error is 0.1861% while the maximum error is 4.514% using MBT. The maximum error for GT is 6.548% and the average error reported is 0.458%. It should be noted down that the author in [118] has not given the results for zone 4, 5, 6 and 7 due to very small number of sample used in that work.

6. 6. 4 Location Result for SD2

Table 6. 14, provides the fault location error for all the sections are presented below.

Table 6.14: Location Error for Zones for SD2

S. No	Zones	GT		MBT	
		Maximum Error	Average Error	Maximum Error	Average Error
1	Zone 1	6.348	3.562	4.9895	2.7022
2	Zone 2	7.856	4.351	4.9393	2.4815
3	Zone 3	5.984	4.885	4.9804	2.3546
4	Zone 4	5.993	4.681	4.7835	2.3255

Using MBT, Zone 1 has the maximum average error of 2.70 m as compared with other zones. Zone 2, zone 3 and zone 4 have almost similar average error of 2.48, 2.35 and 2.32 m respectively. One should not forget that no literature is available for locating faults in IEEE 13 node system since the distances are very small. The results are very promising as it constitutes very negligible error. The maximum error is between 4.9 and 5 m for zone 1, zone 2 and zone 3 and just 4.78m for zone 4. When the GT features are taken into account, the maximum error is 7.856m for zone 2 and the average error is 4.885m for zone 3. The average error is almost double from the average error obtained in MBT. Thereby, the results obtained from MBT are very promising.

Figure 6.15 depicts the fault location error for zone 1 of SD 2. Here, it is found that ABCG fault has the maximum average error of 0.338% as compared with other faults. All the error for these faults is in the range of 0.2% to 0.3%, which turns out to be very appealing. The maximum error for ABCG is 0.498%.The results obtained are very promising. In the figure given below, 1 to 10 refers to different types of faults in sequence: AG, BG, CG, ABG, ACG, BCG, ABCG, AB, AC, and BC respectively when MBT features are employed. In case of GT features, the maximum error is 4.78% for CG fault while maximum average error is 2.55% for BCG fault. The minimum average error is 0.67% for AC.

Table 6.15: Fault Location Error for Zone 1 for SD2

S. No	Faults	GT		MBT	
		Maximum Error	Average Error	Maximum Error	Average Error
1	AG	3.23	1.34	0.4795	0.2271
2	BG	3.67	1.21	0.476	0.258
3	CG	4.78	2.14	0.4762	0.253
4	ABG	3.76	2.46	0.479	0.269
5	ACG	3.23	1.45	0.491	0.333
6	BCG	2.87	2.55	0.493	0.2624
7	ABCG	3.76	2.11	0.498	0.338
8	AB	3.66	0.98	0.476	0.261
9	AC	2.67	0.67	0.452	0.252
10	BC	2.78	0.87	0.457	0.244

Table 6.16: Fault Location Error for Zone 2 for SD2

S. No	Faults	GT		MBT	
		Maximum Error	Average Error	Maximum Error	Average Error
1	BG	1.252	1.778	0.4740	0.2369

It can be observed from table 6.16, that the results for fault location error for zone 2 of SD2 involves only B phase. The maximum error in this zone is 0.474% and average error is 0.2369% in case of MBT while it is 1.252% and 1.778% in case of GT.

Table 6.17: Fault Location Error for Zone 3 for SD2

S. No	Faults	GT		MBT	
		Maximum Error	Average Error	Maximum Error	Average Error
1	**AG**	1.576	0.876	0.447	0.239
2	**BG**	1.436	1.211	0.495	0.283
3	**CG**	1.834	1.433	0.445	0.245
4	**ABG**	1.246	1.021	0.498	0.242
5	**ACG**	1.664	1.025	0.441	0.229
6	**BCG**	1.332	0.876	0.464	0.256
7	**ABCG**	1.021	0.763	0.483	0.223
8	**AB**	0.884	0.675	0.448	0.224
9	**AC**	0.821	0.321	0.424	0.192
10	**BC**	0.764	0.347	0.479	0.216

It is seen from table 6.17, the fault location error for zone 3 of SD2. Zone 3 comprises of all ten types of fault. Here, BCG fault has the maximum average error of 0.256% and AC fault has minimum average error of 0.192%. The maximum error reported is that of AG and BCG with 0.498% and 0.483% respectively using MBT. For GT features, the maximum error is for ACG fault with 1.664%. The average error is for CG fault with 1.433%. Also, the range of average error is from 0.321% to 1.433% which is more than MBT It can be concluded that the results are very effective, since the error is less than 0.5% for MBT as compared to GT.

Table 6.18: Fault Location Error for Zone 4 for SD2

S. No	Faults	GT		MBT	
		Maximum Error	Average Error	Maximum Error	Average Error
1	**AG**	1.45	1.21	0.440	0.253
2	**CG**	1.48	1.23	0.438	0.260
3	**AC**	1.98	1.41	0.411	0.213

Zone- 4 involves two phase A and phase C as seen from table 6.18. Here, CG fault has more average error of 0.260% than AG and AC fault i.e. 0.253% and 0.213% respectively. AG fault has

the maximum error of 0.440% as compared to the error of CG and AC with 0.438% and 0.411% respectively in MBT. While using GT, it is observed that the maximum error is for AC with 1.98% and average error is 1.41%. Both maximum as well as average error is more for GT. Based, on the above results it is therefore concluded that the results of MBT are very promising.

6.7 COMPUTATIONAL TIME

In the figure 6.5, computation time taken for various processes involved for development of algorithm has been presented. It should be noted that all these times were evaluated after calculating the total time taken for each process divided by total no of samples considered. The configuration of the computer on which the algorithm for fault classification and fault location was tested is as: Core*i7* processor, 3.2GHz speed, 12 GB Ram memory.

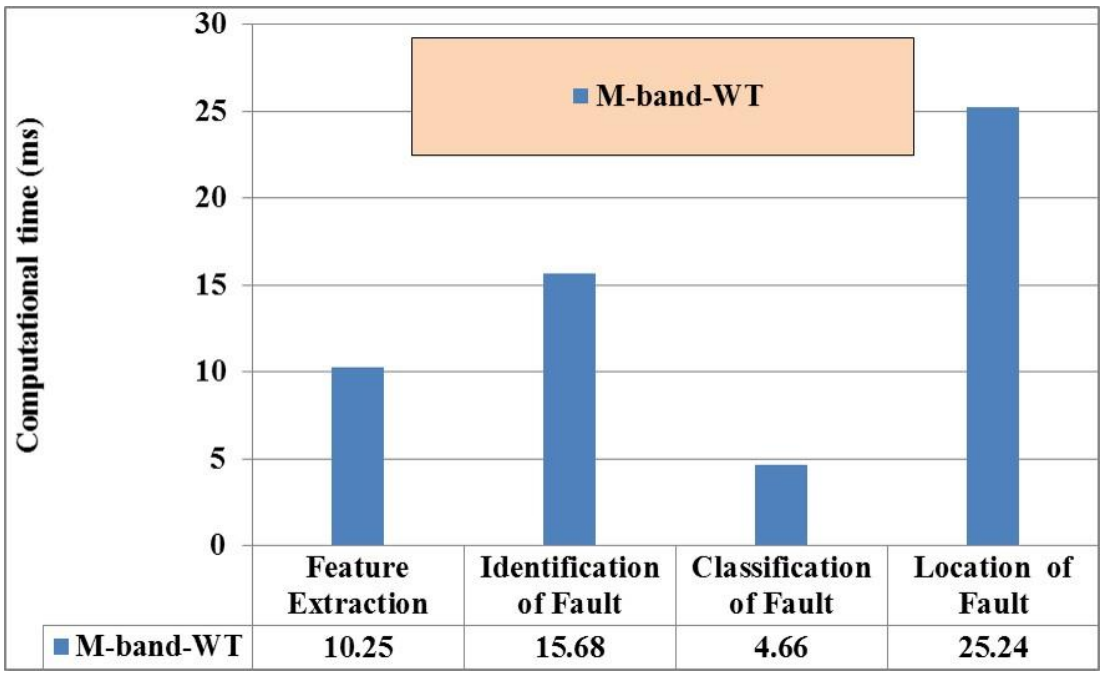

Figure 6.5: Computational Time for Different Evolutionary Process

The feature extraction time is 10.25 ms which is quite high as compared with other signal processing tools. The time taken for identification of faults is 15.68ms, classification of faults is 4.66 ms and for location of fault is 25.24 ms respectively.

6.8 SUMMARY

An algorithm for detection, identification, classification and location of faults is presented in this chapter. Discrimination between load signals and fault signals have also been presented. M- Band Wavelet Transform has not found its use in any other literature for algorithms meant for locating faults in distribution system. The features extracted are basically decomposition of both high frequency as well as low frequency content in the signal in different levels. The results are very promising when the features of MBT are combined with ANN. In case of MBT the accuracy is 99.76% for SD1 and 99.82% for SD2 as compared to 97.56% and 98.68% for GT for SD1 and SD2 respectively. For locating faults, the maximum error is 139.26 m for SD 1 and 4.98 m for SD 2 using MBT as compared to 234.58 m and 4.98 m using GT for SD 1 and SD 2 respectively. Thus, it proves that MBWT provides optimal feature extraction signal for ANN. The results which have been obtained are very promising giving less error in both sample distribution system 1 and sample distribution system 2. The results have been compared with GT and for the particular frequency considered the MBT yields better result as evident from the chapter. The time taken for different evolutionary processes has been given which shows that the feature extraction takes less time.

Dual Tree Complex Wavelet Transform Based Features

Chapter 7

Distribution feeders are the last shackle of the energy chain. It is that part of the network where power is delivered to the customer. This part of electrical power systems is also important as electrical generation and transmission. Distribution feeder is considered to be the prominent part of power by some of the engineers. Power needs to be delivered to consumers without fluctuations in voltage, should have minimal electrical tripping.

The author in [119] has given a complete review of methods meant for fault location. From the traditionally impedance based method, knowledge based to travelling based method [120] each have its own drawback. If impedance based methods were unable to tackle the multiple estimation problem, then the methods based on travelling waves employed huge equipment cost. Since, travelling wave based requires very high sampling frequency. The author in [121] had combined the most commonly used digital signal processing tool wavelet with support vector machine to classify faults in distribution system with distributed generation. The author in [122] and [123] have designed kalman filter and employed decision tree based algorithm to detect high impedance faults in distribution network.

With the advent of time, methods based on amalgamation of signal processing tools and artificial intelligence was employed. In the previous chapters, WT, WPT, GT and MBWT had been utilized to extract features for detection, identification and location of faults in electrical distribution system. Each had its own limitations and advantages. Now, for the work carried out in the present chapter, the sampling frequency was further decreased and also the database was increased. There was a need for another transform to extract the features so that whatever error remains should be decreased.

The use of DTCWT can be found in the field of biometric security [124], image texture retrieval [125], content based image retrieval [126], estimation of motion [127], can be found. But this transform even with lot of edge over the traditional transforms have not been used in detection, identification, classification and location of faults in either transmission or distribution system.

In the present chapter, DTCWT is used for fault identification and location in distribution system. Current and voltage samples have been measured at the substation end for both the sample distribution system as discussed in the Chapter 1. Current samples are used in the purpose of fault identification and classification, whereas voltage samples are used for locating faults. Also, discrimination between load current and fault current has been made.

Further, current and voltage features are collected using Dual Tree Complex Wavelet Transform decomposition. These extracted features are then subjected to ANN for the purpose of fault classification and location of all ten types of fault with perfection. Further, feature extraction time, time taken for identification, classification and location of fault, is also provided. It is worth mentioning that till date Dual Tree Complex Wavelet Transform has not been found for detecting, identifying and locating faults in either transmission or distribution network.

7. 1 SAMPLE DISTRIBUTION SYSTEM

Two sample distribution systems have been considered as already described in section 1.3.1 and 1.3.2 of Chapter 1. The problem of the multiple estimation of location of faults has also been tackled. It arises due to presence of laterals at the same distance in the power distribution network by dividing the network into various zones.

The sample distribution (SD 1) has been divided into 7 zones and sample distribution (SD 2) has been divided into 04 zones. In the first distribution system considered for simulation, zone 1, zone 2 and zone 3 consists of all ten types of faults. Zone 4 and zone 5 consists of only one fault since it involves only phase –b. Similarly, Zone 6 and zone 7 consists of only one fault since it involves only phase –c.

On the other hand, in the second distribution system considered zone 1 and zone 3 comprises of all ten types of fault. While, zone 2 involves 4 types as it involves phase – b and phase – c. Also, zone

4 involves 4 types as it involves phase – a and phase – c respectively. Also, the current and voltage database have been made by increasing the load present in the particular zone to 50%.

In total 15500 samples have been used for evaluating the effectiveness of the algorithm developed. A total of 12428 current and voltage samples for zone 1 and 3072 samples for zone 2 have been collected for preparing the database and used for testing the algorithm. Table 7.1 gives a complete overview of the number of current and voltage samples collected at each zones respectively.

Table: 7 1- Number of current and voltage samples collected

Name	**SD 1**	**SD 2**
No of Zones	7	4
Fault Resistance (Ω)	0.05, 10, 20, 30, 40, 50	0.05, 10, 20, 30, 40, 50
Fault Inception Angle (°)	0, 60, 90, 180	0, 60, 90, 180
Fault Types	10	10
Load (+)	50%	50%
Load (-)	50%	50%
Total Samples	**12428**	**3072**

The sampling frequency considered for the present work is 4.00 kHz. The duration of run for the present simulation in both the cases is 0.5 sec. Fault has been simulated at various inception angles as mentioned in Table 7.1. The solution time step is 125 μs. This is the EMTDC simulation time step. The channel plot step is 250 μs which in turn determines the sampling frequency. This is the time interval at which EMTDC sends data to PSCAD for plotting as well as writing data to output files. It should be kept in mind that more is the sampling frequency; more is the information content in a signal.

7.2 DISCRIMINATION BETWEEN LOAD CURRENT AND FAULT CURRENT

Sometimes, there is a similarity between load data and fault data. Due to which one may consider the load data to be classified as fault. This leads to wrong estimation of fault. In order to overcome this difficulty, current and voltage samples collected at 100% , 50% increased load, as well as 50%

decreased load has been distinguished from fault data by calculating mean and standard deviation and then subjecting it to ANN.

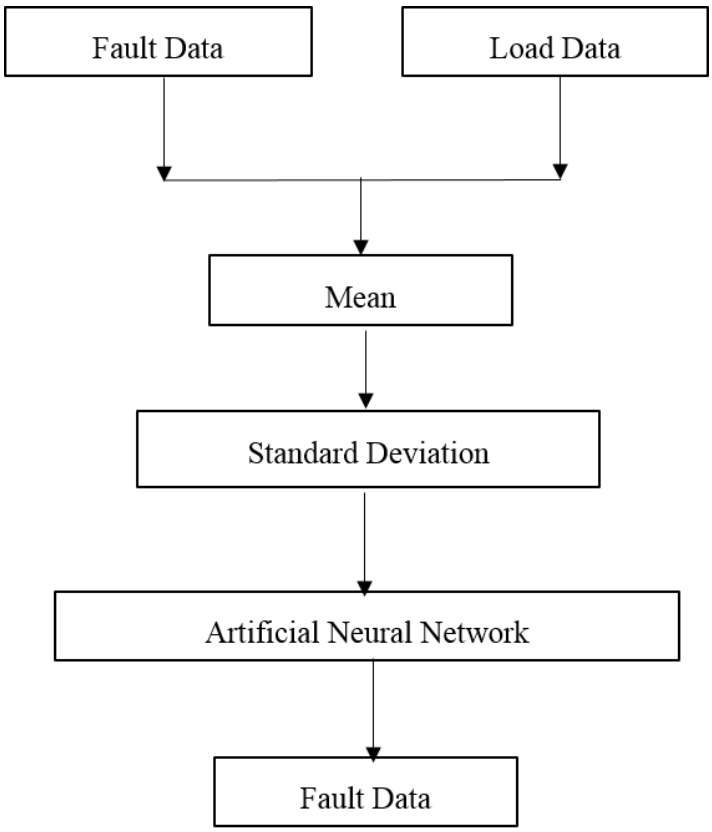

Figure 7.1: Algorithm for Fault and Load Discrimination

7.2.1 Mean

It is the average of current and voltage signal. For a normal signal without fault, its value is zero. During the presence of faults, transients present in the signal makes the value of mean other than zero. Mathematically, it is represented as:

$$\overline{y} = \frac{1}{t_2 - t_1}\int_{t_1}^{t_2} y(t)dt \qquad (7.1)$$

$y(t)$ represent the signal and $\overline{y}$ is its average.

7.2.2 Standard Deviation:

It is the computation of deviation from its mean value. Mathematically, it is given as: $\gamma(t_1,t_2)=(\int_{t_1}^{t_2}(y(t)-\bar{y})^2dt)^{\frac{1}{2}}$

(7.2)

γ: Standard deviation. Standard deviation for a normal signal without fault is one. While, for a transient signal the value deviates from one. Figure 7.1 gives the method adopted to distinguish between load data and fault data.

At first, about 40% of fault data comprising of different phases voltages and current were fed to artificial neural network along with the load data which consists of load voltage and load current for training. Rest 60 % of the data was used for testing. In zone 1 out of 12428 samples only 344 samples were found out to be mismatching i.e. 97.23% of fault data were correctly classified. In zone 2 out of 3072 samples, 42 samples were misclassified i.e. 98.63% of fault data were correctly classified. Now, these samples were considered for classification into ten types of faults as well as its location.

7.3 FEATURE EXTRACTION

As discussed earlier, feature extraction transforms data of high dimension to a lower dimension. But at the same time, the embedded information content is kept intact. In the previous chapter M Band Wavelet transform were used for feature extraction. The M – Band Wavelet is used as discrete wavelet transform with either continuous or discrete input signal. But it suffers from the disadvantage that it has design limitations in two band decomposition: such as orthogonality, realness, symmetry. As mentioned earlier in the present algorithm, Dual Tree Complex Wavelet transform is used as a tool to extract the features of current and voltage samples. Dual Tree Complex Wavelet Transform has not been used for classifying and locating faults in a distribution system as per the literature reported.

7.3.1 Dual Tree Complex Wavelet Transform (DTCWT)

Wavelet based transform are successfully applied in the field of pattern recognition. The major problem of the common decimated Discrete Wavelet Transform (DWT) is its lack of shift invariance. The wavelet coefficients vary substantially when there are shifts of the input signal. Complex Wavelet Transform does not suffer from this problem. But, they generally lack in speed in calculating the coefficients. They also have poor inversion properties [74]. Kingsbury [75, 76] developed Dual-Tree Complex Wavelet Transform (DTCWT) to find the solution for the above problem. It retained the properties of nearly shift invariance as well as directionally selectivity. It consists of a dual tree structure of the wavelet transform.

The first part gives information about the real part while the second gives the imaginary part. The condition of proper reconstruction for WT is satisfied by the use of two different sets of filter. They are designed jointly in order to get an analytical transform. If it is presumed that $h_0(n), h_1(n)$ indicates the low-pass/high-pass filter pair for the upper filter bank, and let $b_0(m), b_1(m)$ is the low-pass/high-pass filter pair for the lower filter bank. It indicates that the two real wavelets associated with each of the two real wavelet transforms as $\phi_a(t), \phi_b(t)$. The filters are designed in such a manner that the complex wavelet $\phi(t) := \phi_a(t) + j\phi_b(t)$ is approximately analytic. Equivalently, they are designed so that $\phi_b(t)$ is approximately the Hilbert transform of $\phi_a(t)$. Filters are themselves real. One of the advantages of DTCWT is that it does not involve complex arithmetic. In order to obtain the inverse of the transform, the real part and the imaginary part are both inverted. The inverse of each of the two real DWTs are used to get two real signals. Final output is obtained by averaging the two real signals.

When the two real DWTs are orthonormal and the $1/\sqrt{2}$ factor is included, the DTCWT gains Parseval's energy theorem: the energy of the input signal is equal to the energy in the wavelet domain

$$\sum_{j.n} \left(|e_a(j.m)|^2 + |e_b(j.m)|^2 \right) = \sum_{m} |s(m)|^2 \tag{7.3}$$

In the present work, decomposition up to two levels is used for fault classification and four levels decomposition have been used for fault location. Figure 7.2 gives the two level decomposition.

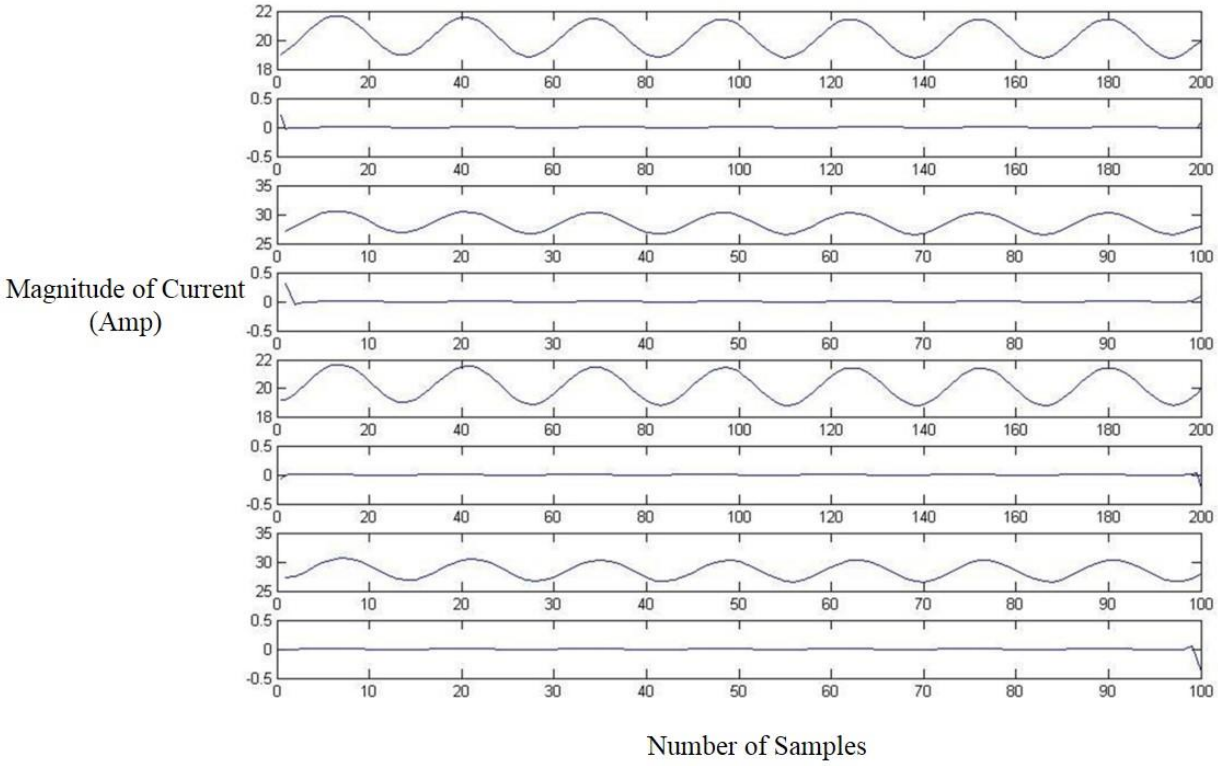

Figure 7.2: Two level decomposition of current signal using DTCWT

7.4 NEURAL NETWORK

In the present work; Levenberg–Marquardt algorithm is employed. The network performance parameters mean square error "mse" was used for the purpose of fault classification and mean square error with regularization "msereg" has been employed for the purpose of location of faults.
In case of fault classification, the features of current samples collected from DTCWT are fed to the neural network. In the present work, the network stops learning when either the mean square error (mse) or number of iterations have reached a predetermined target value which was set to 0.000001 and the number of epochs considered was 3000. The purpose of training is to reduce mse to reasonably low value in few epochs. A maximum of 3000 epochs was considered since as per the configuration of the sample system some samples required approximately 2600 – 2800 epochs to obtain accuracy. Similarly, for the purpose of fault location maximum value of 4000 epoch was

considered. Another feature of the algorithm is that it only involves 20% of the samples for training and rest 80% for testing.

7.5 ALGORITHM

Separate algorithm has been developed for classification and location of faults. The algorithm is effective in giving results by employing less than quarter of full cycle data of the sample collected. Mean and Standard deviation is calculated after feature extraction. They are calculated using equation 7.1 and 7.2 respectively. Further, Skewness [128] is calculated using the equation given below:

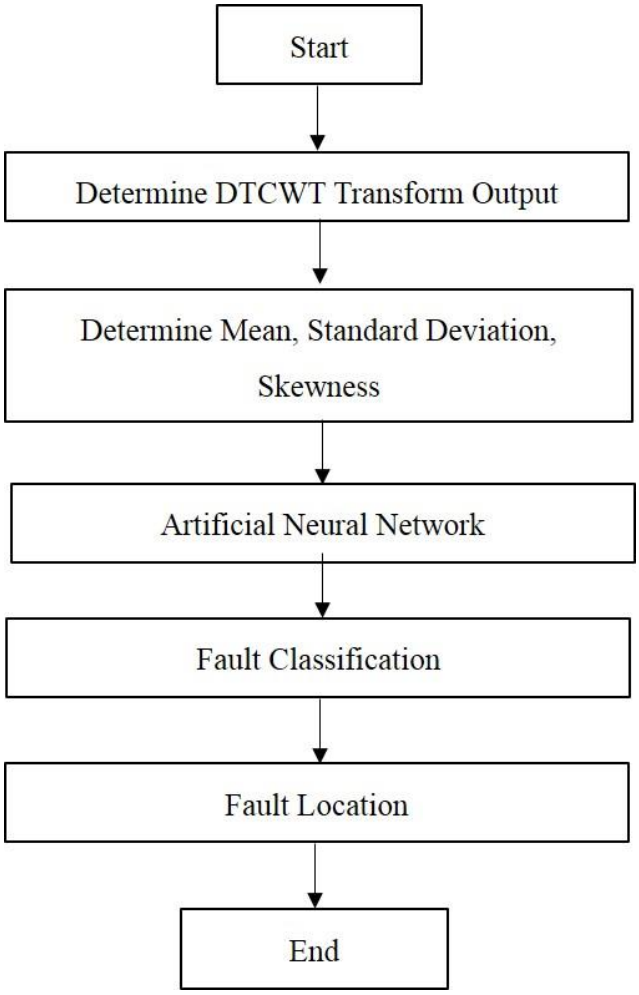

Figure 7.3: Algorithm for Fault Classification and Location

7.5.1 Skewness:

Asymmetry of a given signal with respect to its mean is given by skewness. Its value equals zero for a normal signal. And, it is non – zero for transient signals. Mathematically, it is drafted below as:

$$A(t_1, t_2) = \frac{\int_{t_1}^{t_2} (y(t) - \bar{y})^3}{\gamma} \qquad (7.4)$$

7.6 EXPERIMENTAL RESULTS AND DISCUSSION

7.6.1 Classification Result for SD1

The results are presented below in terms of total classification error; classification error for all sections for both sample 1 and sample 2. Total Classification Error is determined using the same mathematical relationship given by the equation (1.1). The same is given below for ready reference.

$$\text{Total Classification Error } (\%\text{age}) = \frac{\text{Number of Misclassified Samples}}{\text{Total number of samples in that particular zone}} \times 100$$

It is depicted that 99.67% of faults have been accurately classified from the features obtained from DTCWT While 97.116% of faults are classified accurately using MBT. Table 7.3 gives the classification error for all the seven zones of sample distribution system 1 (SD 1).

Table 7.3: Classification Error for Zones for SD1

S. No	Zones	MBT	DTCWT
1	Zone 1	1.086	0.03157
2	Zone 2	0.675	0.0059
3	Zone 3	0.413	0
4	Zone 4	0.332	0
5	Zone 5	0.112	0
6	Zone 6	0.112	0
7	Zone 7	0.114	0

It can be seen from the above figure that the errors obtained are very less. Zone 1 and zone 2 have error of 0.0315% and0.0059% only in DTCWT. It is worth mentioning that zone 3, 4, 5 and 6 are

errorless. On the other hand, using MBT all zones have error including Zone 1 with a maximum error of 1.086% with minimum error in zone 5 and 6 with error %age of 0.112 respectively.

7. 6. 2 Classification Result for SD2

When the algorithm is applied to the features collected from the Dual Tree Complex Wavelet Transform for SD2, the classification accuracy is 99.89% Using DTCWT while, MBT has an accuracy of 98.09%. Table 7.4 gives the zone wise classification error for SD2. It is observed that only zone 4 has an error of 0.111% while other zones are errorless. Using MBT, zone 4 has the maximum error of 0.87% and minimum error of 0.18%. The result turns out to be promising as already discussed zone 1 and zone 3 have maximum samples and zone 4 has very less sample.

Table 7.4: Classification Error for Zones for SD2

S. No	Zones	MBT	DTCWT
1	Zone 1	0.62	0
2	Zone 2	0.18	0
3	Zone 3	0.24	0
4	Zone 4	0.87	0.111

7. 6. 3 Location Result for SD1

Table 7.5 depicts the location error for SD1 for all the sections. The results have not been compared with any other paper due to the fact that the performance evaluation carried out for this work has some additional features such as huge database, and the samples have been collected at relatively lower frequency. But, the work has been compared with the MBT in order to prove the effectiveness of DTCWT since till chapter – 6, MBT has given the best result in comparison with the other transforms used so far.

Table 7.5: Fault Location Error for All Sections for SD1

S. No	Zones	MBT		DTCWT	
		Maximum Error	Average Error	Maximum Error	Average Error
1	Zone 1	7.789	-17.453	4.2957	-5.1627
2	Zone 2	18.987	-3.458	11.6406	-0.0021
3	Zone 3	4.563	2.743	2.222	0.0005
4	Zone 4	6.892	-3.452	0.0167	-0.0034
5	Zone 5	9.845	2.386	0.0272	0.0014
6	Zone 6	7.431	-2.543	0.4172	-0.0212
7	Zone 7	8.432	3.49	5.1412	1.86

In the table shown above, the results obtained from DTCWT features are very promising. As discussed earlier, zone 1, 2 and 3 constitute the maximum number of samples, so the average error is just -5.1627, -0.0021, and 0.0005 m only, which is significantly low. It should be noted clearly that negative sign indicates that the fault was under reach from the exact fault location for zone 1 and 2. It was located beyond the fault point for zone 3. It is obvious from the above figure that the fault was located before the exact location at zone 1, 2, 4 and 6. The maximum error in zone 1 is just 46.27 m. But that is not at all the problem since as per the details of the distance given zone 1 is in kilometer and few meters does not make any operational difference. In case of MBT, it is found that the maximum error is 18.987 m in zone 2 and 9.845 m as compared with DTCWT. Also, the maximum average error is 17.453 m for AG fault which is more than three times the result obtained in DTCWT. It is also observed that the results of MBT are inferior when compared with DTCWT. The results obtained for zone are very much efficient and proves the effectiveness of the algorithm using DTCWT.

Table 7.6: Fault Location Error for Zone 1 for SD1

S. No	Faults	MBT		DTCWT	
		Maximum Error	Average Error	Maximum Error	Average Error
1	**AG**	3.654	-2.234	0.81	-0.66
2	**BG**	4.328	-3.112	0.429	-0.464
3	**CG**	2.018	-2.974	0.7063	-0.641
4	**ABG**	3.467	-2.397	0.110	-0.546
5	**ACG**	2.346	-1.713	0.341	-0.457
6	**BCG**	2.876	-2.124	0.361	-0.476
7	**ABCG**	3.112	-1.765	0.3532	-0.41503
8	**AB**	1.214	-1.674	0.112	-0.5391
9	**AC**	1.876	-8.546	0.4194	-0.42661
10	**BC**	3.231	-1.879	0.3823	-0.53044

Table 7.6 illustrates the location error of zone 1 in % age for all the ten types of fault using MBT and DTCWT. It is quite obvious that all faults were estimated before the fault point. AG has the maximum average error of – 0.66% as compared to other phase faults. ABCG has the minimum fault average with -0.415%. AG fault has the maximum error of 0.81%. But still, the error is less than 1% using DTCWT. But the results obtained using MBT has substantial error. The maximum error is 4.328% in BG fault and the average error is more in AC i. e 8.546%.

Table 7.7 gives the location error of zone 2. It is seen that all faults were located after the location except AG and ABG. The average error is also less than 0.08%. BG constitutes the fault with maximum average error. It also has the maximum error of 1.16% using DTCWT. With MBT, the maximum error is for BG fault with 5.538% and has an average error of 3.112%. ABG and AG fault are under reach from the location of fault.

Table 7.7: Fault Location Error for Zone 2 for SD1

S. No	Faults	MBT		DTCWT	
		Maximum Error	Average Error	Maximum Error	Average Error
1	**AG**	1.654	-1.434	0.31	-0.062
2	**BG**	5.358	3.112	1.16	0.075
3	**CG**	1.718	1.674	0.6066	0.0279
4	**ABG**	2.467	-1.357	0.1812	-0.0934
5	**ACG**	1.336	1.213	0.1989	0.0065
6	**BCG**	1.896	1.124	0.35527	0.0103
7	**ABCG**	1.172	2.345	0.07117	0.0108
8	**AB**	1.264	1.674	0.424	0.0012
9	**AC**	1.836	1.536	0.2254	0.0203
10	**BC**	1.291	1.729	0.239	0.008

The results of zone 3 are presented in table 7.8. Here, except AG, BCG, ABCG, and AC faults were located before the exact location. The average error per fault is even less than 0.01% which does not make any difference. BCG fault has the maximum average error of 0.009%. While the maximum error is 0.222% of AG by using DTCWT. When MBT is used, maximum error of 1.754% is obtained in AG followed by 1.718% in CG. The average error is maximum for ABG with 1.857% and the minimum average error is for AC fault with 1.116%.

Table 7.8: Fault Location Error for Zone 3 for SD1

S. No	Faults	MBT		DTCWT	
		Maximum Error	Average Error	Maximum Error	Average Error
1	**AG**	1.754	-1.433	0.222	-0.004
2	**BG**	1.258	1.712	0.199	0.004
3	**CG**	1.718	1.684	0.074	0.0057
4	**ABG**	1.367	1.857	0.0858	0.004
5	**ACG**	1.236	1.263	0.127	0.009
6	**BCG**	1.766	-1.194	0.129	-0.006
7	**ABCG**	1.372	-1.225	0.0484	-0.005
8	**AB**	1.244	1.644	0.0757	0.004
9	**AC**	1.336	-1.116	0.0466	-0.0008
10	**BC**	1.191	-1.121	0.0624	-0.0021

Table 7.9 depicts the location error of zone 4. The maximum error obtained is 0.0017%, while the average error computed is 0.000% which is almost negligible Using DTCWT. While, the maximum error of 1.583% and average error of 1.554% is obtained using M – Band Transform. Zone 4 consists of only CG fault.

Table 7.9: Fault Location Error for Zone 4 for SD1

S. No	Faults	MBT		DTCWT	
		Maximum Error	Average Error	Maximum Error	Average Error
1	**CG**	1.583	1.554	0.0017	0

It is seen from the table 7.10 the location error of zone 5. The maximum error calculated is 3.7644% while the average error is -0.0837% which is almost negligible using DTCWT. Similarly, using MBT the maximum error is 6.994% and -0.553% respectively. Zone 4 consists of only BG fault. It is seen that the fault was under reach from the fault point.

Table 7.10: Fault Location Error for Zone 5 for SD1

S. No	Faults	MBT		DTCWT	
		Maximum Error	Average Error	Maximum Error	Average Error
1	**BG**	6.994	-0.553	3.7644	-0.0837

It is obvious from figure 7.11 the fault location error for zone 6 is very less. The maximum error reported is 0.0317% while the average error is -0.0011% which is also very good when the features of DTCWT are used. Also, the maximum error is 1.345% and 0.458% using MBT. The error shows that the fault was under reach from the exact fault point. All these error are almost negligible.

Table 7.11: Fault Location Error for Zone 6 for SD1

S. No	Faults	MBT		DTCWT	
		Maximum Error	Average Error	Maximum Error	Average Error
1	**CG**	1.345	-0.458	0.0317	-0.0011

Table 7.12 gives the fault location error of zone 7. By using CTDWT, The average error is 0.0861% while the maximum error is 3.41%. Also, the maximum error using MBT is 4.548% and average error is 0.658% which is more. It should be kept in mind that zone 4, 5, 6 and 7 consists of very less number of samples.

Table 7.12: Fault Location Error for Zone 7 for SD1

S. No	Faults	MBT		DTCWT	
		Maximum Error	Average Error	Maximum Error	Average Error
1	**CG**	4.548	0.658	3.41	0.0861

7. 6. 4 Location Result for SD2

It can be seen from table 7. 13 the fault location error for all the sections are presented.

Table 7.13: Fault Location Error for Zones for SD2

S. No	Zones	MBT		DTCWT	
		Maximum Error	Average Error	Maximum Error	Average Error
1	Zone 1	5.348	3.762	4.78	2.56
2	Zone 2	5.756	3.351	4.66	2.21
3	Zone 3	4.984	5.985	4.91	2.12
4	Zone 4	7.893	3.881	4.783	2.3255

Using DTCWT, Zone 1 has the maximum average error of 2.56 m as compared with other zones. Zone 2, 3 and 4 has almost similar average error of 2.21, 2.12 and 2.32 m respectively. The maximum error is for zone 3 in the range of 4.91 m. It should be kept in mind that no literature is available for locating faults in IEEE 13 node system since the distances are very small. The results are very promising as it constitutes very negligible error. The maximum error is between 4.6 and 5 m for zone 1, zone 2 and zone 3 and just 4.66 m for zone 2. But still they are very promising. When the results are compared with MBT, it is found that the maximum error is 7.893m for zone 4 and the average error is 5.985m for zone 3. The results obtained are inferior if compared with DTCWT.

Table 7.14 depicts the fault location error for zone 1 of SD2. Here, it is found that ABCG fault has the maximum average error of 0.3% as compared with other faults. All the error for these faults is in the range of 0.2% to 0.3%, which is very promising. The maximum error for ABCG is 0.499% using DTCWT. The results obtained from MBT does not give better result as the maximum error is 1.87% for AB fault and the average error is 1.98%. The other errors are also high in this case. The results obtained are very promising for DTCWT.

Table 7.14: Fault Location Error for Zone 1 for SD2

S. No	Faults	MBT		DTCWT	
		Maximum Error	Average Error	Maximum Error	Average Error
1	AG	1.54	0.889	0.475	0.245
2	BG	1.34	0.996	0.492	0.228
3	CG	1.65	0.873	0.493	0.230
4	ABG	1.23	1.34	0.490	0.27
5	ACG	1.34	1.65	0.48	0.29
6	BCG	1.43	1.87	0.46	0.29
7	ABCG	1.32	1.22	0.47	0.23
8	AB	1.87	1.98	0.49	0.27
9	AC	1.34	1.23	0.46	0.27
10	BC	1.36	1.68	0.499	0.3

Table 7.15: Fault Location Error for Zone 2 for SD2

S. No	Faults	MBT		DTCWT	
		Maximum Error	Average Error	Maximum Error	Average Error
1	BG	2.654	1.448	0.475	0.300

It can be seen from table 7.15, that the results for fault location error for zone 2 of SD2 that it involves only B phases. The maximum error in this zone is 0.475% and average error is 0.3% only by using DTCWT. By the use of MBT, the maximum error is 2.654% and the average error is 1.448% respectively.

Table 7.16: Fault Location Error for Zone 3 for SD2

S. No	Faults	MBT		DTCWT	
		Maximum Error	Average Error	Maximum Error	Average Error
1	AG	0.887	0.654	0.483	0.239
2	BG	0.982	0.467	0.481	0.245
3	CG	1.234	0.989	0.498	0.221
4	ABG	1.564	0.653	0.483	0.221
5	ACG	1.348	0.884	0.476	0.250
6	BCG	1.223	1.218	0.447	0.215
7	ABCG	1.008	1.266	0.496	0.281
8	AB	0.987	1.253	0.472	0.261
9	AC	0.884	1.348	0.499	0.300
10	BC	0.926	1.118	0.476	0.222

It is seen from table 7.16 the fault location error for zone 3 of SD2. Zone 3 comprises of all ten types of fault. Here, AC fault has the maximum average error of 0.3% and BCG fault has minimum average error of 0.221%. The maximum error reported is that of AC followed by CG with 0.499% and 0.498% respectively in case of DTCWT. While, using MBT the maximum error is 1.564% in ACG fault and average error of 0.467%. Also, it is observed that the maximum error are in the range between 1.564% and 0.884%. While, the average error obtained is 0.467% which is twice the error obtained for DTCWT. It can be concluded that the results are very promising for DTCWT, since the error is less than 0.5%.

Table 7.17: Fault Location Error for Zone 4 for SD2

S. No	Faults	MBT		DTCWT	
		Maximum Error	Average Error	Maximum Error	Average Error
1	AG	1.25	0.98	0.468	0.306
2	CG	1.38	1.03	0.483	0.290
3	AC	1.18	1.11	0.450	0.191

Zone- 4 involves two phase A and phase C as seen from table 7.17. Here AG fault has more average error of 0.306% than CG and AC fault i.e. 0.290% and 0.191% respectively. CG fault has the maximum error of 0.483% as compared to the error of AG and CG with 0.468% and 0.450% respectively in the case of DTCWT. When the features from MBT are used, it is observed that the maximum error is of 1.38% for CG fault and the average error is 1.11% for AC fault. Needless to say that all the errors obtained in MBT are more than DTCWT. Based, on the above results it is therefore concluded that the results obtained from DTCWT are very promising.

7.7 COMPUTATIONAL TIME

In the figure 7.4, computation time taken for various processes involved for the development of algorithm has been presented. It should be noted that all these times were evaluated after calculating the total time taken for each process divided by the total no of samples considered. The configuration of the computer on which the algorithm for fault classification and fault location was tested is as: Core*i7* processor, 3.2GHz speed, 12 GB Ram memory.

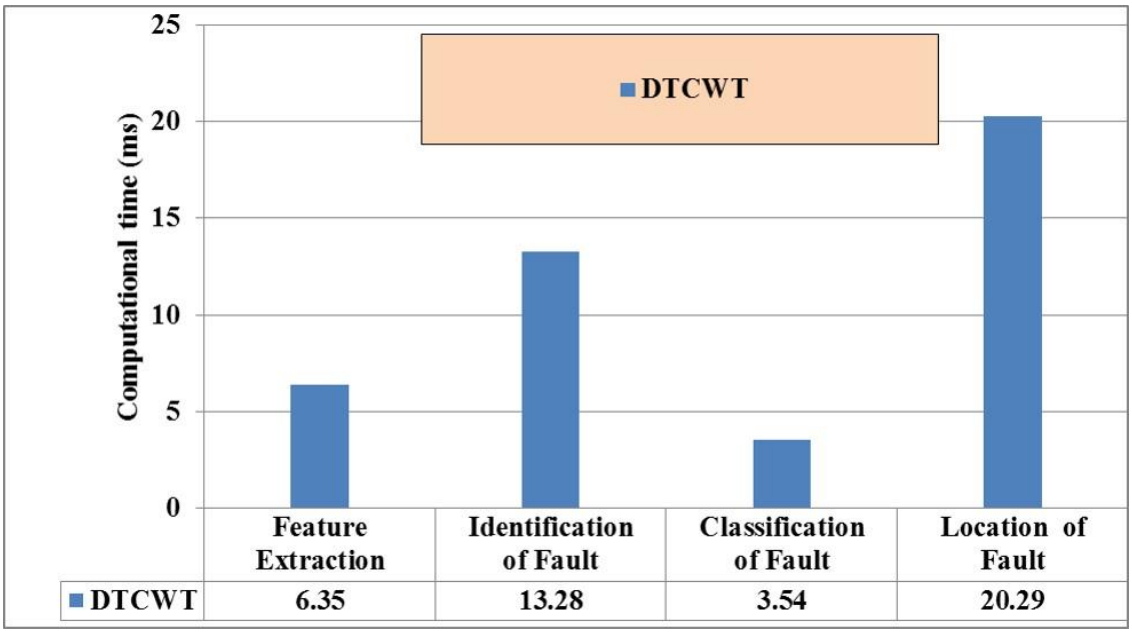

Figure 7.4: Computational Time for Different Evolutionary Process

The feature extraction time is 6.25 ms which is quite low as compared with other signal processing tools. The time taken for identification of faults is 13.28ms, classification of faults is 3.54 ms and for location of fault is 20.29 ms respectively.

7.8 SUMMARY

An algorithm for detection, identification, classification and location of faults is presented in this chapter. Discrimination between load signals and fault signals have also been presented. DTCWT has not found its use in any other literature for algorithms meant for locating faults in distribution system. The features extracted are basically decomposition of both high frequency as well as low frequency content in the signal in different levels. The results are very promising when the features of DTCWT are combined with ANN. It is evident that classification accuracy of about 99.67% for SD 1 and 99.89% for SD 2 is fetched using DTCWT. Whereas, MBT gives classification accuracy of only 97.116% for SD 1 and 98.09% for SD2 respectively. Also, in case of location, the maximum error reported for SD1 is 11.64 m using DWT, while using MBT the error is 18.98 m. Further, the location error obtained for SD2 using DTCWT is just 4.91 m while using MBT is 7.89 m respectively. Thus, it proves that DTCWT provides optimal feature extraction signal for ANN. The results have been compared with MBT and hence, the results of DTCWT which have been obtained are very promising giving less error in both sample distribution system 1 and sample distribution system 2. The times taken for different evolutionary processes have been given which shows that the feature extraction takes less time.

FCM and Statistical Based Approach

Chapter 8

Distribution system comprises of number of radial feeders which has to be highly reliable and efficient under normal and emergency condition. As already discussed, the methods proposed for fault location in transmission lines are not easily applicable to distribution systems.

The author in [129] – [130] has presented a complete overview of the work carried out for detecting, identifying and locating faults in a distribution system. The author in [131] – [132] has presented algorithm for estimating the error as well as identifying in the faults in a series compensated transmission line. Needless to mention that these techniques are basically based on the modern day algorithms were more than one algorithm is developed for detection, identification, classification and location of faults. Support Vector Machine as classifier has been used. Other work includes locating faults on underground cable [133] – [134], use of artificial intelligence [135], considering the sags in voltage for location of fault [136] etc are few works which have been carried out in the direction of fault location in distribution system. The author in [137] – [138] has also located fault in distribution system but they have considered the phases which involved the ground. Even, the present day scenario of detecting fault in distributed generation has been dealt in [139].

With the introduction of digital signal processing tools in power system, wavelet transform came into play for extraction of current features that can be subjected to algorithm meant for appropriate location of faults but yet an errorless fault location could not be achieved. Also, methods based on amalgamation of signal processing tools and artificial intelligence was employed. In the previous chapters, WT, WPT, GT, MBWT and DTCWT had been utilized to extract features for detection, identification and location of faults in electrical distribution system. Each had its own limitations and advantages. But these approaches were based on extraction of features by use of digital signal processing tools and were developed keeping in mind the present scenario.

In the present chapter, the current samples collected from the sample distribution systems are subjected to FCM to obtain clusters and fed to expectation maximization algorithm [13]. This

chapter attempts to presents a solution to tackle the problem of interruption in service in distribution system. A current sample database collected from the measurements at substation end has been statistically modeled. It is an attempt to detect, identify and locate fault in distribution system with a permissible accuracy.

8. 1 SAMPLE DISTRIBUTION SYSTEM

Two sample distribution systems have been considered as already described in section 1.3.1 and 1.3.2 of Chapter 1. The problem of the multiple estimation of location of faults has also been tackled. It arises due to presence of laterals at the same distance in the power distribution network by dividing the network into various zones.

The sample distribution (SD 1) has been divided into 7 zones and sample distribution (SD 2) has been divided into 04 zones. In the first distribution system considered for simulation, zone 1, zone 2 and zone 3 consists of all ten types of faults. Zone 4 and zone 5 consists of only one fault since it involves only phase –b. Similarly, Zone 6 and zone 7 consists of only one fault since it involves only phase –c.

On the other hand, in the second distribution system considered zone 1 and zone 3 comprises of all ten types of fault. While, zone 2 involves 4 types as it involves phase – b and phase – c. Also, zone 4 involves 4 types as it involves phase – a and phase – c respectively.

Table: 8 1- Number of current and voltage samples collected

Name	SD 1	SD 2
No of Zones	7	4
Fault Resistance (Ω)	0.05, 10, 20, 30, 40, 50	0.05, 10, 20, 30, 40, 50
Fault Inception Angle (°)	0, 60, 90, 180	0, 60, 90, 180
Fault Types	10	10
Total Samples	**1428**	**320**

In total 1748 samples have been used for evaluating the effectiveness of the algorithm developed. A total of 1428 current and voltage samples for zone 1 and 320 samples for zone 2 have been

collected for preparing the database and used for testing the algorithm. Table 8.1 gives a complete overview of the number of current and voltage samples collected at each zones respectively.

The sampling frequency considered for the present work is 2.00 kHz. The duration of run for the present simulation in both the cases is 0.5 sec. Fault has been simulated at various inception angles as mentioned in Table 8.1. The solution time step is 250 μs. This is the EMTDC simulation time step. The channel plot step is 500 μs which in turn determines the sampling frequency. This is the time interval at which EMTDC sends data to PSCAD for plotting as well as writing data to output files. It should be kept in mind that more is the sampling frequency; more is the information content in a signal.

8.2 APPROACHES FOR FAULT LOCATION

An approach to resolve the problem of fault location in distribution system subjected to different kinds of fault by examining system behavior is presented. After simulating a distribution system with different types fault over a range of fault resistance and at various locations, current waveforms are recorded at the substation end. These samples are pre-processed in PSCAD to obtain the r.m.s value. Each and every sample in the created database has sufficient information about the system. It basically gives the outcome of the different conditions that occur in the system. It helps in the process of data classification, while establishing certain classes in the model. At first data has been analyzed by considering the distribution system into groups where fault can be easily detected and located. The objective is set in such a manner that these particular groups correspond to zones so that a relationship is established data classification and fault location. Fuzzy c- mean is then applied on these current samples thus obtained and are subjected to expectation – maximization algorithm for fault classification and fault location of zones respectively. A detailed algorithm for FCM and EM-algorithm applied for the above purpose is presented below:

8.2.1 Fuzzy c-Means (FCM) Clustering

Dunn [140] introduced the concept of Fuzzy c-means (FCM) clustering in 1974. It was further simplified by Bezdek [141] in 1981 and has since being admired. It is considered as a derivative of k-means clustering. Clustering data allows the conformation of meaningful groups in an analytical

way, which helps to classify data according to similarities or affinities. The clustering algorithms are developed by computing the metric differences for the distance calculation. Various types of clustering methods have been developed. Out of them fuzzy clustering finds its vital representation in the field of data mining, artificial intelligence, numerical taxonomy, pattern recognition, image analysis, image processing, and medicine. It is widely used because of fuzzy membership, as it allows membership functions to all clusters in a data set making it appropriate for analysis of the clusters. Fuzzy C-means algorithm is based on the minimization of a criterion function. FCM clustering algorithm is applied because of good performance and less execution time to obtain clustered data. In the proposed work, authors have used algorithm [142] to fix the number of clusters.

If one consider a matrix of a data elements (fault signal), each of size $s(s=3)$ is represented as $B=(b_1,b_2,.....,b_n)$. The clustering are established by FCM through an iterative procedure that minimizes the objective function as drafted in Equation (8.1)

Objective function: $$O_m(U,C)=\sum_{i=1}^{c}\sum_{j=1}^{n}U_{ij}^{m}D^2(x_j,C_i) \quad (8.1)$$

Constraint: $$\sum_{i=1}^{c}U_{ij}=1;\quad \forall j \quad (8.2)$$

Where, U_{ij} is membership of the j^{th} data in the i^{th} cluster C_i, m stands for the fuzziness of the system $(m=2)$ and D represents the distance between the cluster center and data point.

8.3 FCM Algorithm

The Flow chart of FCM algorithm is shown in figure 8.1. The implementation steps are given below:

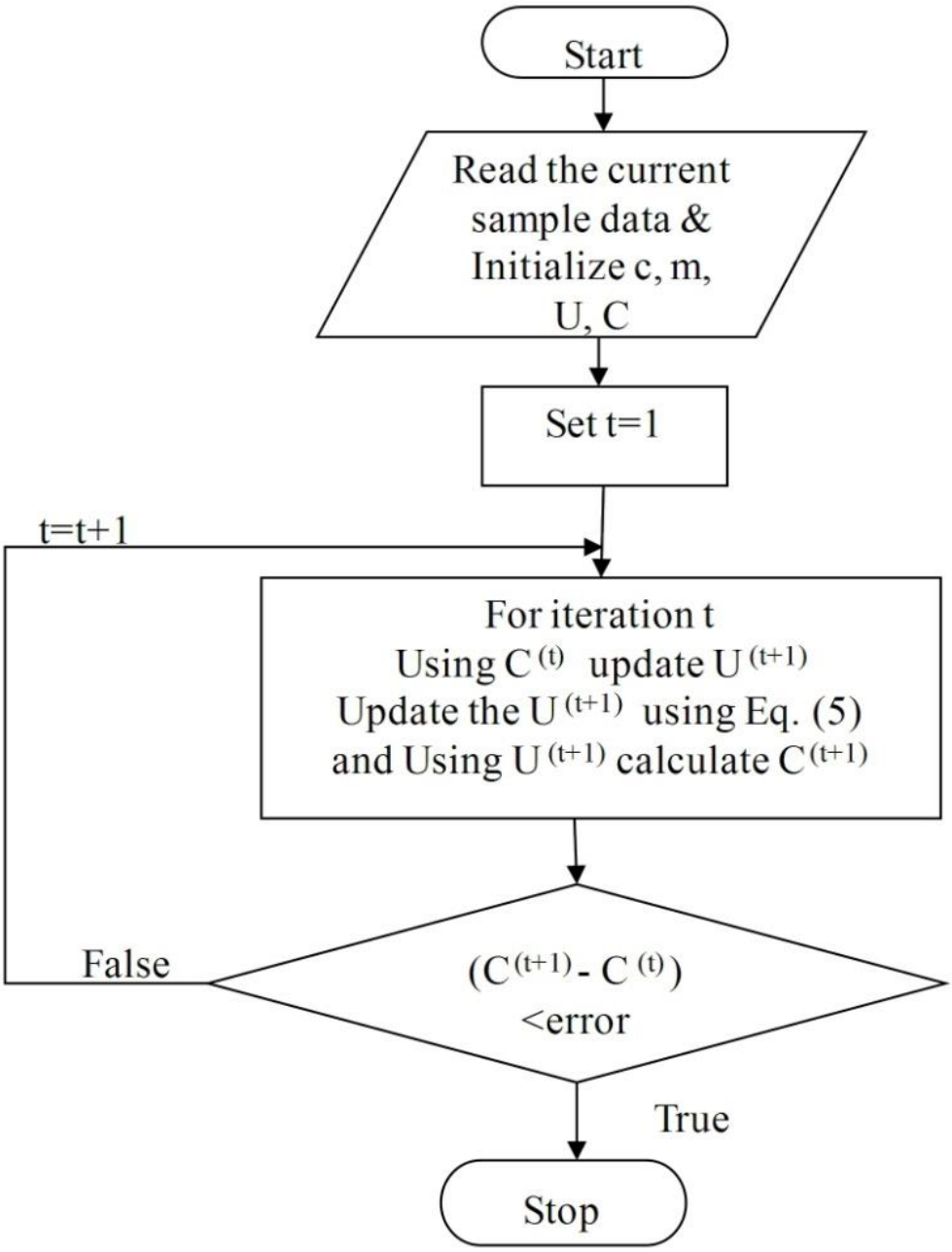

Figure 8.1: Flowchart for FCM algorithm

Input: fault signal data; Output: Clustered data;

- Initialize the cluster centers C_i .

- The distance is computed by D between the cluster center and data point by using equation (8.3)

$$D^2(x_j, C_i) = \left\| x_j - C_i \right\|^2 \tag{8.3}$$

- The membership values are evaluated by using equation (8. 4)

$$U_{ij} = \left(\sum_{k=1}^{c} \left(\frac{D(x_j, C_i)}{D(x_j, C_k)} \right)^{2/(m-1)} \right)^{-1} \tag{8.4}$$

- The cluster centers are updated using equation. (8.5)

$$C_i = \frac{\sum_{j=1}^{n} U_{ij}^m x_j}{\sum_{j=1}^{n} U_{ij}^m} \tag{8.5}$$

- The iterative process starts:

1. The membership values are renewed U_{ij} by using equation (8.4)
2 the cluster centers are updated C_i by using equation (8.5).
3 The distance is revised D using equation (8.3).
4 If $\left| C_{new} - C_{old} \right| > \varepsilon; \quad (\varepsilon = 0.001)$ then move to step1.
5 Else stop the process

- Each fault signal is assigned a specific cluster for which the membership is maximal.

8.4 EXPECTATION – MAXIMIZATION ALGORITHM

Initial values for the centers are calculated using the knowledge of the groups, obtained using the FCM algorithm. The initial value of covariance matrix is used as the identity matrix. The mixture coefficients are then evaluated maintaining the proportionate of data in each group, in relation to the sample. Once initial parameters are obtained, the estimation of the mixture model parameters is initiated by the Expectation - Maximization algorithm [143] – [144], which is an iterative procedure until the desired convergence is achieved. It is an iterative approach to maximum likelihood estimation. Each iteration of an EM algorithm involves two steps: an Estimation (E) step and a Maximization (M) step. The M step involves the maximization of a likelihood function that

is redefined in each iteration by the E step. The results are the final values of parameters μ **(mean vector),** V (covariance matrix) and p (weight/ coefficient of mixture) of each group. The steps of the Expectation – Maximization algorithm are as follows:

1. The number of components of the mixture is computed by using the fuzzy cluster-mean algorithm.
2. The initial values of parameter are evaluated for each component $(\mu^{(0)}, V^{(0)}, p^{(0)})$.
3. Estimate the posterior probability for each observation (Expectation-steep) as shown in the following equations:

$$\hat{\tau}_{ij} = \frac{p_i \phi(x_j; \mu_i, V_i)}{f(x_j)} \tag{8.6}$$

$$f(x_j) = \sum_{g=1}^{G} p_g \phi(x_j; \mu_g, V_g) \tag{8.7}$$

Where $\hat{\tau}_{ij}$ represents the posterior probability of x_j corresponding to the i term, $\phi(x_j; \mu_i, V_i)$ is the normal multivariate density and $f(x_j)$ corresponds to the estimated mixture of distributions for the i terms evaluated in x_j and j is an index which indicates the total amount of data.

4. Update, μ , V , p of each component (maximization-step) by using equations (8.8) – (8.10). p_i, μ_i, V_i are the updated estimations.

$$p_i = \frac{1}{n} \sum_{j=1}^{n} \hat{\tau}_{ij} \tag{8.8}$$

$$\mu_i = \frac{1}{n} \sum_{j=1}^{n} \frac{\hat{\tau}_{ij} x_j}{p_i} \tag{8.9}$$

$$V_i = \frac{1}{n} \sum_{j=1}^{n} \frac{\hat{\tau}_{ij} (x_j - \mu_i)(x_j - \mu_i)^T}{p_i} \tag{8.10}$$

5. Repeat steps 3 and 4, until desired convergence is obtained.

Subsequently, the groups are organized in classes associated to faults. It is based on the probability of appearance in each group as presented by the mixture model in the following equation:

$$f_{FM}(x) = \sum_{g=1}^{G} p_g \phi_g(x; \mu_g, V_g) \tag{8.11}$$

Where $f_{FM}(x)$ corresponds to mixture model of sample (x) which corresponds to random sample of n observations of dimension d.

Based on the statistical model, fault location is based on the response obtained from the model. Current waveforms which have been recorded are used to locate the answer for this problem. Each and every sample in the created database has sufficient information about the system. It basically gives the outcome of the different conditions that occur in the system. It helps in the process of data classification, while establishing certain classes in the model. It should be kept in mind that each class corresponds to a zone within the distribution network. The distribution network has been taken divided into several zones. The work focuses to establish the match between fault location and data classification within zones. Since, the groups are known; the current samples collected are subjected to Fuzzy Cluster Means algorithm, in order to evaluate the centers of groups so that the method is initialized. Further, the shape and final proportion of groups within the distribution is defined by using EM algorithm and the initial estimation. At this step, the shape of the covariance matrices for each distribution and the shape of each group is determined by a heterocedastic model. Further, the coefficients obtained are mapped within the group to determine the occurrence of the fault.

8. 5 RESULTS AND DISCUSSION

A brief analysis of the result is presented below for both the sample distribution system considered

8.5.1 Sample Distribution System 1

The results of sample distribution system have been compared with the results reported in [145]. Table: 8.2 give the classification result. From the above table, it is obvious that the result obtained for classification after subjecting the current samples to FCM is far promising as compared from Reference [145]. It can be observed that the results of Single –phase to line faults and line to line faults does not make any difference, But the results obtained for ABG, BCG and CAG faults are far promising as 95.12%, 90.05% and 90.01% as compared to 81.25%, 79.16%, 77.08% respectively. Even, the result for ABCG fault i.e. 90% is given which is not available in the reported paper. The results prove the worth of FCM algorithm as compared to k-mean algorithm. The location result is represented in Table 8.3.

Table 8.2: The Classification Result for SD1

Sr. No	Types of Fault	Name of the Fault	REF [13]	PM
1	Single – Phase to Ground Fault	AG	100%	100%
2		BG	100%	100%
3		CG	100%	100%
4	Line to Line Fault	AB	100%	100%
5		BC	100%	100%
6		CA	100%	100%
7	Double Line to Ground Fault	ABG	81.25	95.12%
8		BCG	79.16	90.05%
9		CAG	77.08	90.01%
10	Three Phase to Ground Fault	ABCG	NA	90%

Table 8.3: The Location Result for SD1

Sr. No	Types of Zone	REF [13]	PM
1	Zone 1	99.43%	99.98%
2	Zone 2	95.17%	98.25%
3	Zone 3	82.62%	94.52%
4	Zone 4	56.49%	78.77%
5	Zone 5	NA	80.25%
6	Zone 6	NA	81.43%
7	Zone 7	NA	84%

The results obtained give the probability of the samples which are given to the zones. As seen from the result, Proposed method i.e. the samples obtained from FCM yields far better results as compared to the K- mean algorithm. Specially, for zone 4, the difference in result is almost about 20%. The results for other zones have not been reported but still they can be said promising because these zones contain very few samples.

8.5.2 Sample Distribution System 2

The classification result of the current samples obtained from IEEE 13 node feeder is presented in Table: 8. 4. It's worth mentioning that the results have not been compared with anyone since no result for this feeder is reported. The results obtained are very promising since all the faults are accurately classified into different types of faults.

Table. 8.4: Classification Result for SD 2

Sr. No	Types of Fault	Name of the Fault	PM
1	Single – Phase to Ground Fault	AG	100%
2		BG	100%
3		CG	100%
4	Line to Line Fault	AB	100%
5		BC	100%
6		CA	100%
7	Double Line to Ground Fault	ABG	100%
8		BCG	100%
9		CAG	100%
10	Three Phase to Ground Fault	ABCG	100%

Table 8.5 gives the location result of the sample distribution system2. It should be kept in mind that zone 1 and zone 3 gives 100% result as it comprises of all the three phases. While, zone 2 and zone 4 gives 75% and 78.77% result as it involves two phases and consists of less number of sample.

Table 8.5: Zone Classification Result for SD 2

Sr. No	Types of Zone	PM
1	Zone 1	100%
2	Zone 2	75%
3	Zone 3	100%
4	Zone 4	78.77%

8.6 SUMMARY

A probabilistic based method for location of faults in distribution systems has been given in this chapter. The approach is based on statistical modeling of the samples obtained after been clustered by the use of FCM. Results obtained after the clusters are administered to expectation – maximization algorithm for the given feeder is promising It should be kept in mind that the proposed algorithm has not been applied to current samples of distribution system as per the literature available till date.

The selection of the number of groups or zones is the drawback for the proposed method if other distribution system is considered. But for the two sample distribution system, the groups have been defined. This method allows an optimization for classification of data which enables good model accuracy. Also, this method if implemented is economically viable.

Conclusion and Future Perceptive

Chapter 9

Distribution system comprises of number of radial feeders which has to be highly reliable and efficient under normal and emergency condition. As already discussed, the methods proposed for fault location in transmission lines are not easily applicable to distribution systems due to the configuration of the network.

The database was collected over range of different sampling frequency starting from 16.00 kHz to 02.00 kHz. Also, several digital signal processing tools were used to extract the feature and provide good results. The algorithms have been designed to almost accurately detect, identify, classify and locate faults in electrical distribution system. The problem of multiple estimation that arouse in the algorithms developed from impedance based calculation has been dealt off.

Two sample distribution networks have been considered as a standard database in order to test the effectiveness of the algorithm. These databases are the standard databases employed for testing the algorithm. The features have been extracted from wavelet transform, wavelet packet transform, Gabor Transform, Multi band Wavelet Transform and Dual Tree Complex Wavelet Transform. Among, all DTCWT has given the best results. It has been successful in computing fault distances without any error. The results obtained for classification is more than 99% for sample distribution system 1 and more than 98.5% respectively. Similarly, the results for location of faults for sample distribution system 1 are less than 1% and sample distribution system 2 is less than 2% respectively.

A comparative analysis of the result between wavelet and wavelet packet transform over different "*daubechies"* has been presented for the purpose of classification. As per the result obtained even though the classification accuracy is 99.61% in case of WPT and 99.03% in case of WT for SD1, the location accuracy obtained is more in case of WPT. It is quite evident from the results obtained that the feature extracted from WPT yield better result as compared to WT. for both SD1 and SD2. It should also be kept in mind that the sampling frequency considered for this case is 15.360 kHz.

In the case of GT classification an accuracy of 99.94% is obtained in comparison to 97.294% in case of WPT for SD1. Similarly, the maximum error attained by using GT features is equal to 139.27 m as compared with WPT where the error in location is 248.76m. For SD2, the classification accuracy is 99.73% for GT as compared to 98.69% in case of WPT. Similarly, the location error in terms of WPT is almost approximately double when compared with GT features where the maximum error is 8.456 m as compared to 4.99 m. Thus, it proves that GT provides optimal feature extraction signal for ANN. The results which have been obtained are very promising giving less error in both sample distribution system 1 and sample distribution system 2. It is worth reminding that the sampling frequency considered in the present case is 12.00 kHz.

The results are very promising when the features of MBT are combined with ANN. In case of MBT the accuracy is 99.76% for SD1 and 99.82% for SD2 as compared to 97.56% and 98.68% for GT for SD1 and SD2 respectively. For locating faults, the maximum error is 139.26 m for SD 1 and 4.98 m for SD 2 using MBT as compared to 234.58 m and 4.98 m using GT for SD 1 and SD 2 respectively. Thus, it proves that MBWT provides optimal feature extraction signal for ANN. The results which have been obtained are very promising giving less error in both sample distribution system 1 and sample distribution system 2. The results have been compared with GT and for the particular frequency considered the MBT yields better result as evident from the chapter. The sampling frequency considered in the present case is 8.00 kHz.

It is evident that classification accuracy of about 99.67% for SD 1 and 99.89% for SD 2 is fetched using DTCWT. Whereas, MBT gives classification accuracy of only 97.116% for SD 1 and 98.09% for SD2 respectively. Also, in case of location, the maximum error reported for SD1 is 11.64 m using DWT, while using MBT the error is 18.98 m. Further, the location error obtained for SD2 using DTCWT is just 4.91 m while using MBT is 7.89 m respectively. Thus, it proves that DTCWT provides optimal feature extraction signal for ANN at 4.00 kHz. Hence, it can be concluded that DTCWT will provide better classification and location results at low frequency.

In an attempt to present non transform based technique, as an extension to transform based techniques, a new statistical approach which is nowadays very popular is presented. With this feeling the author has attempted to give a new methodology to classify and locate faults by using FCM in an attempt to detect, identify and locate fault in distribution system. The method is found to give improved accuracy to that of transformed based tools. As discussed in chapter -2, clustering

methods are very popular methods in classification. Hence, the detection, identification and classification of faults have also been carried out by the use of Fuzzy cluster means and expectation maximization algorithm. The purpose had been to correctly classify the faults and locate the particular zones associated with it. It is worth to mention that in the proposed algorithm current samples are used instead of conventionally used voltage samples."

Other important feature of the work reported is that computational time for carrying out different evolutionary process has also been discussed. The feature extraction time, time taken for identification, classification and location of faults have been successfully derived. The time has been computed for each sample.

Among all, Gabor Transform takes the maximum time followed by Wavelet Packet Transform, M Band DWT, DTCWT and WT. The reason have been explained in the thesis.

9.1 THESIS OUTCOME

After investigation of all the developed algorithms with a large number of fault cases with all possible types of faults, faults parameters and system parameters variations, following outcomes of this work can be listed:

- The fault classification, fault zone identification and fault location algorithms developed in this work show considerable improvement in terms of accuracy compared to the methods available in the literature.
- All algorithms in this work are developed for single end measurement only. This eliminates the requirement of measurements from other end, communication channel and installation of high frequency based travelling wave's detector.
- All fault detection, identification, classification and location algorithms are developed to work with measurements of three phase currents and voltages
- All fault classification and fault zone identification algorithms designed in this work are developed to work with less than quarter cycle post fault measurements only. This reduces the processing time of the algorithms thereby, making them quite fast for practical implementation.

- Among the features collected by different signal processing tools, DTCWT presents superior result. The orders in which features have been extracted and good results have been obtained are in sequence as follow: DTCWT, M – Band DWT, Gabor Transform, WPT and WT.
- Statistical based method employing the use of Fuzzy Cluster Mean and Expectation Maximization algorithm has also been used.

9.2 FUTURE PERSPECTIVES

- Fault needs to be detected, identified and classified in multi ring feeder system. As per the available literature very little work has been reported. Barely two or three papers have been successful in the above purpose.
- Faults needs to be located in the distribution systems with underground cables. These cables are also the part of the network. Most of the researchers neglect the underground cables and develop the algorithm.
- Detection of high impedance fault is also an important issue which needs to be addressed. High impedance faults cause major destruction to the equipment installed in the network.
- Nowadays, distributed generation has found a significant role in the distribution networks. Faults needs to be detected, identified and located in distribution network with distributed generation.

List of Publications

International Journals:

1. Pratul Arvind, Rudra Prakash Maheshwari, "A Gabor Filter Based Approach for Locating Faults in Distribution", Advanced Materials Research, vol. 403, pp. 5007 – 5014.
2. Pratul Arvind, Rudra Prakash Maheshwari, "FCM and Statistical Based Approach for Classification and Location of Faults in Electrical Distribution System", International Journal of Power System Operation and Energy Management, vol. 1, pp. 64 – 68.

Communicated Journals:

1. Pratul Arvind, Rudra Prakash Maheshwari, "Introspecting Wavelet and Wavelet Packet Transform Features for Fault location in Distribution System, International Review of Electrical Engineering.(PraiseWorthy)
2. Pratul Arvind, Rudra Prakash Maheshwari, "A Gabor Transform Based Approach for Locating faults in Distribution System", International Journal of Electrical Power and Energy Systems (Elsevier)
3. Pratul Arvind, Rudra Prakash Maheshwari, "A M - Band Transform Based Approach for Locating faults in Distribution System", International Journal of Electrical Power System Research(Elsevier)
4. Pratul Arvind, Rudra Prakash Maheshwari, "A Complex Dual Tree Wavelet Transform Based Approach for Locating faults in Distribution System", IET Generation Transmission and Distribution

International Conferences:

1. Pratul Arvind, Rudra Prakash Maheshwari, "Comparison between wavelet and wavelet packet transform features for classification of faults in distribution system", American Institute of Physics Conference Proceedings, pp. 25– 30, August 2012.
2. Pratul Arvind, Rudra Prakash Maheshwari, "A wavelet packet transform approach for locating faults in distribution system", IEEE Symposium on Computers & Informatics (ISCI), Penang, Malaysia, pp. 113 – 118, March 2012.
3. Pratul Arvind, Rudra Prakash Maheshwari, "Simulation of IEEE 13-node feeder and Its wavelet decomposition", Proceedings of ICOPS, vol. 10, pp. 423– 430, December 2011.
4. Pratul Arvind, Rudra Prakash Maheshwari, "A Wavelet Transform and Rule Based Approach for Identification of Faults in Electrical Distribution System", Proceedings of International Conference on Electrical Power and Energy System, MANIT, Bhopal, pp. 351– 356, August 2010.

BIBLIOGRAPHY

[1] IEEE Standard, "IEEE guide for protective relay applications to distribution lines," IEEE Power Engineering Society, pp.1-100, February 2008.

[2] D. P. Kothari, I. J. Nagrath, "Power system engineering", New Delhi: Tata McGraw Hill, pp.886–890, 2009.

[3] Ministry of Law and Justice, "The electricity act", New Delhi, June 2, 2003.

[4] Electrical Power Protection, "Faults types and effects", IDC Technologies Tech Briefs (Electrical), 2000.

[5] M. M. Saha, Ratan Das, et-al, "Review of fault location techniques for distribution systems," Power Systems and Communications Infrastructures for the future," Beijing, pp.1-6. Sept. 2002.

[6] R. Das, "Determining the location of faults in distribution system," Ph. D. dissertation, University of Saskatchewan, Saskatoon, Canada, 1998.

[7] IEEE Distribution Planning Working Group Report, "Radial distribution test feeders," IEEE Transaction on Power System, vol. 6, no. 3, pp. 975 – 985, August 1991.

[8] "PSCAD, User Guide," Manitoba Research Centre, Canada.

[9] James Burke, "Hard to find information about distribution systems", ABB Reference Manual, pp. 1-55, August.2002.

[10] D. T. W. Chan, C. Z. Lu, "Distribution system fault identification by mapping of characteristic vectors," International Journal of Electric Power Systems Research, vol. 57, pp.15-23, 2001.

[11] Anoop Arya, Yogendra Kumar, A comparative survey of fault section estimation methods in electric distribution system," Proceedings of Fifteenth National Power Systems Conference (NPSC), IIT Bombay, pp 154-158, December 2008.

[12] Biswarup Das, "Fuzzy logic-based fault-type identification in unbalanced radial power distribution system," IEEE Transactions on Power Delivery, vol. 21, no. 6, pp.278-285, January 2006.

[13] Wael Al-Hasawi, Mahmoud Gilani, "Proposed techniques for identifying open and short circuit sections in distribution systems," WSEAS Transactions on Power Systems, pp 372-381, vol 4, no 12, December 2009.

[14] Le Xu, Mo-Yuen Chow, "A classification approach for power distribution systems fault cause identification," IEEE Transactions on Power Delivery, vol. 21, no. 1, pp.53-60, February 2006.

[15] Xuping Xu, James. F. Peters, "Rough set methods in power system fault classification," Proceedings of IEEE Canadian Conference on Electrical and Computer Engineering, Manitoba, pp. 100-105, 2002.

[16] K. L. Butler, J. A. Momoh, "Detection and classification of line faults on power distribution systems using neural networks, Proceedings of 36th Midwest Symposium on Circuit and Systems, pp 368-371, 1993.

[17] Y. Tang, H.F. Wan et al., "Fault indicators in transmission and distribution systems," Proceedings of IEEE International Conference on Electric Utility Deregulation and Restructuring and Power Technologies, City University, London, pp. 238-243, April 2000.

[18] U. D. Dwivedi, S. N. Singh, S. C. Srivastava, "A wavelet based approach for classification and location of faults in distribution systems," Proceedings of INDICOM 2008, vol.2, pp. 488-493, December 2008.

[19] A. Campoccia, et-al, "A generalized methodology for distribution systems faults identification, location and characterization," Proceedings of IEEE International Conference on Power Technology, Russia, pp. 1-7, 2005.

[20] A. Campoccia, et-al, "GA-based feature selection for faults identification in electrical distribution systems," pp. 186, Proceedings of IEEE International Conference on Electrical Power Engineering, 1999.

[21] Karen Rezende, Caino De Oliveira, et-al, "Faulted branch identification on power distribution systems under noisy environment", Japan, pp. 1-5, 2009.

[22] Mats Ostman, "The pros and cons of alternative grounding systems," Wartsila Technical Journal, pp. 27 -31, January 2009.

[23] Wang Nian-bin, et-al, "Study on line selection of grounded fault in non-effectively earthed system based on wavelet packet and chaotic neural networks," Proceedings in IEEE Second International Conference on Intelligent Computation Technology and Automation, China, pp. 476 - 480, October 2009.

[24] Pan Zhencun, et-al., “Single-Phase to ground fault line identification and section location method for non-effectively grounded distribution systems based on signal injection,” Transactions of Tianjin University and Springer Verlag, vol. 14, no.2, pp. 96 - 93, January 2008.

[25] Fan Zhang, Zhencun Pan, et-al, “A new principle of fault line selection in non solidly earthed network based on direction travelling wave,” Proceedings in IEEE Eight International Conference Power Engineering Conference, Singapore, pp. 1121-1125, December 2007.

[26] Tao Ji, Qingle Pang and Xinyun Liu, “Study on fault line detection based on genetic artificial neural network in compensated distribution system,” Proceedings in IEEE International Conference on Information Acquisition, China, pp. 1427 - 1431, August 2006.

[27] Qingle Pang, “Rough Set Neural Network Based Fault Line Detection for Neutral Non-Effectively Grounded System,” Proceedings of World Congress on Intelligent Control and Automation, pp. 6550 - 6554, China, June 2008.

[28] Xinzhou Dong, Shenxing Shi, “Identifying single-phase to ground fault feeder in neutral non-effectively grounded distribution system using wavelet transform,” IEEE Transaction on Power Delivery, vol. 23, no. 4, October 2008.

[29] R. N. Mahanty, P. B. Dutta Gupta, “Comparison of Fault Classification Methods Based on Wavelet Analysis and ANN,” International Journal of Electric Power Components and Systems, vol. 34, pp. 47–60, 2006.

[30] M. M. Saha, Ratan Das, et-al, “Review of fault location techniques for distribution systems,” Power Systems and Communications Infrastructures for the future,” Beijing, pp.1-6. Sept. 2002.

[31] J. Mora-Fl`orez, J. Mel´endez, G. Carrillo-Caicedo, “Comparison of impedance based fault location methods for power distribution systems”, Electric Power Systems Research, vol. 78, pp. 657 - 666, 2008.

[32] J. Zhu D. L. Lubkerman, A. A. Girgis, “Automated fault location and diagnosis on electric power distribution feeders”, IEEE Transactions on Power Delivery, vol. 12, no. 2, pp. 801 - 809, 1997.

[33] E. C. Senger, G. Jr. Manassero, C. Goldemberg, E.L. Pellini, “Automated fault location system for primary distribution networks”, IEEE Transactions on Power Delivery, vol. 20, no. 2, pp. 1332 – 1340, 2005.

[34] A. A. Girgis, C. M. Fallon, D. L. Lubkerman, "A fault location technique for rural distribution feeder", IEEE Transaction on Industry Application", vol. 29, no. 6, pp. 1170-1175, 1993.

[35] M. M Saha, F. Provost, E. Rosolowski, "Fault location method for MV cable network", Seventh International Conference on Developments in Power System Protection, Amsterdam, Netherlands, pp 323-326, 2001.

[36] S. Santoso, R. C. Dugan, J. Lamoree, A. Sundaram, "Distance estimation technique for single line-to-ground faults in a radial distribution system", Proceedings of IEEE Power Engineering Society Winter Meeting, no.4, pp.2551-2555, 2000.

[37] R. Das., M. S. Sachdev, T.S. Sidhu, "A fault locator for radial sub transmission and distribution lines", Proceedings of IEEE PES Summer Meeting, pp. 443-448, 2000.

[38] M. Choi, S. Lee, D. Lee, B. Jin, "A new fault location algorithm using direct circuit analysis for distribution systems", IEEE Transactions on Power Delivery, vol. 19 no. 1, pp. 35 - 41. 2004.

[39] Y. Liao, "Algorithms for power system fault location and line parameter estimation", 39th South-eastern Symposium on System Theory, Mercer University, Macon, GA. 2007.

[40] D. Thomas, R. Carvalho, E. Pereira, "Fault location in distribution systems based on traveling wave", Proceedings of Power Technology Conference, vol.2, pp 468 – 472, 2003.

[41] Z. Q. Bo, G. Waller, M. A. Redfren, "Accurate fault location technique for distribution system using fault generated high – frequency transient voltage signals", IEE Proceedings in Generation, Transmission and Distribution, vol. 146, no. 1, pp. 73 -79, 1999.

[42] Y. Tang, H. F. Wang, R. K. Aggarwal, A. T. Johns, "Fault indicator in transmission and distribution systems", Proceedings of Electric Utility Deregulation And Restructuring And Power Technologies, London, UK, pp: 238 - 243.

[43] F. H. Magnago, A. Abur, "A new fault location technique for radial distribution systems based on high frequency signals", Proceedings of IEEE PES Summer Meeting, pp. 426 – 431, 1999.

[44] A. Borgheti, S. Corsi, C.A. Nucci, M. Paolone, L. Pereto and R. Tinarelli, "On the use of continuous-wavelet transform for fault location in distribution power systems", Electrical Power and Energy Systems, vol. 28, pp.608 - 617, 2006.

[45] T. Bi., Y. Ni, C.M. Shen, F. F. Wu, "Efficient multiway graph partitioning method for fault section estimation in large-scale power networks". IEE Proceedings Generation Transmission and Distribution, vol. 149, no. 3, pp. 289 - 294, 2002.

[46] T. Bi, Y. Ni, C. M. Shen, F. F. Wu, "An on-line distributed intelligent fault section estimation system for large-scale power networks", Electric Power Systems Research, vol. 62, no. 3, pp. 173-182, 2002.

[47] M. Al - Shaher, M. M. Sabra, A.S. Saleh, "Fault location in multi-ring distribution network using artificial neural network," Electric Power Systems Research, vol. 64, no.2, pp 87 – 92, 2003.

[48] F. S. Wen, C. S. Chang, "Probabilistic approach for fault-section estimation in power systems based on a refined genetic algorithm", IEE Proceedings on Generation Transmission and Distribution, vol. 144, no. 2, pp. 160 – 168, 1997.

[49] D. Thukaram, H.P. Khincha, L. Jenkins and K. Visakha, "A three phase fault detection algorithm for radial distribution networks", Proceedings of IEEE Region 10 Conference on Computers, Communications, Control and Power Engineering, vol. 2, pp. 1242 – 1248, 2002.

[50] W. H Chen, C. W. Liu, M. S. Tsai, "On-line fault diagnosis of distribution substations using hybrid cause-effect network and fuzzy rule based method", IEEE Trans on Power Delivery, vol. 15, no .2, pp. 710-717, 2002.

[51] J. Mora-Fl`orez, J. Cormane-Angarita, G. Ordónez-Plata, "K-means algorithm and mixture distributions for locating faults in power systems", Electrical Power System Research, vol. 79, pp. 714 – 721, 2009.

[52] L. S. Martins, J. F. Martins, C. M. Alegria, V.F. Pires, "A network distribution power system fault location based on neural eigenvalue algorithm", Proceeding of IEEE Bologna Power Tech Conference, Bologna, Italy. 2003.

[53] L. Sousa, J. F. Martins, V.F. Martins, Pires, C.M. Alegria, "A neural space vector fault location for parallel double-circuit distribution lines", International Journal of Electric Power and Energy Systems, vol. 27, no. 3, pp. 225 – 231, 2005.

[54] C Wang, H. Nouri, T. S. Davies, "A mathematical approach for identification of fault sections on the radial distribution systems", 10th Mediterranean Electro - Technical Conference (MELECON), vol. 3, pp 882 - 886, 2000.

[55] H Mokhlis, H. Y. Li, "Fault location estimation for distribution system using simulated voltage sags data", UPEC, 2007.

[56] M. Kezunovic, Y. Liao, "Fault location estimation based on matching the simulated and recorded waveforms using genetic algorithms", International Conference on Development in Power System Protection, Amsterdam, the Netherlands, pp 399-402, 2002.

[57] P Järventausta, P. Verho, J. Partanen, "Using fuzzy sets to model the uncertainty in the fault location process of distribution networks", IEEE Transaction on Power Delivery, vol. 9, no. 2, pp. 954-960, 1994.

[58] W. Zhong, W. H. Liu, 1996, "Application of a fuzzy set method in distribution system fault location", Proceedings of IEEE International Symposium on Circuits and Systems, vol. 1, 617 – 620, 1997.

[59] S. J. Lee, M. S. Choi, S. H. Kang, B. G. Jin, D. S. Lee, "An intelligent and efficient fault location and diagnosis scheme for radial distribution systems", IEEE Transactions on Power Delivery, vol. 19, no. 2, pp. 524 – 532, 2004.

[60] A. Khosravi, J. A, Llobet, "A hybrid method for fault detection and modeling using modal intervals and ANFIS", Proceeding of American Control Conference, New York, USA, 2007.

[61] J. Mora-Fl`orez, G. Carrillo, L. Pérez, "Fault location in power distribution systems using anfis nets and current pattern, "IEEE PES Transmission and Distribution Conference and Exposition, Latin America, Venezuela, 2003.

[62] V. Ziolkowski,, I. N. D'Silva, R. A. Flauzino, "Automatic identification of faults in power systems using neural network technique", 16th IEEE International Conference on Control Applications: Part of IEEE Multi-conference on Systems and Control, Singapore, 2007.

[63] F. Chunju, K. K. Li, W .L. Chan, Y. Weiyong, Z. Zhaoning, "Application of wavelet fuzzy neural network in locating single line to ground fault (slg) in distribution lines", Electric Power and Energy System, vol. 29, pp. 497-503. 2007.

[64] C. H. Kim, Raj Aggrawal, "Wavelet Transform in Power System", Power Engineering Journal, pp.81-87, April 2000.

[65] K. R. Soman, K. I. Ramachandran, "Insight into wavelets", PHI Pvt. Ltd., 2nd Edition, October 2006.

[66] Yanqiu Bi, Jianguo Zhao and Dahai Zhang, “Single-phase-to-ground fault feeder detection based on transient current and wavelet packet,” Proceedings in IEEE International Conference on POWERCON, Singapore, November. 2004.

[67] Wang Nian-bin, et-al, “Study on line selection of grounded fault in non-effectively earthed system based on wavelet packet and chaotic neural networks,” Proceedings in IEEE Second International Conference on Intelligent Computation Technology and Automation, China, pp. 476-480, October 2009.

[68] D. Gabor, "Theory of Communication", J. Inst. Elec. Engineering, pp.429-457, 1946.

[69] Tamer A. Kawady, et al, “Gabor transform based fault locator for transmission lines,” Proceeding of IEEE Eleventh International Middle East Power System Conference, Egypt, pp. 123 – 128, December 2006.

[70] S. Mallat, “A theory for multiresolution signal decomposition: the wavelet representation,” IEEE Transactions on Pattern Analysis and Machine Intelligence, vol. 11, no. 7, pp. 674 - 693, 1989.

[71] I. Daubechies, “Orthonormal bases of compactly supported wavelets”, Communications on Pure and Applied Mathematics, vol. 41, pp 909 – 996, 1988.

[72] H. Zou, and A. H. Tewfik, “Discrete orthogonal M – Band wavelet decompositions”, In Proceedings of International Conference on Acoustic Speech and Signal Processing, vol. 4, pp. IV-605-IV-608, 1992.

[73] R. A. Gopinath, C. S. Burns, Wavelets and filter banks, in : C. K. Chui (Ed.), wavelets: A tutorial in theory and applications, Academic Press, San Diego, C.A., pp. 603 – 654, 1992.

[74] N. Julia. S. Gabriele, “Dual-tree complex wavelet transform in the frequency domain and an application to signal classification”, Technical Report/Department for Mathematics and Computer Science, University of Mannheim, 2003.

[75] N.G Kingsbury, “The dual-tree complex wavelet transform: a new efficient tool for image restoration and enhancement”, Proceedings of European Signal Processing Conference, , pp. 319–322, Sept. 1998

[76] N.G Kingsbury, “Shift invariant properties of the dual-tree complex wavelet transform”, Proceedings of International Conference, ICASSP’99, Phoenix, Arizona, USA, vol. 1, pp. 1221–1224, March. 1999.

[77] N.G Kingsbury, "A dual-tree complex wavelet transform with improved orthogonality and symmetry properties", Proceedings of International Conference on Image, pp. 375–378, Sept. 2000.

[78] H. Choi, J. Romberg, R.G. Baraniuk, and N. Kingsbury, "Hidden markov tree modeling of complex wavelet transforms," Proceedings of IEEE International Conference on Acoust, Speech, Signal Processing (ICASSP), vol. 1, pp. 133–136, June 5–9, 2000.

[79] P. L. Dragotti and M. Vetterli, "Wavelet footprints: Theory, algorithms, and applications", IEEE Transactions on Signal Processing, vol. 51, no. 5, pp. 1306–1323, May 2003.

[80] N.G. Kingsbury, "Image processing with complex wavelets", Philos. Trans. R. Soc. London A, Math. Phys. Sci., vol. 357, no. 1760, pp. 2543–2560, Sept. 1999.

[81] N.G. Kingsbury and J.F.A. Magarey. "Wavelet transforms in image processing," Proceedings of 1st European Conf. Signal Analysis. Prediction, Prague, pp. 23–34, June 24–27, 1997.

[82] J. Romberg, H. Choi, R.G. Baraniuk, and N.G. Kingbury, "Multi scale classification using complex wavelets and hidden Markov tree models, Proceedings of IEEE Int. Conf. Image Processing, Vancouver, BC, Canada, vol. 2, pp. 371–374, Sept. 10–13, 2000.

[83] J.K. Romberg, M. Wakin, H. Choi, N.G. Kingsbury, and R.G. Baraniuk, "A hidden Markov tree model for the complex wavelet transform," Rice ECE, Tech. Rep., Sept. 2002.

[84] N.G. Kingsbury, "The dual-tree complex wavelet transform: A new techniquefor shift invariance and directional filters," Proceedings of. 8th IEEE DSP Workshop, Utah, paper no. 86, Aug. 9–12, 1998.

[85] N.G. Kingsbury, "Complex wavelets for shift invariant analysis and filtering of signals," Appl. Comput. Harmon. Anal., vol. 10, no. 3, pp. 234–253, May 2001.

[86] E.P. Simoncelli, W.T. Freeman, E.H. Adelson, and D.J. Heeger, "Shiftable multi-scale transforms," IEEE Trans. Inform. Theory, vol. 38, no. 2, pp. 587–607, March. 1992.

[87] O. P. Malik, " Application of Neural Networks in Transmission Line Protection, Power Engineering Society General Meeting, pp. 1-6, 2007.

[88] R. N. Mahanty, P. B. Dutta Gupta, "ANN based fault classifier with wavelet MRA generated inputs", International Journal of Engineering Intelligent Systems, Vol. 16, No. 2, pp. 75-85, June 2008.

[89] Fan Chunju , K.K. Li , W.L. Chan , Yu Weiyong , Zhang Zhaoning , "Application of wavelet fuzzy neural network in locating single line to ground fault (SLG) in distribution lines," International Journal of Electric Power Systems Research, vol.29, pp.497-503, 2007.

[90] D. Thukaram, et al, "Artificial neural network and support vector machine approach for locating faults in radial distribution systems," IEEE Transaction on Power Delivery, vol. 2,no. 20, pp. 710–720, April 2005.

[91] Shashidhara. H.L and Vikram M. Gadre, "Introduction to Wavelets and Wavelet Transforms", Invited paper, Proceedings of National Conference on Applications of Fourier and Wavelet Analysis in Engineering and technology (NACWET-99), Chickballapur, pp 58 – 65, May 1999.

[92] D.C. Roberston, et al, "Wavelet and electromagnetic power system transients," IEEE Transaction on Power Delivery, vol. 11, no. 2, pp. 624–629, April 1995.

[93] Gaurav Bhatnagar, Q. M. Jonathan Wu, Balasubramanian Raman, "Discrete fractional wavelet transform and its application to multiple encryptions". Journal of Information Science (Elseivier), vol. 223, pp. 297- 316, 2013.

[94] Gaurav Bhatnagar, Q. M. Jonathan Wu, Balasubramanian Raman, "A New Fractional Random Wavelet Transform for Fingerprint Security", IEEE Transactions on Systems, Man, and Cybernetics, Part A, vol. 42, no. 1, pp. 262 – 275, 2012.

[95] Ali –Reza Sedighi, Mahmood – Reza Haghifam, O. P. Malik, "High Impedance Fault Detection Based on Wavelet Transform and Statistical Pattern Recognition, IEEE Transactions on Power Delivery, vol.20, no.4, pp. 2414 – 2421, October 2005.

[96] A. H. Osman, O. P. Malik, "Protection of Parallel Transmission Line using Wavelet Transform, IEEE Transactions on Power Delivery, vol. 19, no. 1, pp. 49 – 55, January 2004.

[97] Bhavesh Bhalja, R. P. Maheshwari, "Protection of double-circuit line using wavelet transform", Institution of Engineers. India, vol. 87, no. 2, pp. 67 –7 0, September 2006.

[98] Bhavesh Bhalja, R. P. Maheshwari, "Percentage differential protection of double-circuit line using wavelet transform", Electrical. Power Components and System, vol. 35, no. 8, pp. 945 – 954, August 2007.

[99] E. Y. Hamid, Z. I. Kawasaki, "Wavelet-based data compression for power disturbances using minimum description length data," IEEE Transactions. Power Delivery, vol. 17, no. 2, pp. 460– 466, April 2002.

[100] M. da Silvaa, M. Oleskoviczb, D. V. Coury, “A Hybrid fault locator for three terminal lines based on wavelet transform, International Journal of Electric Power System Research, vol 78, pp. 1980 - 1988, May 2008.

[101] Prakash Ishwar, V.M. Gadre, Munish Moudgil, “A wavelet network approach to the non-linear discrete system identification problem”, Second National Conference on Communications (NCC), Bombay, India, pp. 193-197, 1996.

[102] A.H.A. Bakar, M.S. Ali, Chia Kwang Tan, H. Mokhlis, H. Arof, H.A. Illias, "High impedance fault location in 11 kV underground distribution systems using wavelet transforms", International Journal of Electrical Power and Energy System, vol. 55, pp. 723 - 730, February 2014.

[103] Mohd Syukri Ali, Ab Halim Abu Bakar, Hazlie Mokhlis, Hamzah Arof and Hazlee AzilIllias, "High-impedance fault location using matching technique and wavelet transform for underground cable distribution network", IEEJ Transactions on Electrical and Electronic Engineering, vol.9, no. 2, pp. 176 - 182, March 2014.

[104] Mohd Syukri Ali, A. B Halim Abu Bakar, Hazlie Mokhlis, Hamzah Aroff, Hazlee AzilIllias, Muhammad Mohsin Aman, "High impedance fault localization in a distribution network using the discrete wavelet transform", 6th International Power Engineering and Optimization Conference PEOCO2012 ,pp.349 - 354, 6-7 June 2012.

[105] Wang Ke, Chen Weirong, Li Qi, “Power system fault identification method based on multi – wavelet packet and artificial neural network”, Proceedings of International Conference on ISDEA, pp. 1457 – 1452, 2012.

[106] E. Ortiz, V. Symos, “Support vector machines and wavelet packet analysis for fault detection and identification”, Proceedings of IJCNN, pp. 3449 – 3456, 2006.

[107] R. Das, M. S. Sachdev, T. S. Sidhu, “A fault locator for radial sub transmission and distribution lines,” IEEE Power Engineering Society Summer Meeting, Washington, July 16-20, 1998.

[108] S. R. Samantaray, P. K. Dash, G.Panda, “Transmission line fault detection using time-frequency analysis, Proceedings in IEEE INDICOM Conference, Chennai, pp. 162-166, December 2005.

[109] A. E. Ibrahim, Tamer A. Kawady, et.al., “Generalized 1- D gabor transform application to power system signal analysis,” Proceeding of IEEE ISIE Conference, Canada, pp. 624 – 629, July 2006.

[110] Tamer A. Kawady, et.al., "A gabor transform-based universal fault detector for transmission lines," Proceeding of IEEE Twelfth International Middle East Power System Conference, Egypt, pp. 265 – 269, March 2008.

[111] T. A. Kawady, N. I. Elkalashy, A. E. Ibrahim, A. I. Taalab, "Arcing fault identification using combined gabor transform – neural network for transmission lines," vo. 61, pp. 248-258, 2014.

[112] G. Morales – Espana, J. Mora Florez, "A complete fault location formulation for distribution systems using k-nearest neighbour for regression and classification", IEEE Transmission and Distribution Conference and Exposition, Latin America, pp. 810-815, 2010.

[113] Ali –Reza Sedighi, Mahmood – Reza Haghifam O. P. Malik, "Soft Computing Applications in high impedance fault detection in distribution systems, Electrical Power System Research, vol.76, pp. 136 – 144, 2005.

[114] Seema Kulkarni, V. M. Gadre and Sudhindra V. Bellary, "Non uniform M-Band wave packets for Transient Signal Detection", IEEE Transactions on Signal Processing, pp. 1803-1807, June 2000.

[115] P. G. Patwardhan and V. M. Gadre, "Design of 2-D M-th Band low pass FIR eigen filters with symmetries", IEEE Signal Processing Letters, vol. 14, no. 8, pp. 517-520, August 2007.

[116] Q.Saifee, P.G. Patwardhan, V.M.Gadre, "On parallelepiped-shaped pass bands for multidimensional non separable Mth-band low-pass filters", IEEE Transactions on Circuits and Systems II: Express Briefs, vol. 55, no 8, pp.786 – 790, August 2008.

[117] C. Chaux, L. Duval, and J.C. Pesquet, "2D dual-tree m-band wavelet decomposition," Proceedings in IEEE (ICASSP), Philadelphia, vol. 4, pp. 537–540, Mar. 2005.

[118] G. Mora Espana, J. Mora Florez, H. Vargas, Torres, "Fault location method based on determination of the minimum fault reactance for uncertainty loaded and unbalanced power system", IEEE Transmission and Distribution Conference and Exposition, Latin America, pp. 803-809, 2010.

[119] M. Mirzaei, M.Z. A Ab Kadir, E. Moazami, H. Hizam, "A review of fault location methods for distribution power system", Australian Journal of Basic and Applied Sciences, vol. 3, pp. 2670 – 2676, 2009.

[120] Zhang Xiaoli, Zeng Xiangjung, et al, “Fault location using wavelet energy spectrum analysis of travelling wave,” Proceeding of IEEE 8th International Power Engineering Conference pp. 1129 – 1130, 2007.

[121] A Samui, S. Samantaray, “Wavelet singular entropy based islanding detection in distributed generation", IEEE Transactions on Power Delivery, vol.18, no.-1, pp. 411-418, 2013.

[122] S. Samantaray, G. K. Panda, “High impedance fault detection in distribution feeders using extended kalman filter and support vector machine”, European Transactions on Electrical Power, vol. 20, no. 3, pp. 382 - 393, April 2010.

[123] S. Samantaray, G. K. Panda, “Ensemble decision trees for high impedance fault detection in power distribution network", International Journal of Electrical Power and Energy Systems, Elsevier Science, vol. 43, no. 1, pp 1048-1055, December 2012.

[124] Gaurav Bhatnagar, Q. M. Jonathan Wu, Balasubramanian Raman, “Fractional dual tree complex wavelet transform and its application to biometric security during communication and transmission”, Future Generation Computer System, vol. 28, no.1, pp. 254-267, 2012.

[125] P.F.C. de Rivaz, N. G. Kingsbury, “Complex wavelet features for fast texture image retrieval”, Proc. IEEE Int. Conf. Image Processing, Kobe, vol. 1, pp. 109–113. Oct. 1999.

[126] M. Kokare, P. K. Biswas, and B. N. Chatterji, “Rotation invariant texture features using rotated complex wavelet for content based image retrieval”, Proc. IEEE Int. Conf. Image Processing, Singapore, vol. 1, pp. 393–396, Oct. 2004.

[127] J.F.A. Magarey and N.G. Kingsbury, “Motion estimation using a complex-valued wavelet transform,” IEEE Trans. Signal Processing, vol. 46, no. 4, pp. 1069–1084, Apr. 1998.

[128] P. Ray, B. K. Panigrahi, N Senroy, “Hybrid methodology for fault distance estimation in series compensated transmission line, IET Generation, Transmission and Distribution, vol. 7, no. 5, pp. 431 – 439, 2013.

[129] J. Mora, J. Meléndez, et al, “An overview to fault location methods in distribution system based on single end measures of voltage and current”, Proceeding of ICREPQ’04 – International Conference on Renewable Energy and Power Quality, Barcelona, April 2004.

[130] Tom Short, J. Kim, C. Melhorn, “Update on distribution system fault location technologies and effectiveness,” Proceeding in International Conference on Electricity Distribution, Prague, June 2009.

[131] Venkatesh. C and K. S. Swarup, "Steady State Error Estimation in Distance Relay for Single Phase to Ground Fault in Series- Compensated Parallel Transmission Lines", IET Generation, Transmission & Distribution, vol. 8, no. 7, pp. 1318-1337, Jul. 2014.

[132] Venkatesh. C and K. S. Swarup, "Faulty Line Identification by Distance Relay In Series-Compensated Parallel Transmission Lines", IEEE Power and Energy Society General Meeting 2014, Washington, USA, July 2014.

[133] Zhihan Xu, T. S. Sidhu, "Fault location methods based on single – end measurements for underground cables", IEEE Transactions on Power Delivery, vol. 26, no. 4, pp. 2845 – 2854.

[134] T. S. Sidhu, Zhihan Xu, " Detection and classification of incipient faults in underground cables in distribution system, IEEE Transactions on Power Delivery, vol. 25, no. 3, July 2010.

[135] S. Sahoo, P. Ray, K. B. Panigrahi, N. Senroy, "A computational intelligence approach for fault location in transmission lines", Joint International Conference on Power Electronics, Drives and Energy Systems, pp. 1 – 6.

[136] Lilik Jamilatul Awalin, Hazlie Mokhlis, Ab Halim Abu Bakar, Hasmaini Mohamad, Hazlee A. Illias, "A generalized fault location method based on voltage sags for distribution network", IEEJ Transactions on Electrical and Electronic Engineering, vol.8, no S1, pp S38 - S46, Nov 2013.

[137] Soon-Ryul Nam, Jin-Man Sohn, Sang-Hee Kang, Jong-Keun Park, "Ground-fault location algorithm for ungrounded radial distribution systems," Springer-Verlag Journal, vol. 89, pp 503 - 508, May 2006.

[138] S. Herraiz, J. Meléndez, G. Ribugent,et al, "Application for fault location in electrical power distribution systems," Proceeding of 9th International Conference on Electrical Power Quality and Utilisation, 9 -11 October 2007.

[139] K. M. Sharma, K. P. Vittal, P Seshagiri, "A heuristic approach for distributed generation source location and capacity evaluation in distribution systems", IEEE Region 10 Conference (TENCON), pp. 1- 6.

[140] Dunn, J. C., A Fuzzy Relative of the ISODATA Process and Its Use in Detecting Compact Well-Separated Clusters, Taylor & Francis Journal of. Cybernetics and Systems, vol. 3, no. 3, 32–57, 1974.

[141] J. C. Bezdek, Pattern Recognition with Fuzzy Objective Function Algorithms, Plenum Press, New York, 1981.

[142] Haojun Sun, S. Wang and Q. Jiang, "FCM-Based Selection Algorithm for Determining the Number of Clusters," Elsevier J. Pattern Recognition, vol. 37, pp. 2027-2037, 2004.

[143] J. Hair, R. Anderson, R. Tatham, W. Black, Multivariable Data Analysis, Prentice Hall, Madrid, 1999.

[144] M. Jordan, R. Jacobs, "Hierarchical mixture of experts and the EM algorithm, IEEE Transactions on Neural Computation, vol.6, pp. 181-214, 1994.

[145] J. Mora - Florez, et a, "k –mean algorithm for locating faults in power system," Electric Power System Research, vol. 79, no. 4, pp. 714 – 721, 2009.

[146] Qing Yang, Jingran Guo, Dongxu Zhang, Chang Liu, "Fault Diagnosis based on Fuzzy C-means (FCM) algorithm of the optimal number of clusters and probabilistic neural network", International Journal of Intelligent Engineering and Systems, vol. 4, no. 2, pp. 51 -59, 2011.

[147] Karwan Qader, Mo Adda, "A survey of network fault classification using clustering techniques", International Journal of Advance Research in Computer and Communication Engineering, vol. 2, no.10, pp 4028 – 4032, 2013.

[148] Xiaofeng Liu, Lin Ma, Sheng Zhang, Joseph Mathew, "Using fuzzy c-means and fuzzy intergals for machinery fault diagnosis", pp. 1-9, Proceedings of International Conference on Condition Monitoring, England, 2005.

[149] I. W. C. Lee, P. K. Dash, "S-transform-based intelligent system for classification of power quality disturbance signals", IEEE Transactions on Industrial Electronics, vol. 50, no.3, pp. 800 – 805, August 2003.

[150] Stuti Shukla, S. Mishra, Bhim Singh, "Empirical-mode decomposition with hilbert transform for power-quality assessment", vol. 24, no.4, pp. 2159 – 2165, October 2009.

APPENDIX - A

Electrical Parameters of SaskPower Distribution System:

Equivalent Distribution System Source Data:

Base Voltage (kV)	Base Capacity (MVA)	Positive and Negative Sequence Impedance (p.u.)	Zero Sequence Impedance (p.u.)
25	10	0.68283+j2.98139	0.09496+j1.39289

Line Data:

Section between nodes	Length of Section (km)	Series Impedance (Ohms/km)		Shunt Admittance (Mhos/km)	
		Positive & Negative Sequence	Zero Sequence	Positive & Negative Sequence	Zero Sequence
1 & 2	2.414	0.3480+j0.5166	0.5254+j1.7040	j3.74 E-06	j2.49 E-06
2 & 6	16.092	0.3480+j0.5166	0.5254+j1.7040	j3.74 E-06	j2.49 E-06
6 & 7	4.023	0.3480+j0.5166	0.5254+j1.7040	j3.74 E-06	j2.49 E-06
7 & 8	5.150	0.5519+j0.5390	0.7290+j1.727	j3.59 E-06	j2.39 E-06
8 & 9	2.414	0.5519+j0.5390	0.7290+j1.727	j3.59 E-06	j2.39 E-06
9 & 10	4.506	0.5519+j0.5390	0.7290+j1.727	j3.59 E-06	j2.39 E-06
10 & 11	2.414	0.3480+j0.5166	0.5254+j1.7040	j3.74 E-06	j2.49 E-06
6 & 12	2.414	0.3480+j0.5166	0.5254+j1.7040	j3.74 E-06	j2.49 E-06
8 & 13	2.414	7.3977+j0.8998	7.3977+j0.8998	j2.51 E-06	j2.51 E-06

13 & 14	2.414	7.3977+j0.8998	7.3977+j0.8998	j2.51 E-06	j2.51 E-06
13 & 15	2.414	7.3977+j0.8998	7.3977+j0.8998	j2.51 E-06	j2.51 E-06
15 & 16	2.414	7.3977+j0.8998	7.3977+j0.8998	j2.51 E-06	j2.51 E-06
15 & 17	2.414	7.3977+j0.8998	7.3977+j0.8998	j2.51 E-06	j2.51 E-06
9 & 18	2.414	7.3977+j0.8998	7.3977+j0.8998	j2.51 E-06	j2.51 E-06
18 & 19	2.414	7.3977+j0.8998	7.3977+j0.8998	j2.51 E-06	j2.51 E-06
18 & 20	3.219	7.3977+j0.8998	7.3977+j0.8998	j2.51 E-06	j2.51 E-06
20 & 21	3.219	7.3977+j0.8998	7.3977+j0.8998	j2.51 E-06	j2.51 E-06

Load data:

Node Number	Phase	Connected Size (kVA)	Composition (%)		
			Heating	Lighting	Motor
1	A	15.0	99.8	0.1	0.1
2	A	15.0	99.8	0.1	0.1
7	B	15.0	99.8	0.1	0.1
11	A, B & C	1000.0	0.1	0.1	99.8
12	A, B & C	67.5	99.8	0.1	0.1
14	B	15.0	99.8	0.1	0.1
15	B	15.0	99.8	0.1	0.1
16	B	7.5	99.8	0.1	0.1

17	B	15.0	99.8	0.1	0.1
18	C	25.0	99.8	0.1	0.1
19	C	15.0	99.8	0.1	0.1
21	C	15.0	99.8	0.1	0.1

Power Factor of Loads:

Type of Load	Power Factor
Heating	1.0
Lighting	0.85 lag
Motor	0.8 lag

APPENDIX - B

Electrical Parameters of IEEE 13 – Node Feeder:

Load Model Codes:

Code	Connection	Model
Y-PQ	Wye	Constant kW and kVAr
Y-I	Wye	Constant Current
Y-Z	Wye	Constant Impedance
D- PQ	Delta	Delta Constant kW and kVAr
D-I	Delta	Delta Constant Current
D-Z	Delta	Delta Constant Impedance

Load Data:

Node	Load Model	Ph-1 kW	Ph-1 kVAr	Ph-2 kW	Ph-2 kVAr	Ph-3 kW	Ph-3 kVAr
634	Y-PQ	160	110	120	90	120	90
645	Y-PQ	0	0	170	125	0	0
646	D-Z	0	0	230	132	0	0
652	Y-Z	128	86	0	0	0	0
671	D-PQ	385	220	385	220	385	220
675	Y-PQ	485	190	68	60	290	212
692	D-I	0	0	0	0	170	151
611	Y-I	0	0	0	0	170	80

Shunt Capacitor Bank:

Node	Ph-A	Ph-B	Ph-C
	kVAr	kVAr	kVAr
675	200	200	200
611			100

Overhead Line Spacing:

Spacing ID	Type
500	Three – Phase, 4 wire
505	Two – Phase ,3 wire
510	Single – Phase , 2 wire

Overhead Line Spacing:

Config.	Phasing	Phase	Neutral	Spacing	Configuration.
		ACSR	ACSR	ID	
601	B A C N	556,500 26/7	4/0 6/1	500	601
602	C A B N	4/0 6/1	4/0 6/1	500	602
603	C B N	1/0	1/0	505	603
604	A C N	1/0	1/0	505	604
605	C N	1/0	1/0	510	605